Technical University of Munich
TUM School of Engineering and Design

Study on the Multi-Timescale Complex Dynamic Characteristics of Modular High-Temperature Gas-Cooled Reactors

Jiaxuan Zhang

Complete reprint of the dissertation approved by the TUM School of Engineering and Design of the Technical University of Munich for the award of the

Doktor der Ingenieurwissenschaften (Dr.-Ing).

Chair: Prof. Dr.-Ing. Harald Klein

Examiners:

1. Prof. Rafael Macián-Juan, Ph.D.
2. Prof. Pengfei Wang, Ph.D.

The dissertation was submitted to the Technical University of Munich on 14.02.2025 and accepted by the TUM School of Engineering and Design on 20.06.2025.

KURZFASSUNG

Diese Dissertation befasst sich mit den komplexen dynamischen Eigenschaften modularer Hochtemperaturreaktoren (HTGR) über verschiedene Zeitskalen hinweg, mit besonderem Fokus auf den HTR-PM. Die HTGR-Technologie stellt einen bedeutenden Fortschritt im Kernreaktordesign dar, da sie eine hohe Effizienz, inhärente Sicherheitsmerkmale und vielseitige Anwendungsmöglichkeiten wie die Stromerzeugung und die Wasserstoffproduktion bietet. Die Technologie der Hochtemperaturreaktoren, hervorgegangen aus mehreren Jahrzehnten Forschung und Entwicklung, bietet wesentliche Vorteile gegenüber herkömmlichen Reaktordesigns, darunter höhere Betriebstemperaturen und verbesserte Sicherheitsmerkmale. Der HTGR verwendet Helium als Kühlmittel und Graphit als Moderator, was hohe Austrittstemperaturen ermöglicht, die in verschiedenen industriellen Prozessen über die reine Stromerzeugung hinaus genutzt werden können. Die Entwicklung der HTGR-Technologie hat zur Entstehung modularer Reaktoren wie dem HTR-PM geführt, die sowohl auf hohe Effizienz als auch auf Sicherheit ausgelegt sind.

Im ersten Teil wurde das HCP (HTR Code Package) entwickelt, um verschiedene bestehende Codes in ein einheitliches System zu integrieren, das in der Lage ist, das komplexe Verhalten von HTGRs zu simulieren. Die Motivation zur Erweiterung von HCP liegt in der Notwendigkeit eines umfassenden Werkzeugs, das sowohl kurzfristige als auch langfristige dynamische Szenarien präzise abbilden kann. Diese Erweiterung ist entscheidend, um die Einschränkungen bestehender Modelle zu überwinden, die für die Gewährleistung der Reaktorsicherheit und -effizienz wesentlich sind.

Der zweite Teil dieser Arbeit konzentriert sich auf die Erweiterung von HCP um ein flexibles Vorhang-Steuerstabmodell. Steuerstäbe spielen eine entscheidende Rolle bei der Leistungsregelung des Reaktors und bei der Gewährleistung eines sicheren Stillstands. Das flexible Vorhangmodell simuliert die Bewegung der Steuerstäbe durch Anpassung der Nuklidkonzentrationen in den Steuerstabregionen und ermöglicht so das dynamische Ein- und Ausfahren während der Simulationen. Die Methodik umfasst die Integration dieses Modells in das bestehende HCP-Framework, insbesondere in die Module MGT-N (Neutronik) und MGT-FD (Strömungsmechanik). Verifikations- und Validierungsprozesse (V&V) werden unter Verwendung vereinfachter Reaktormodelle durchgeführt, mit Benchmark-Vergleichen gegenüber etablierten Codes wie SERPENT und ATHLET. Die Ergebnisse bestätigen die Genauigkeit und Wirksamkeit des flexiblen Vorhangmodells, wodurch eine präzise Simulation des Steuerstabverhaltens ermöglicht und die Gesamtfähigkeit von HCP bei der Analyse dynamischer Szenarien verbessert wird.

Der dritte Teil behandelt die Entwicklung detaillierter neutronenphysikalischer und thermohydraulischer Modelle für den HTR-PM innerhalb des HCP-Frameworks. Das Neutronikmodell, basierend auf dem MGT-N-Modul, unterteilt den Reaktorkern in zahlreiche radiale und axiale Zonen, um die räumliche Verteilung des Neutronenflusses und reaktivitätsabhängige Rückkopplungsmechanismen präzise zu erfassen. Das thermohydraulische Modell, implementiert im MGT-FD-Modul, beschreibt den Wärmeübergang und das Strömungsverhalten im Reaktorkern und im Primärkreislauf. Diese Modelle sind entscheidend für die Simulation kurzfristiger dynamischer Szenarien, wie z. B. Steuerstabbewegungen, Leistungsfluktuationen und Schwankungen der Eintrittstemperatur. Die Simulationen bestätigen die Auslegungssicherheit des HTR-PM unter verschiedenen Betriebsbedingungen und zeigen die Fähigkeit des Reaktors, auch während transienter Ereignisse Stabilität und Leistung aufrechtzuerhalten.

Der vierte Teil der Dissertation untersucht Brennstoffmanagementstrategien und deren Auswirkungen auf den kurz- und langfristigen Reaktorbetrieb. Das SHUFLE-Modul wird eingesetzt, um die Bewegung der Brennstoffkugeln im Kern mithilfe des Seepage- und Flowtube-Modells zu simulieren. Diese Modelle liefern entscheidende Erkenntnisse zu optimalen Beladungsmustern und Nachfüllstrategien, die für die Aufrechterhaltung der Reaktorleistung und -sicherheit über längere Zeiträume hinweg wesentlich sind. Das TNT-Modul wird verwendet, um Abbrandketten dynamisch anhand aktueller Kerndaten anzupassen, wodurch die Genauigkeit von Abbrand- und Isotopenzusammensetzungsprognosen verbessert wird. In diesem Abschnitt wird auch die Kombination kurz- und langfristiger dynamischer Szenarien betrachtet, wobei die Ergebnisse aus dem flexiblen Vorhang-Steuerstabmodell und den thermohydraulischen Analysen integriert werden. Durch die Simulation verschiedener Brennstoffzyklen, einschließlich des OTTO-Konzepts (Once Through Then Out) und mehrerer Umläufe, wird der Einfluss unterschiedlicher Betriebsstrategien auf die Effizienz und Sicherheit des Reaktors bewertet.

Diese Dissertation stellt eine umfassende Untersuchung der komplexen dynamischen Mehrzeitskalen-Eigenschaften modularer HTGRs mit besonderem Fokus auf den HTR-PM dar. Die Arbeit erweitert das HCP-Framework um ein flexibles Steuerstabmodell, verbessert die neutronenphysikalischen und thermohydraulischen Simulationen und untersucht fortschrittliche Strategien im Brennstoffmanagement. Die Ergebnisse leisten einen wesentlichen Beitrag zum Verständnis des Betriebs und der Sicherheit von HTGRs und bieten eine solide Grundlage für zukünftige Entwicklungen. Das erweiterte HCP-Framework erweist sich als leistungsfähiges Werkzeug zur Analyse des dynamischen Verhaltens von HTGRs und unterstützt deren Rolle als Schlüsseltechnologie für eine nachhaltige und sichere Energieversorgung.

ABSTRACT

This dissertation delves into the multi-timescale complex dynamic characteristics of modular high-temperature gas-cooled reactors (HTGR), focusing on the HTR-PM. HTGR technology represents a significant advancement in nuclear reactor design, offering high efficiency, inherent safety features, and versatile applications such as electricity generation and hydrogen production. High-Temperature Gas-Cooled Reactor technology, emerging from several decades of research and development, offers notable advantages over traditional reactor designs, including higher operational temperatures and enhanced safety features. The HTGR employs helium as a coolant and graphite as a moderator, allowing for high outlet temperatures that can be utilized in various industrial processes beyond electricity generation. The evolution of HTGR technology has led to the development of modular reactors like the HTR-PM, designed for both high efficiency and safety.

In first part, The HCP was developed to integrate various legacy codes into a unified system capable of simulating the complex behaviors of HTGRs. The motivation for extending HCP lies in the need for a comprehensive tool that can accurately simulate both short-term and long-term dynamic scenarios. This extension is crucial for addressing the limitations of existing models, which are essential for ensuring reactor safety and efficiency.

The second part of this research focuses on extending the HCP to include a flexible curtain control rod model. Control rods play a vital role in regulating reactor power and ensuring safe shutdown operations. The flexible curtain model simulates the movement of control rods by adjusting the nuclide concentrations in the control rod regions, allowing for dynamic insertion and withdrawal during simulations. The methodology involves integrating this model into the existing HCP framework, specifically within the MGT-N (neutronics) and MGT-FD (fluid dynamics) modules. Verification and validation (V&V) processes are conducted using simplified reactor models, with benchmark comparisons against established codes such as SERPENT and ATHLET. The results confirm the accuracy and effectiveness of the flexible curtain model, enabling precise control rod behavior simulation and enhancing the overall capability of HCP in dynamic scenario analysis.

The third part addresses the development of detailed neutronics and thermal-hydraulic models for the HTR-PM within the HCP framework. The neutronics model, based on the MGT-N module, subdivides the reactor core into numerous radial and axial zones to capture the spatial distribution of neutron flux and reactivity feedback mechanisms accurately. The thermal-hydraulic model, implemented in the MGT-FD module, encompasses the heat transfer and fluid flow dynamics within the reactor core and primary circuit. These models are crucial for simulating short-term dynamic scenarios, such as control rod movements, power fluctuations, and variations in inlet temperatures. The simulations validate the design safety of HTR-PM under various operational conditions, demonstrating the reactor's ability to maintain stability and performance during transient events.

The fourth part of the dissertation explores fuel management strategies and their implications for both short-term and long-term reactor operation. The SHUFLE module is employed to simulate fuel pebble movement within the core, utilizing the seepage and flowtube models. These models provide critical insights into optimal fuel loading patterns and refueling strategies, essential for sustaining reactor performance and safety over extended periods. The TNT module is used to dynamically adjust depletion chains based on real-time nuclear data, enhancing the accuracy of burnup and isotopic composition predictions. This section also examines the combination of short-term and long-term dynamic scenarios, integrating the results from the flexible curtain control rod model and the thermal-hydraulic analyses.

By simulating various fuel management cycles, including the OTTO (once through then out) and multi-pass refueling strategies, the research evaluates the impact of different operational approaches on reactor efficiency and safety.

This dissertation presents a comprehensive study on the multi-timescale complex dynamic characteristics of modular HTGRs, with a particular emphasis on the HTR-PM. The research extends the HCP framework to include a flexible curtain control rod model, enhances the neutronics and thermal-hydraulic simulations, and explores advanced fuel management strategies. The findings significantly contribute to the understanding of HTGR operation and safety, providing a robust foundation for future reactor design and development efforts. The enhanced HCP framework emerges as a powerful tool for simulating and analyzing the dynamic behaviors of HTGRs, ensuring their role as a pivotal technology in the pursuit of sustainable and secure energy systems.

ABBREVIATION

AVR	- Arbeitsgemeinschaft Versuchsreaktor
ATHLET	- Analysis of Thermal-Hydraulics of Leaks and Transients
BWRs	- Boiling Water Reactors
CNNC	- China National Nuclear Corporation
SiC	- Silicon Carbide
PyC	- Pyrolytic Carbon
GWe	- GigaWatts electric
GRS	- Gesellschaft für Anlagen und Reaktorsicherheit gmbH
HTGR	- High Temperature Gas Cooled Reactor
HTGRs	- High Temperature Reactors
HCP	- HTR Code Package
KEFF	- The Effective Multiplication Factor
LOCA	- Loss of Coolant Accident
LWR	- Light Water Reactor
MGT	- Multi Group TINTE
MGT-FD	- MGT Fluid Dynamic
MGT-N	- MGT Neutronics
NSSS	- Nuclear Steam Supply System
PWRs	- Pressurized Water Reactors
PBRs	- Pebble Bed Reactors
RPV	- Reactor Pressure Vessel
SHUFLE	- Software for Handling Universal Fuel Elements
STACY	- Source Term Analysis Code System
OTTO	- Once Through Then Out

PLOFC	- Pressurized Loss of Forced Cooling
TNT	- Topological Nuclide Transmutation
TRISHA	- neutron Transport Integral Spectrum and Homogenization Application
TRISO	- Tri-isotropic
VSOP	- Very Superior Old Program
VHTGR	- Very High Temperature reactor

1. INTRODUCTION

1.1. Background

Energy is the driving force behind global economic development and serves as a vital material foundation for human survival and progress. With the increasing severity of global climate change and environmental pollution issues, sustainable and clean energy has become a key strategy for global energy transformation. According to data released by the International Energy Agency (IEA), the proportion of renewable energy in the global energy structure has been gradually increasing since the 1970s, especially with the rapid development of new energy sources such as wind and solar energy. However, despite the rapid growth of renewable energy, its share in the global energy supply remains relatively low. At the same time, fossil fuels still dominate, while nuclear energy, as a reliable low-carbon energy source, is gradually gaining prominence in the global energy structure.

According to the World Energy Outlook 2023 New Policies Scenario, coal demand is projected to rise by 0.2% annually from 2014 to 2040. Gas demand is expected to grow at a rate of 1.5% per annum, while oil demand is forecasted to increase by 0.5% annually over the same period. In terms of electricity generation, coal usage is anticipated to surge by 35% by 2040, resulting in a decrease in its share of generation from 40% to 28%. Meanwhile, nuclear output is forecasted to expand by almost 80% by 2040, primarily driven by a surge in new power station construction in China. Additionally, renewables, excluding hydro, are projected to increase nearly five-fold over the same period [1].

As a sustainable and clean form of energy, nuclear power is increasingly prominent in the global energy transition. According to statistics from the International Atomic Energy Agency (IAEA) as of 2022, there are a total of 443 nuclear reactors worldwide, with a total installed capacity of 397 gigawatts-electric (GWe). Among them, countries such as France, the United States, and China have leading nuclear power installed capacities globally. Taking China as an example, China's nuclear power installed capacity has grown from about 9 million kilowatts in 2010 to about 52 million kilowatts in 2022, with an average annual growth rate exceeding 20%, making it an important driving force for global nuclear energy development.

Nuclear energy, as a clean energy source, has significant environmental advantages compared to traditional fossil fuels. According to data from the U.S. Energy Information Administration (EIA), nuclear power generation does not produce carbon dioxide or other greenhouse gases during the process, resulting in minimal impact on the atmosphere. Therefore, it is considered one of the important means to address climate change. Taking France as an example, France is one of the countries with the most extensive use of nuclear energy in the world, with nuclear power accounting for more than 70% of its electricity generation. However, its carbon emissions are much lower than other developed countries, which to some extent proves the environmental friendliness of nuclear energy.

In 2021, nuclear reactors produced a combined output of 2653 TWh, marking an increase of 100 TWh compared to the 2553 TWh generated in 2020, as depicted in Figure 1. This figure represents the third-highest global nuclear generation total to date, falling just shy of the 2657 TWh recorded in 2019 and the 2660 TWh in 2006. Moreover, this resurgence reaffirms the upward trajectory observed in nuclear generation since 2012 [2].

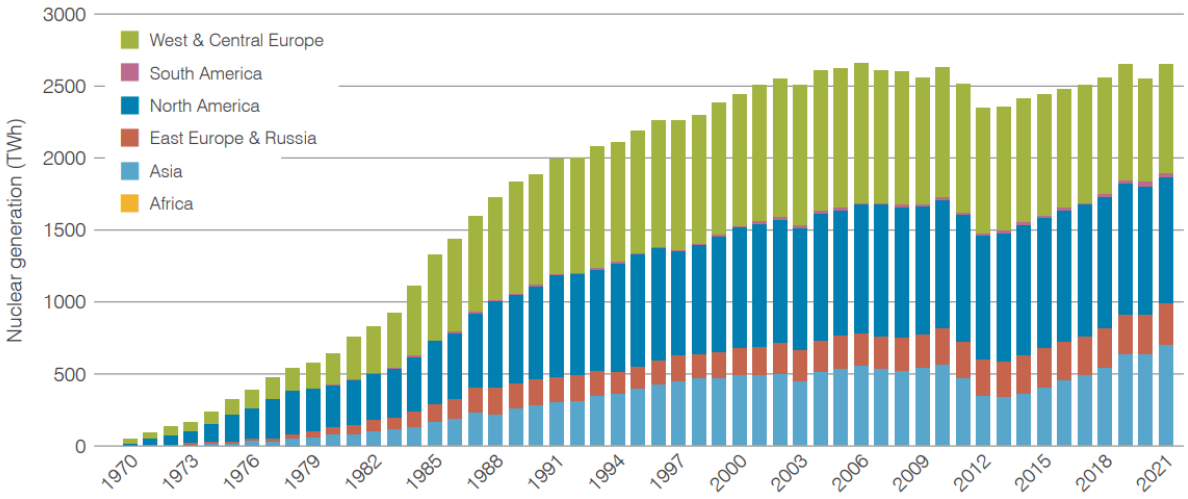

Figure 1 Nuclear electricity production [2]

Since the first achievement of nuclear power generation in the United States in 1951, after nearly 70 years of research and accumulation, nuclear energy technology has evolved from prototype reactors used in nuclear experiments to large-scale commercial nuclear power plants, experiencing four generations of development. The first-generation nuclear power plants, developed from the 1950s to the early 1960s, primarily consisted of experimental prototype nuclear power units using light water reactors. The second-generation nuclear power plants, developed from the 1960s to the early 1990s, commercialized large-scale nuclear power plants based on the first-generation designs. The third-generation nuclear power plants, developed from the late 1990s to the 2010s, represented by advanced light water reactors with optimized and standardized designs, exhibited improved safety and economics compared to second-generation plants. Currently, operational or under-construction nuclear power plants worldwide are mainly based on second and third-generation technologies. In comparison to second-generation nuclear power plants, third-generation technology has seen improvements in nuclear safety and economics. However, there are still some shortcomings. Major nuclear accidents such as the core meltdown and radioactive release incident at the Three Mile Island Nuclear Generating Station in the United States, the reactor explosion accident at the Chernobyl Nuclear Power Plant in the former Soviet Union, and the severe nuclear leakage incident at the Fukushima Daiichi Nuclear Power Plant in Japan have sounded the alarm for the importance of nuclear safety. Fourth-generation nuclear energy technology was first proposed by the US Department of Energy in June 1999 and represents the cutting-edge technological development trend for future advanced nuclear power plants. The goal of fourth-generation nuclear energy systems is to sustainably develop the economy, improve global ecology, and enhance nuclear power safety by increasing the economics of nuclear power, developing inherent proliferation resistance, and reducing nuclear waste. Table 1 gives a principal overview on the reactors systems belonging to the different generations

Table 1 Reacotr systems belonging to the different generations of reactor development

Types	Example	Characteristics
Generation I	Prototypes and first commercial plants	Experimental reactors prototype, first phase of commercial reactors
Generation II	PWR, BWR, CANDU, etc.	Commercial reactors
Generation III	EPR, ABWR, AP1000, etc.	Improved commercial reactors
Generation IV	HTGR, LFR, MSR, etc.	Future reactors

In the current phase of nuclear development, advancements in Pressurized Water Reactors (PWRs), Boiling Water Reactors (BWRs), CANDU reactors, and fast reactors are of primary importance. This phase focuses on expanding power generation capacity while striving to lower specific investment costs. Enhancements in safety are also a key priority, exemplified by initiatives such as the implementation of core catchers, double-walled containments, and enhancements in decay heat removal systems. As highlighted in Table 1, ongoing efforts in nuclear technology are directed towards Generation IV systems, a collaborative endeavor involving numerous countries.

The high-temperature gas-cooled reactor, as one of the advanced reactor types of the fourth- generation nuclear power plants, has several advantages compared to traditional PWRs. Firstly, HTGRs can achieve high operating temperatures, typically exceeding 700°C and even reaching above 1000°C. This high-temperature coolant can be utilized in various industrial processes such as thermal cracking and hydrogen production, enabling efficient energy utilization and improving energy conversion efficiency. Secondly, due to the use of gas coolant, HTGRs do not rely on external water sources, significantly reducing the heat exchange between the nuclear reactor and the external environment, thereby lowering the risk of severe accidents that may occur in water-cooled reactors. Furthermore, HTGR designs incorporate multiple passively safe features, enhancing their safety and stability. As a clean energy source, the nuclear reaction process in HTGRs does not produce greenhouse gases such as carbon dioxide, resulting in minimal negative impact on the atmospheric environment. Against the backdrop of addressing climate change and environmental pollution issues, the low carbon emissions and environmental characteristics of HTGRs will be increasingly valued. Due to its high-temperature coolant, HTGRs have broad prospects for applications in various fields. In addition to electricity generation, HTGRs can provide high-temperature heat sources for industrial production, fuel hydrogen production, petrochemical industry, molten salt reactors, etc., offering new possibilities for achieving energy diversification and efficient utilization. With continuous technological innovation and development, the performance and economics of HTGRs will be further improved. The application of new materials and processes will solidify the position of HTGRs in the field of nuclear energy, providing a more sustainable and clean energy solution for human society. In conclusion, HTGRs offer advantages such as high efficiency, safety, low carbon emissions, multi-field applications, and potential

for technological innovation and development. They will provide new impetus and choices for global energy transition, becoming an important force driving the development of clean energy.

1.2. Overview of HTGR

1.2.1. Principle Characteristics of HTGR

HTGR represents an innovative reactor system designed for electricity generation and process heat production. Initially, the aim was to harness elevated coolant temperatures exceeding 500°C to generate high-pressure steam efficiently. Additionally, graphite exhibits minimal neutron absorption, rendering it advantageous for neutron economy within this system. As nuclear technology and energy economics progress, the utilization of nuclear process heat and the development of systems with highly favorable safety profiles become increasingly significant.

The physical properties of carbon are of significant relevance to nuclear reactors: its atomic mass and extremely low neutron capture cross-section render it a highly suitable candidate for moderate-speed reactions. Hence, graphite is employed as a moderator or structural component in many thermal neutron reactors.

The coolant must have certain properties, such as chemical inertness, resistance to phase changes, immunity to neutron activation, and efficient heat exchange. Helium stands out as the sole coolant capable of meeting these stringent requirements, while also being naturally abundant in sufficient quantities. Drawing upon previous and contemporary design experiences, the outlet temperature of HTGRs typically ranges between 750°C and 950°C, with an inlet temperature around 250°C. This lower limit is dictated by the Wigner effect. Given the high operating temperatures, metallic fuel coatings are impractical, necessitating fission product retention at a microscopic level, often achieved through the utilization of ceramic-coated fuel particles.

Graphite serves as the primary structural material for both the fuel elements and the reflectors within the system. The coolant utilized is high-pressure helium, circulating through the core from top to bottom. Its temperature increases significantly, from approximately 250°C to 750°C in facilities employing steam generators.

As is shown in Figure 2, The HTGRs features two primary core design schemes: the prismatic core design and the pebble bed core design. The pebble bed core consists of numerous fuel spheres stacked together, offering greater fluidity compared to the prismatic core design, enabling continuous reloading and unloading of the core, thereby enhancing the efficiency of nuclear power plants. On the other hand, modular design enhances both the safety and the economies of scale of nuclear power plants, thus driving HTGRs towards a multi-module direction. Based on the fluid pebble bed core and modular design, the pebble bed modular HTGR exhibits excellent thermal and chemical stability, primarily demonstrated by:

(1) The use of ceramic coatings for encapsulating fuel particles in the pebble bed modular HTGR, which can withstand higher temperatures compared to metallic cladding fuel rods.

(2) The pebble bed core employs chemically stable graphite as the structural material, devoid of any metallic components. Graphite cores offer advantages such as high thermal capacity and excellent safety performance.

(3) In the pebble bed modular HTGR, single-phase helium gas serves as the coolant for the primary reactor loop. Helium has highly stable physical and chemical properties, meaning that it does not affect the reactivity of the reactor or react with graphite.

(4) The pebble bed modular HTGR features a favorable negative feedback temperature coefficient and a passive residual heat removal system, enabling inherent reactor safety. This design prevents core material temperatures from exceeding limits and avoids core meltdown accidents under any circumstances. Its inherent passive characteristics limit the power density and core size of the high-temperature gas-cooled reactor, resulting in lower power levels for individual modular units.

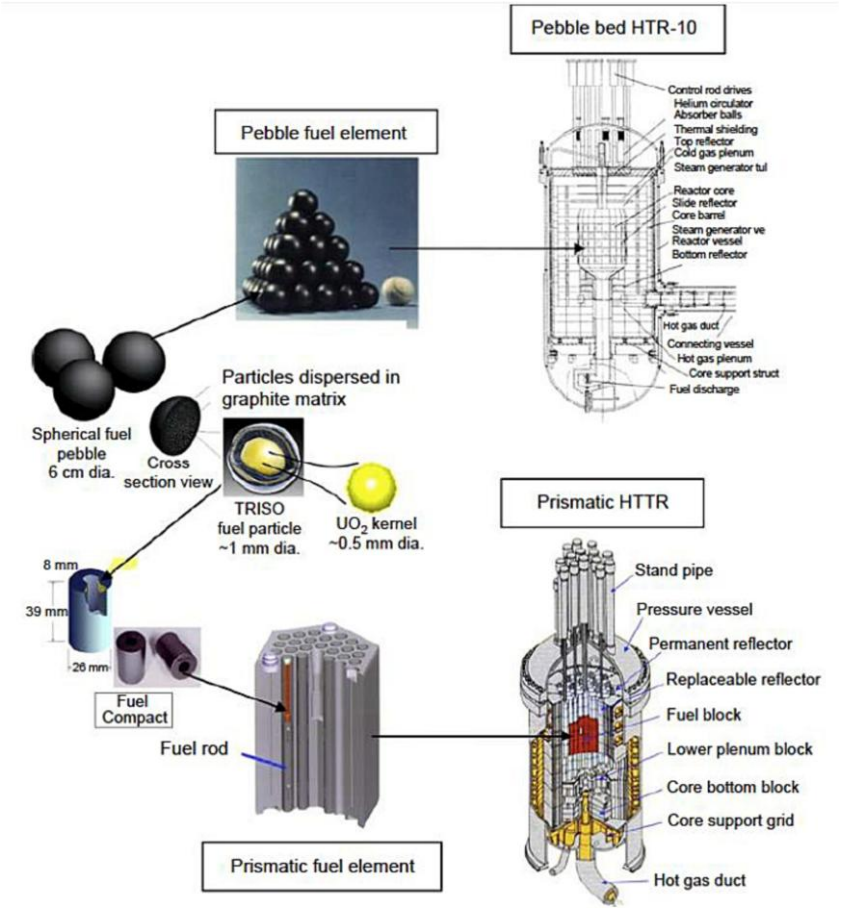

Figure 2 Comparison of Pebble Bed Reactor and Prismatic Type Reactor[3]

1.2.2. Fuels for HTGRs

The original concept of coated fuel particles was proposed by R. Huddle in 1957[5]. Since that time, a wide range of coated particle designs have been created, produced, and deployed around the world. One of the key advantages of High Temperature Gas-cooled Reactors (HTGRs) is their exceptional versatility in accommodating various fuel cycles. As a result, different fuel cycles, such as High Enriched Uranium (HEU), Low Enriched Uranium (LEU), Uranium-Thorium (U, Th), Uranium-Plutonium (U-Pu), and Plutonium (Pu), have been tested and applied in various HTGR systems. The two most commonly used types of coated particle fuel are bi-isotropic (BISO) and tri-isotropic (TRISO)

particles, as depicted in Figure 3. Since the 1980s, only the TRISO coated particle design has been permitted due to updated fuel quality and performance criteria.

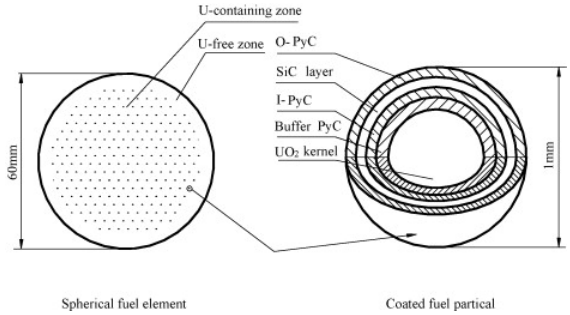

Figure 3 HTGR spherical fuel element[4]

The TRISO-coated particle design comprises four layers arranged in the following sequence: a porous buffer layer, an inner PyC (Pyrolytic Carbon) layer, a SiC (Silicon Carbide) layer, and an outer PyC layer.

Each layer of the TRISO fuel coating is carefully engineered to fulfill specific roles, such as containing fission products, resisting creep deformation, mitigating shrinkage under irradiation, and improving overall irradiation performance. While the majority of fission products are produced and confined within the fuel kernel, the porous buffer layer acts as a sacrificial shield, preventing energetic fission products from escaping. This layer is crucial for shielding the inner PyC from radiation damage and creating enough void space to accommodate fission gases and kernel swelling. The inner PyC layer serves to limit the diffusion of gaseous fission products and chlorine gas produced during SiC deposition, ensuring the SiC layer remains under compression. The primary function of the SiC layer is to retain metallic fission products and maintain the structural stability of the fuel. Finally, the outer PyC layer acts as the last barrier against gaseous fission products, reducing tensile stress on the SiC while also providing a bonding interface for the graphite matrix.

The fuel composition consists of coated particles integrated into the graphite matrix of spherical fuel elements, with a thermal neutron spectrum. Given the low parasitic absorption of graphite, an efficient neutron economy is achieved. High burn-up levels, ranging from 80,000 to 100,000 MWd/t of heavy metal, corresponding to enrichments of 8 to 10%, can be attained. Further details on TRISO-coated particles are provided in Figure 3. The fuel consists of UO_2 in the form of small kernels, approximately 500 μm in diameter. Surrounding the kernel is an initial buffer layer (about 50–90 μm thick) that is porous and capable of capturing migrating fission products. The subsequent layers (C/SiC/C) are thin (40 μm/35 μm/40 μm) but form a strong pressure vessel, effectively retaining fission products during normal operations and preventing their release even during severe accidents, up until the fuel temperature reaches around 1600°C.

The fuel zone is surrounded by a 5-mm-thick graphite shell, free of fuel and made from the same material as the fuel matrix, ensuring a strong connection between the two. A new fuel element typically holds 7–10 g of heavy metal in oxide form, depending on the core's specific configuration. This design provides a thermodynamic benefit by promoting nearly uniform heat generation throughout the fuel element. The graphite's high thermal conductivity effectively regulates the temperature distribution within the fuel, enabling the reactor to achieve high coolant temperatures while maintaining relatively low fuel temperatures compared to other reactor designs.

1.2.3. HTGR application

High-temperature reactors have the capability to supply steam cycles and can be directly integrated into gas turbine cycles or combined cycles. Depending on the parameters of the cycles, efficiencies between 40% and 50% can be achieved.

Figure 4 depicts the schematic flow sheet of a hot steam process with reheat, seamlessly integrated into the primary circuit. This flow diagram, based on the provided data, was implemented in the THTGR plant.

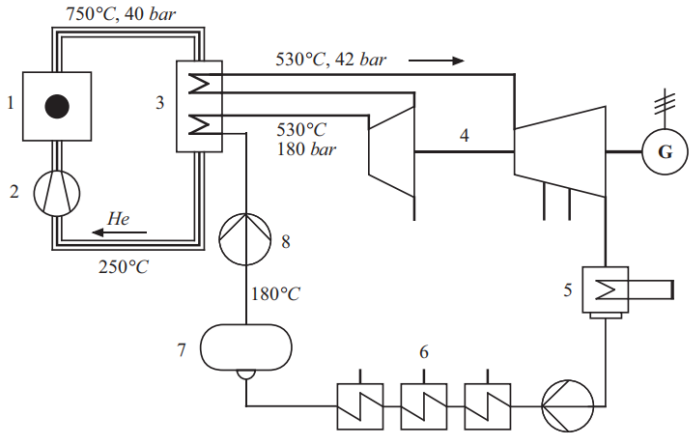

Figure 4 Principle of a hot steam cycle with reheat by helium [6]

(1: reactor, 2: helium circulator, 3: steam generator with reheater, 4: turbo machinery, 5: condenser, 6: feedwater preheating, 7: feedwater storage vessel, 8: feedwater–pump)

Due to the elevated helium outlet temperature from the core reaching 750°C, it became feasible to generate hot steam at 530°C/180 bar and hot reheated steam at 530°C/45 bar. The plant operated with a net efficiency of 40%, which encompassed the utilization of a dry air cooling tower for the disposal of process waste heat.

The significant increase in reactor outlet temperature has paved the way for integrating nuclear reactors with hydrogen production systems utilizing high-temperature electrolysis or thermochemical water splitting methods. By coupling nuclear reactors with advanced thermochemical cycles for hydrogen production, it becomes feasible to achieve large-scale hydrogen generation that is efficient, cost-effective, and entirely carbon-free. This strategy not only enhances the load-following capability of nuclear power plants—allowing them to switch flexibly between electricity and hydrogen production—but also boosts their economic viability by providing hydrogen as a valuable resource for transportation and chemical industries. Currently, many countries and regions are actively advancing research and development in fourth-generation nuclear reactors and thermochemical water-splitting-based hydrogen production technologies.

Figure 5 illustrates a typical schematic cycle configuration of a nuclear hydrogen production system based on Very High Temperature Reactor (VHTGR) and the I-S cycle. Clearly, the I-S cycle and the power cycle are arranged in series. For this series system, the high-temperature helium gas produced by the VHTGR sequentially passes through the Intermediate Heat Exchanger (IHX) and the Steam Generator (SG), providing thermal energy for hydrogen production and electricity generation, respectively [7].

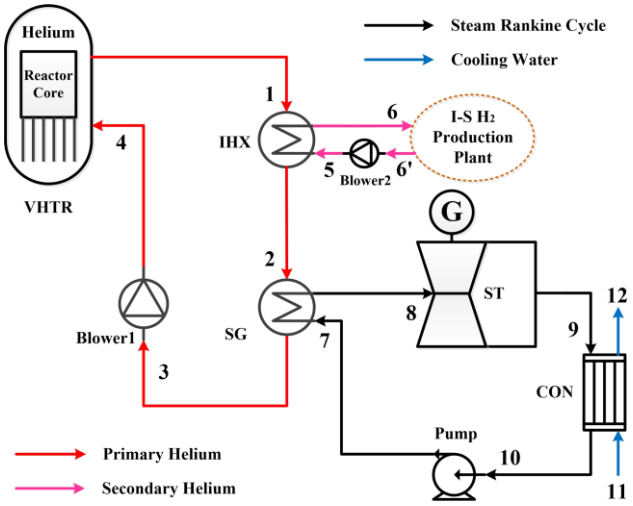

Figure 5 Schematic diagram of the typical SCS [8]

In addition to the production of electrical energy and hydrogen, future nuclear energy can also be utilized in the heat market. Co-generation plants can be operated, enabling the delivery of both electricity and heat for various purposes. Notable applications include providing district heating, process steam for refineries and chemical plants, and heat for seawater desalination. Additionally, for enhanced oil recovery, which is expected to play a significant role in the coming decades, large quantities of superheated steam are required.

1.2.4. History of HTGRs

1) Germany

The foundational idea of high-temperature gas-cooled reactors with a prismatic core structure was first explored at the Atomic Energy Research Establishment in Harwell in early 1966. Concurrently, research in Western Germany concentrated on the pebble bed design, where the core is composed of a randomly packed bed of spherical fuel elements. The efforts at Harwell culminated in the construction of the 20 MW reactor experiment under the OECD High Temperature Reactor Project (DRAGON) at Winfrith, England, which reached its design power output in April 1966. Building on this success, the Harwell design was further advanced with the development of the Peach Bottom Reactor by the Philadelphia Company in partnership with General Atomic of San Diego, achieving full operational power in May 1967.

HTGRs have been a topic of interest in Germany due to their potential as a next-generation nuclear power technology offering enhanced safety features and potential applications in both electricity generation and industrial processes. Germany has a long history of nuclear research dating back to the mid-20th century. In the 1960s and 1970s, German scientists and engineers began exploring HTGR concepts for their inherent safety features, such as passive heat removal and high-temperature operation.

One of the significant milestones in German HTGR development was the construction and operation of the Arbeitsgemeinschaft Versuchsreaktor (AVR) in Jülich, as is shown in Figure 6 [10], which began operation in 1966. In 1956, a working group consisting of nine utility companies was established to pave the way for the construction of the AVR, or Experimental Reactor. Within two years, despite key components such as fuel not being fully developed for market readiness, a concept was approved. The experimental pebble-bed high-temperature gas-cooled reactor (AVR), with a thermal capacity of 46

MW, began construction in 1961 and commenced operation in 1967 (see Figure 10). The AVR operated for over 750 weeks until its final shutdown in 1988. During its operational lifespan, the total cumulative electricity generated by the AVR amounted to 1.6 billion kWh, corresponding to a time utilization rate of 67.2%, a remarkable achievement for the first AVR-class reactor system. A significant milestone was achieved in 1976 when the AVR operated continuously for 111 days, marking the longest uninterrupted run since the plant's inception. That same year, the availability reached its peak at 91.9%. The AVR was an experimental HTGR designed to investigate the feasibility and performance of this reactor concept. It operated until 1988 and provided valuable data and experience

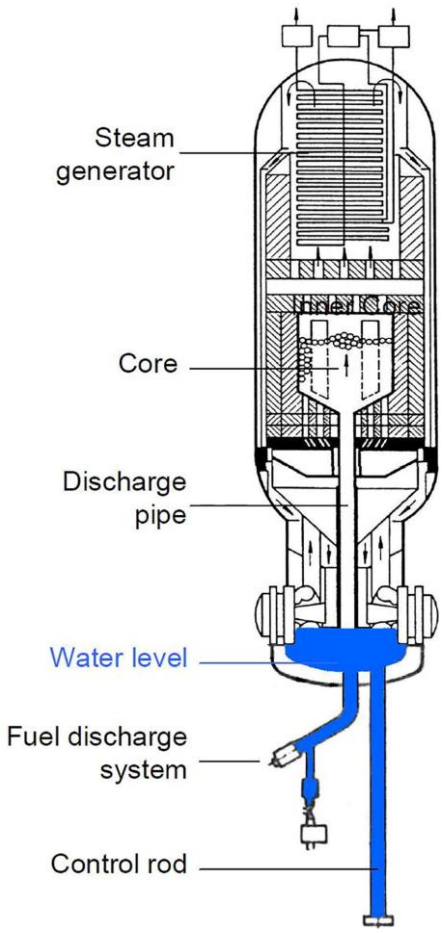

Figure 6 Schematic of AVR reactor[10]

Building on the experience gained from the AVR, Germany embarked on a larger-scale HTGR project with the construction of the THTGR-300 (Thorium High-Temperature Reactor 300) in Hamm-Uentrop. The 300 MWe THTGR-300(Figure 7) was designed as a steam cycle power plant and construction began in 1971 in Schmehausen near Hamm/Westfalia. A pioneering effort was made with the installation of dry cooling towers using a rope net design. Several design changes were implemented compared to the AVR, including the adoption of prototype components such as prestressed concrete reactor pressure vessels containing six steam generators arranged in parallel (interchangeable), helium coolant flowing from top to bottom, a 3-fold increase in power density, or control rods driven by the pebble-bed core, necessitated by the 6 m diameter movable core. Initially, the construction was scheduled for 61 months. However, challenges arose in establishing regulatory standards for new components and corresponding calculation regulations, as well as changes in safety concepts leading to

comprehensive verification, new configurations, and redesigned requirements during the licensing process, resulting in years of delay in commissioning and significantly increased construction costs. The direct transfer of pressurized water reactor requirements to high-temperature reactors, ignoring the specific operating characteristics of high-temperature reactors, even led to significant changes in safety concepts. A major change involved multiple modifications to the pipeline system in the secondary circuit, controlling double-ended pipe ruptures at any position in the circuit by retrospectively installing numerous pipe whip restraint devices.

THTGR-300 finally achieved initial criticality in September 1983 and delivered the first batch of electricity to the grid in November 1985. In September 1986, the reactor achieved full power operation for the first time, thereby achieving the goal of demonstrating the industrial service capability of the pebble-bed reactor, ready for handover to utility companies. Technical issues arose during operation: fuel discharge devices were initially not allowed to operate at full power during reconfiguration, 35 out of 2600 difficult-to-access screws were lost in the fixed hot gas ducts, and fuel ball ruptures occurred due to multiple unexpected shutdowns during startup (Schwarz and Bäumer, 1987), necessitating the insertion of control rods into the core. These technical issues could be addressed through improved design and construction.

Despite the challenges faced by the THTGR-300 project, research on HTGR technology continued in Germany, often in collaboration with international partners. German organizations such as the Forschungszentrum Jülich (Jülich Research Centre) and industry players like Siemens have been involved in research and development efforts aimed at improving HTGR designs and addressing technical challenges.

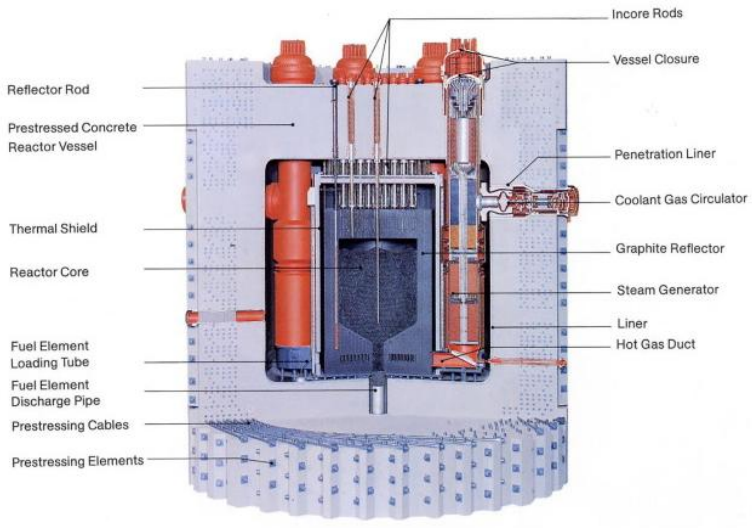

Figure 7 THTGR-300 core components[10]

As of recent years, Germany's nuclear energy policy has shifted towards phasing out nuclear power in favor of renewable energy sources. This has influenced the direction of nuclear research and development in the country, with less emphasis on traditional reactor technologies. However, HTGRs continue to attract interest globally, particularly in countries looking for safe, reliable, and carbon-neutral energy sources.

The German HTGR-200 module (HTGR-module, as is shown in Figure 8) concept plant remains a significant reference design for several reasons. Firstly, its comprehensive documentation status makes it well-suited for various benchmarks and studies. The ongoing construction of the HTR-PM in China, based on the HTGR-200 design, marks a significant advancement in this reactor concept, with operations expected to commence in 2023. The HTGR module has been developed as a modular heat source suitable for both cogeneration and process heat applications. In cogeneration scenarios, the helium outlet temperature from the core is designed to reach 700°C, with steam conditions set at 530°C and 180 bar. For process heat applications, such as integration with the steam reforming process or intermediate heat exchangers, the helium outlet temperature is targeted to range between 900 and 950°C. Figure 8 provides an overview of the basic design of such a modular unit when coupled with a steam generator. The reactor core and steam generator are housed in separate steel vessels, connected by a linking vessel containing a coaxial hot gas duct. The core comprises 360,000 fuel elements containing UO_2 in TRISO-coated particle form, housed within a 3-meter diameter core standing 9.43 meters tall. This design deviates from traditional reactor designs with a near 1 H/D ratio, optimized for neutron balance. The chosen H/D ratio facilitates heat dissipation in the event of a loss of coolant accident, limiting maximum fuel temperature to below 1600°C. Additionally, all shut-down elements are operated within the side reflector, further constraining the core diameter to 3 meters. The core's average power density is set at 3 MW/m^3 given these conditions. Helium cooling gas flows from top to bottom, heating up from 250°C to 700°C for steam generation. The hot gas is directed to a chamber below the core and then to the steam generator, featuring a helical tube bundle. Feedwater enters at the bottom, with steam exiting via samplers at the top. Walls of the primary circuit are cooled by a flow of cold gas at 250°C, maintaining a small pressure difference between the hot and cold gas sides in the hot gas duct.

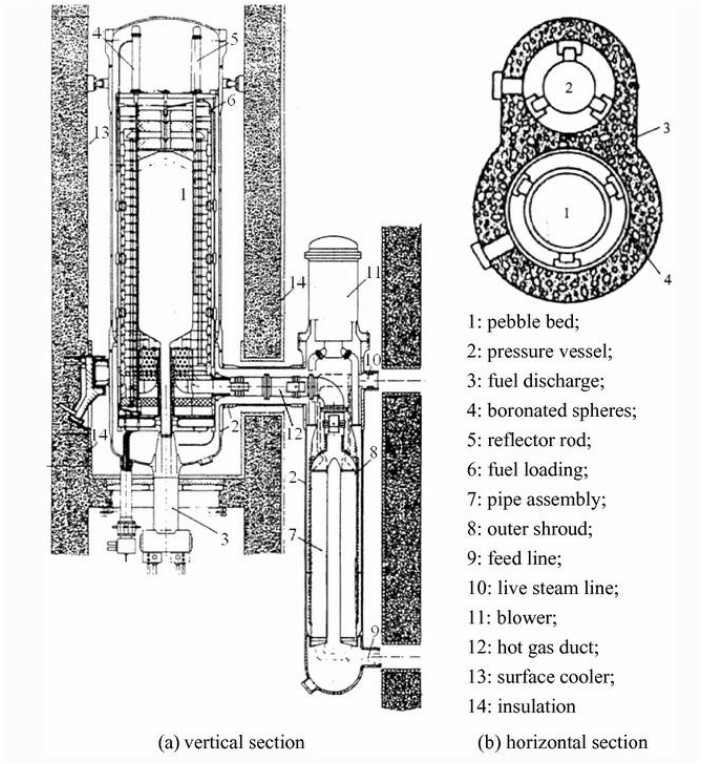

Figure 8 Arrangement of the primary components of the HTGR-Module[42]

2) Japan

HTGRs have emerged as a significant avenue in the pursuit of advanced nuclear energy technologies, promising enhanced safety features, improved efficiency, and diverse applications. Within this landscape, Japan has played a pivotal role, leveraging its scientific expertise and technological prowess to pioneer innovations in HTGR development.

Japan's engagement with HTGRs dates back to the mid-20th century, propelled by a burgeoning interest in harnessing nuclear energy for peaceful purposes. Early research initiatives laid the groundwork for subsequent advancements, as Japanese scientists and engineers sought to explore novel reactor concepts capable of operating at elevated temperatures while ensuring robust safety standards.

The establishment of experimental facilities, such as the Japan Atomic Energy Agency's (JAEA) Oarai Research and Development Center, provided a fertile ground for HTGR research and development. These facilities served as crucibles for innovation, facilitating the design, construction, and testing of prototype reactors aimed at demonstrating the feasibility and viability of HTGR technology.

A landmark achievement in Japan's HTGR journey came with the commissioning of the Fugen Experimental Reactor (FER) in Tsuruga, Fukui Prefecture. FER, inaugurated in 1979, represented Japan's maiden venture into commercial-scale HTGR deployment. With its utilization of helium as a coolant and graphite as a moderator, FER showcased pioneering advancements in reactor design and operational capabilities. The operational legacy of FER, spanning several decades, yielded invaluable insights into high-temperature operation, fuel performance, and safety protocols, shaping Japan's HTGR program for years to come.

Building upon the success of FER, Japan embarked on the construction of the High-Temperature Test Reactor (HTTR) at the Oarai Research and Development Center. The HTTR project(Figure 9)

, inaugurated in 1998, aimed to further advance HTGR technology, serving as a testbed for research initiatives and experimental campaigns. HTTR's achievements, including its demonstration of high-temperature capabilities and safety validation, underscored Japan's commitment to fostering innovation and excellence in nuclear energy research.

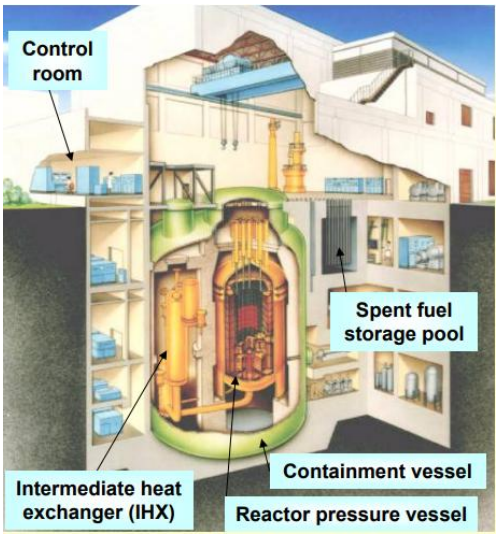

Figure 9 Graphite-moderated/helium gas-cooled HTGR [9]

In parallel, Japan has actively pursued next-generation HTGR projects, such as the Advanced High-Temperature Reactor (AHTGR) and Very-High-Temperature Reactor (VHTGR) initiatives. These projects exemplify Japan's forward-thinking approach to nuclear energy, seeking to enhance reactor performance, expand operational envelopes, and explore novel applications beyond electricity generation.

3) China

China's engagement with high-temperature gas-cooled reactors can be traced back to the latter half of the 20th century when China embarked on ambitious nuclear energy plans to meet the growing demand for electricity. Early research initiatives laid the groundwork for the development of high-temperature gas-cooled reactors, driven by the exploration of alternative reactor concepts with inherent safety features and high-temperature operation capabilities.

The establishment of research institutions and experimental facilities provided a conducive environment for the study and innovation of high-temperature gas-cooled reactors. Institutions such as the China Institute of Atomic Energy (CIAE) and the Institute of Nuclear and New Energy Technology at Tsinghua University (INET) became focal points for scientific exploration, fostering collaboration among academia, industry, and government agencies.

The research and development of high-temperature gas-cooled reactor technology in China began in the late 1970s, primarily led by the Institute of Nuclear and New Energy Technology at Tsinghua University. The R&D process can be broadly divided into three phases:

The first phase, spanning from 1974 to 1990, was the early exploration stage. The main progress during this period included the inclusion of key projects in the field of nuclear energy in the national high-tech research and development program and the initiation of research on critical technologies.

The second phase, from 1990 to 2003, focused on the construction of experimental reactors. This period saw the construction of the 10 MW high-temperature gas-cooled experimental reactor, HTR-10, at Tsinghua University.

The third phase, from 2003 to 2020, saw significant advancements. Supported by the national high-tech research and development program, operational and safety tests were conducted on the 10 MW high-temperature gas-cooled experimental reactor. Additionally, with support from the national nuclear energy development program, preliminary and key technology research was conducted for industrial demonstration power plants. Under the auspices of the national "2006-2020" major science and technology projects, the demonstration project for the Shidao Bay 200,000-kilowatt-level nuclear power plant (HTR-PM) was constructed.

In 1988, an agreement was signed between industrial sectors and research centers in Germany and China, aiming to design and construct a small modular pebble-bed reactor, with the core and steam generator arranged side by side, resembling the concept of high-temperature gas-cooled reactor modules. Collaboration between INET and SIEMENS/INTERATOM ultimately led to the conceptual design of the HTR-10 [11]. The Chinese government approved the construction of this experimental reactor near Beijing in 1992. The HTR-10 achieved initial criticality in 2000 and attained full operational status in 2003. Extensive testing was conducted simultaneously to demonstrate various safety aspects of high-temperature gas-cooled reactors.

The construction and operation of China's first prototype high-temperature gas-cooled reactor, the HTR-10(Figure 10 [42]), marked a significant milestone in the country's HTGR development journey. Commencing operation at the China Institute of Atomic Energy (CIAE) in 2000, the HTR-10 served as

a testbed to validate HTGR technology, showcasing its feasibility and operational capabilities. The successful operation of the HTR-10 laid the groundwork for subsequent advancements in HTGR design and engineering.

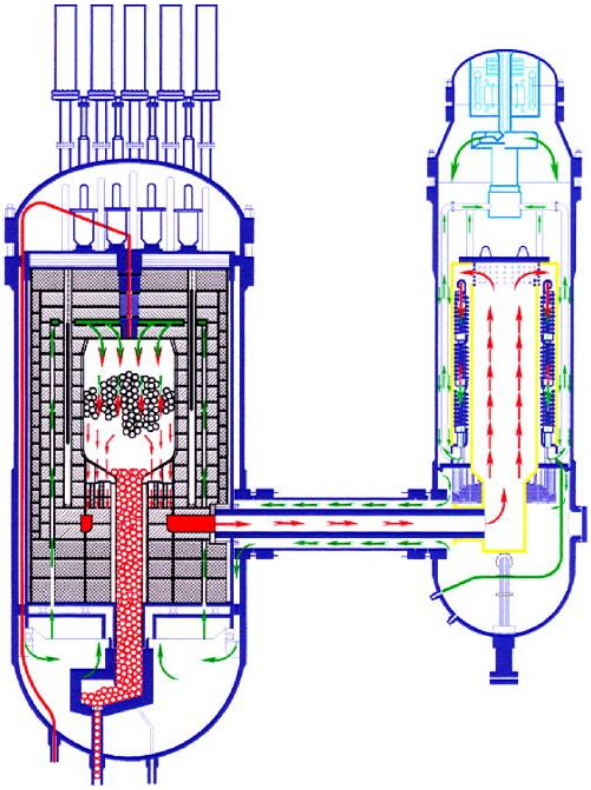

Figure 10 Chinese 10 MW high-temperature gas-cooled test reactor (HTR-10).

Building upon the success of the HTR-10, China embarked on larger-scale high-temperature gas-cooled reactor projects, such as the HTR-PM (High-Temperature Reactor Pebble-Bed Module) demonstration project. Led by Tsinghua University and the China National Nuclear Corporation (CNNC), the HTR-PM adopts a pebble-bed modular reactor design, representing a significant leap forward in high-temperature gas-cooled reactor technology.

The HTR-PM is slated for construction in China, serving as the demonstration plant for the country's advancement in high-temperature reactor technology. The modular system will have a thermal power output of 2 × 250 MWth. The heat generated by the reactor plant will be utilized to produce steam at 566°C/13.25 MPa for driving a steam turbine cycle, resulting in an electrical power output of 212 MW. Seawater will be employed for cooling the power cycle. The modular HTGR will feature a pebble-bed core utilizing a Low Enriched Uranium (LEU) fuel cycle and TRISO-coated particles.

Meanwhile, China actively sought international cooperation and partnerships to accelerate the development of high-temperature gas-cooled reactors. Collaboration with countries such as the United States, South Africa, and South Korea facilitated knowledge exchange, joint research, and technology transfer, enriching China's HTGR projects with diverse perspectives and expertise.

As China continues to address the complexities of energy transition and sustainable development, high-temperature gas-cooled reactors remain a cornerstone of its clean, reliable, and safe energy future

strategic vision. The development journey of China's high-temperature gas-cooled reactors is characterized by perseverance, innovation, and collaboration, underscoring China's leadership in nuclear energy innovation and its commitment to addressing global energy challenges.

1.3. HTGR codes

The importance of developing reactor simulation and simulation system code in the field of nuclear energy cannot be overstated. These codes play a crucial role in the development and application of nuclear energy.

Reactor simulation and simulation codes assist engineers and researchers in conducting comprehensive evaluations and analyses of reactor operation. By simulating various operating conditions, accident scenarios, and emergency measures, these codes can assess the safety performance of reactors under different circumstances, providing vital insights for design and operation. They are also essential for optimizing reactor design. Through simulating different design schemes, material choices, and process parameters, engineers can evaluate their impact on reactor performance, efficiency, and costs, guiding rational design decisions.

In the event of reactor malfunction or abnormal conditions, simulating fault processes, evaluating system responses, and predicting impacts can effectively reduce accident risks, ensuring personnel and environmental safety. Furthermore, these codes serve as important tools and resources for training and education. By simulating reactor operations and accident scenarios, they help operators and maintenance personnel familiarize themselves with the principles of reactor systems, operating procedures, and safety regulations, enhancing their ability to respond to emergencies. Lastly, simulation and simulation codes provide robust support for reactor technology research and development. Researchers can utilize simulation results and data to conduct various scientific experiments, engineering tests, and theoretical analyses, exploring new reactor designs, material applications, and operational strategies, thus driving innovation and progress in nuclear energy technology.

In the simulation of high-temperature gas-cooled reactors, it is necessary to involve multiple aspects of system codes to comprehensively simulate and analyze various characteristics and behaviors of the reactor. These mainly include the following aspects:

Neutron transport code: This code is used to simulate processes such as neutron generation, transport, absorption, and scattering, as well as neutron flow and reactions within the reactor. Therefore, the accuracy and reliability of neutron transport codes are crucial for the safety and performance of the reactor.

Thermal-hydraulic code: This code is used to simulate thermal processes such as temperature distribution, heat conduction, convective heat transfer, and fluid flow within the reactor. It plays an important role in the safety and stability of the reactor.

Radiation transport code: This code is employed to simulate processes such as radiation transport, absorption, and scattering of neutrons and photons within the reactor, as well as the distribution of radiation fields in the surrounding environment. It has significant implications for the safety of the reactor environment and personnel.

Material behavior code: This code is used to simulate behaviors such as expansion, deformation, fission product release, oxidation, and corrosion of materials within the reactor. It addresses the mechanical, thermodynamic, and chemical properties and evolution processes of materials within the reactor, which significantly impact the structural integrity and lifespan of the reactor.

Kinetics code: This code is utilized to simulate reactive changes, power response, and control measures under steady-state and transient conditions within the reactor. It addresses the dynamic processes of reactor reactivity and power changes, which are crucial for the stability and control of the reactor.

In summary, the simulation of reactors requires the involvement of multiple aspects of system codes to comprehensively simulate and analyze various characteristics and behaviors of the reactor. The accuracy and reliability of these system codes are essential for ensuring the safety, efficiency, and stability of the reactor.

1.3.1. VSOP

VSOP is a system code designed for high-temperature gas-cooled reactor physics calculations and fuel cycle by the Institute of Energy and Climate Research (IEK-6) at the Juelich Research Center [12]. The high-temperature gas-cooled reactor research at IEK-6 initially concentrated on the development of pebble-bed reactor designs. Currently, the primary focus is on evaluating and enhancing the safety characteristics of these reactors under both normal operating conditions and accident scenarios. To support this objective, a range of computer codes have been developed, validated, and optimized to simulate various safety and operational aspects of high-temperature gas-cooled reactors. These codes are extensively used and have played a key role in recent licensing processes, including those for China's HTR-PM project. The code infrastructure currently in use is shown in Figure 11[39].

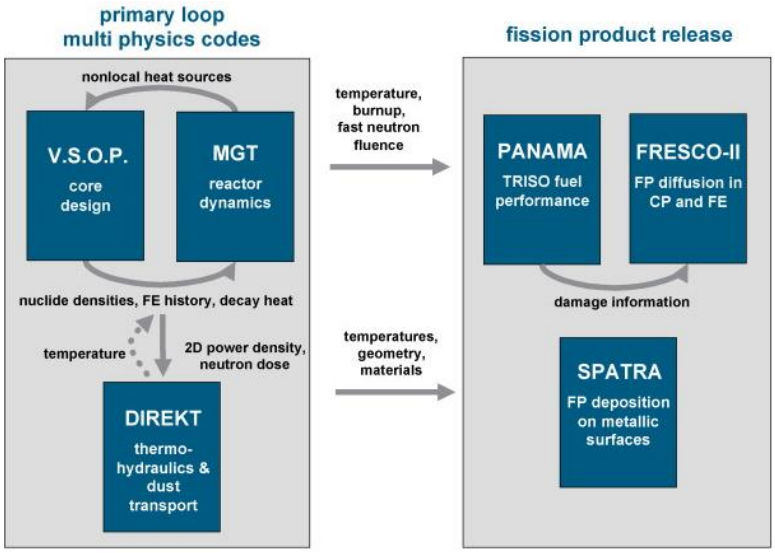

Figure 11 Overview of the HTR code infrastructure presently being used

VSOP is an extensive suite of integrated codes for neutronics and thermo-fluid dynamics, incorporating features such as control rod modeling, fuel shuffling, fuel cost analysis, and specialized extensions for specific calculations. Its primary focus is on simulating both steady-state and transient operating conditions. The code is limited to 30 neutron energy groups and operates with 2D geometries. The thermo-fluid dynamics module within VSOP is known as THERMIX, with the coupling between the two established in 1985. Multiple versions of the code are in different stages of development, making it difficult to identify a single definitive version.

The code is derived from the MAFIA-II code developed by L. Massimo [21]. Similar to its predecessor, the system is structured into seven distinct chain links, with the sequence of their loading determined

by the code. While retaining the overall framework, all subroutines of VSOP have been either completely rewritten or replaced. Originally developed for use with all types of thermal reactors, VSOP has undergone substantial upgrades and extensions to support simulations specifically for HTGRs.

1.3.2. TINTE/MGT/MGT-3D/

TINTE/MGT serves as the predecessors to MGT-3D[12-15], a multi-energy group 3D reactor dynamics code specifically designed for high-temperature reactors. The primary objective of the code is to offer dependable simulations spanning from reactor equilibrium scenarios to all safety-critical short, medium, and long transients. Originally developed as TINTE, the code underwent substantial enhancements to meet the demand for more precise steady-state calculations and the simulation of a broad spectrum of transients. The most crucial data originated from the pebble bed test reactor AVR1, which provided insights into coupled neutronics–thermal-hydraulics[15]. Additionally, the SANA experiment contributed temperature and natural convection data[16], while the VELUNA experiment provided information on coupled forced flow, temperatures, and corrosion[17]. Subsequently, TINTE has been extensively employed in numerous HTGRs projects globally.

The demand for heightened numerical accuracy raises the question of the precision offered by the two-group approximation in comparison to a multi-group model. In response to this inquiry, a multi-group derivative of TINTE, referred to as MGT (multi-group TINTE), has been developed. In MGT (Multi-Group Transport), rather than solving the diffusion equations analytically for each mesh and two neutron energy groups, a broader approach utilizing up to 43 energy groups can be employed. This results in a banded matrix that necessitates numerical solution methods. Additionally, inline spectrum calculations for cross-section calculations can be executed for every time step and location within the reactor.

MGT-3D represents the evolution of its predecessor, MGT, boasting a range of enhancements that significantly elevate its capabilities. Among these improvements are the extension to 3D calculations in cylindrical coordinates and pseudo XYZ, allowing for a more comprehensive analysis of complex systems. Furthermore, the introduction of a new solution for the time-dependent momentum conservation equation enhances accuracy and fidelity in simulations. Additionally, the incorporation of a new radiative heat transfer equation further refines the model's predictive power. Notably, advancements in heat conduction equations within the mesh grid and pebble have been made, alongside the integration of new materials for calculating convective heat transfer between meshes. The inclusion of features such as block-fuel heterogeneous temperature calculation and explicit fuel kernel temperature calculation demonstrates a commitment to addressing nuanced aspects of thermal dynamics. Moreover, optimizations, such as minimized limits for thermo-fluid dynamic calculation time steps, ensure efficiency without compromising precision. With increased capacity for major mesh grids and components, as well as improvements in 1D network calculation, MGT-3D emerges as a comprehensive and sophisticated tool for thermal analysis in diverse applications.

As a complement to special conditions, such as those associated with HTGR rapid depressurization accidents, specific issues have been addressed using the DIREKT code[21]. Subsequently, the determination of power and temperature histories, along with relevant burnup and isotopic compositions, can be utilized for operating fission product release and fuel performance codes, such as FRESCO-II [18]and PANAMA [19]. These codes extract computed temperatures from VSOP and MGT to ascertain release rates of important isotopes. SPATRA[20] is capable of simulating the transport and location of fission products on metal surfaces.

1.3.3. HTR Code Package(HCP)

In order to document and preserve decades of expertise gained in the field of HTGR safety research, in 2010, the individual programs developed at RWTH Aachen University and Forschungszentrum Jülich were integrated into a unified code package, employing state-of-the-art programming techniques and standards[22]. For specific HTGR-related issues, new modeling approaches were employed, utilizing more advanced programming techniques. HCP integrates relevant and recently applied physical models in a highly integrated manner. This allows for the simulation of both steady-state and transient operating conditions of complete 3D reactor models, including physical aspects such as fission product release calculations for each core region or simulations of dust generation and transport, enabling more in-depth safety analyses.

In order to consolidate and preserve the wealth of expertise accumulated over decades in the field of safety research for high-temperature gas-cooled reactors, individual programs developed by Aachen University and the Juelich Research Center began to be integrated into a unified code package in 2010, employing state-of-the-art programming techniques and standard [22]. For certain HTGR-specific issues, new modeling approaches were utilized, employing more advanced programming techniques. HCP (High-Temperature Code Package) couples relevant and recently applied physics models in a highly integrated manner. This allows for the simulation of steady-state and transient operating conditions of complete 3D reactor models, including physics aspects such as fission product release calculations for each core region or simulations of dust generation and transport, thus enabling deeper safety analyses.

The backbone software of HCP, written in C++, manages all input/output operations, data handling, and overall program control. Several specialized modules are integrated into this framework, each addressing distinct physical aspects of the high-temperature gas-cooled reactor core and its main circuit. The neutron kinetics module (MGT-N) and the fluid dynamics module (MGT-FD) originate from the MGT-3D code, which was refactored and partially rewritten in Fortran 90 to create standalone MGT-N and MGT-FD modules. Spectrum calculations are handled by the TRISHA module. The burnup calculation (TNT) and fuel management (SHUFLE) algorithms are adapted from the VSOP code system, with significant enhancements and a complete rewrite in C++. While the VSOP code system itself is not directly integrated into HCP, it serves as a reference for validation purposes. The STACY module supersedes and improves upon the earlier FRESCO-II, FRESCO-I, and PANAMA codes, focusing on simulating fuel performance and modeling the release and transport of fission products within the reactor core. The STAR module is designed to address the deposition and resuspension of carbon dust.

Based on the aforementioned description, the current prototype of HCP includes modules such as MGT-FD, MGT-N, TRISHA, TNT, SHUFFLE, etc. In some published thesiss, initial validation has been conducted using simple models and past experimental data, including comparisons with international codes such as SERPENT.

The initial version of HCP has successfully replicated many functionalities of currently available standalone computational programs, allowing for a more accurate description of key issues in the reactor core. While the program is primarily used for simulating pebble-bed reactors, developers have also focused on developing new program sections that are independent of reactor type. For instance, the combustion module TNT is essentially applicable to pressurized water reactors, reactors used for medical radioisotope production, or nuclear material conversion facilities.

In terms of software, HCP is based on the C++ and Fortran 90 programming languages and adopts flexible and user-friendly input structures such as XML and advanced software libraries. HCP can be

used to simulate small-scale models, such as the irradiation of individual fuel components, as well as complex reactor cores. In the latter case, preferred core conditions during normal operation can be simulated. To do so, we conduct coupled simulations of fluid dynamics, neutron kinetics, and fuel management. This equilibrium core serves as the starting point for actual reactor operation, including dynamic behavior and accident scenarios.

Since the previously independent neutron kinetics and fluid dynamics calculation modules (MGT-3D) have been integrated into HCP, apart from transients caused by control rod procedures, HCP can also replicate other transient conditions. Its main advantage lies in its ability to determine the initial state at the onset of a transient. In other aspects such as the behavior of fission products and graphite dust, HCP can utilize additional modules for research (currently only using standalone STACY and STAR computer programs).

The central part is the so-called "backbone" (see Figure 12). This section combines higher-level tasks that were previously implemented separately in individual schemes. These include, for example, input and output, data management, and scheme flow control. Various calculation modules for reactor core or primary circuit physics are coupled with this central module. Both the neutron kinetics (MGT-N) and fluid dynamics (MGT-FD) modules are based on MGT-3D. The TRISHA spectrum module replaces the spectrum modules of MGT-3D and VSOP. SHUFLE takes over fuel management. STACY combines tasks covering the performance range of obsolete schemes such as FRESO-II, PANAMA, and FRESCO-I, covering tasks in the area of fission product release and fuel behavior. Dust behavior has only been addressed since the implementation of STAR in the TARGET project. The functionality description of HCP modules is as follows. As mentioned earlier, in some aspects of HCP simulation, existing computational programs were not integrated; instead, new computational modules were developed. These modules comprehensively incorporate existing knowledge and models and also address new issues.

1.4. MOTIVATION

As mentioned earlier, as a fourth-generation high-temperature gas-cooled reactor, modular high-temperature gas-cooled reactors have many advantages, including high inherent safety and good economy. The development of HTGRs is of great significance for promoting the development of the nuclear energy industry, improving energy utilization efficiency, strengthening energy security, and protecting the ecological environment.

In reactor dynamic analysis, consideration of multiple time scales, both short-term and long-term, is crucial. These time scales range from instantaneous reactions on the order of microseconds to hours, days, or even years of long-term operation. For short-term time scales, in the range of microseconds to milliseconds, nuclear reactions and energy release in the reactor are very rapid. This is critical for fast neutron physics and transient response. For instance, during sudden events such as abrupt load changes or accidents, dynamic analysis at this time scale can help predict and control the reactor's instantaneous behavior. For mid-term time scales, ranging from seconds to minutes, the response of control systems, changes in fuel rod temperatures, and performance of cooling systems become important. Maintaining the stability and performance of the reactor is upheld and optimized at this time scale during routine operation. For long-term time scales, spanning from hours to years, factors such as fuel depletion, fuel rod decay, system degradation, and equipment maintenance come into play. For the long-term operation and life management of reactors, these factors need to be considered to ensure the safe, stable, and economical operation of the reactor.

Considering these different time scales simultaneously in dynamic analysis can better predict and control various issues and challenges that may arise at different time scales, thus ensuring the safety of reactor operation. Additionally, optimizing the performance of the reactor based on the requirements and changes at different time scales can enhance its efficiency and reliability. Moreover, it enables better management of the reactor's lifespan, extending its operational life and minimizing the impact of equipment wear and degradation. Therefore, dynamic analysis of HTGRs across long- and short-term-time scales is crucial for ensuring the safety, stability, and economical operation of the reactor.

A variety of individual computer codes have been developed, validated, and optimized to simulate different aspects of HTGRs, facilitating the mentioned safety analyses. For example, MGT is more suitable for observing the dynamic behavior of HTGRs on shorter time scales, such as changes in power, forced flow, and natural convection heat transfer. Conversely, VSOP has advantages in simulating the long-term core design, fuel cycle, and reactor operation of HTGRs. This includes handling fission product release and fuel performance, previously addressed by FRESO-II, PANAMA, and FRESCO-I, as mentioned earlier. The calculation of power history with correlated burnup and isotope compositions can be utilized to run decay heat calculation codes such as NAKURE [23].

Undoubtedly, for the same HTGR model, there will inevitably be corresponding errors in analyzing its long-term and short-term dynamics if different software models are used due to the different emphases of each software model. HCP addresses this issue effectively by employing advanced programming techniques and standards. It allows for the study of various aspects of HTGR core safety and the analysis of its long-term and short-term dynamic response characteristics through a single reactor model input.

The new HCP will overcome the limitations and drawbacks in terms of functionality and flexibility caused by the heterogeneous infrastructure of computer codes, and the development of the HCP has the potential to make significant contributions to the safety assessment of high-temperature gas-cooled reactors, especially pebble-bed reactors. Moreover, through an integrated design approach, it can also reduce the complexity of HTGR reactor design. Unfortunately, due to some reasons, FJZ and RWTH stopped further development of HCP after 2014 [10].

In prior work, The HCP project led by RWTH and FJZ have been roughly completed, including the majority of the modules linking and functional validation of the HTR code package. However, in the brief and hurried knowledge transfer process, a significant number of files, including some test and validation cases, and other related documents, were lost, and the early developers had not drafted the complete programmer and user manuals. In addition, in spite of remarkable achievement accomplished, there are still some open issues to be fixed out. For example, the control rod system is not implemented yet which limits the performance and flexibility of safety analysis, and the STACY and STAR modules are not fully coupled with HCP. Meanwhile, there are some logic issues and inefficiencies within the source code, especially in the backbone, leading to memory leakage in certain scenarios. Moreover, there is considerable space for the optimization of the program structure, various components, and their interfaces. In summary, further development and optimization of the current HCP are needed to better simulate the long-term and short-term dynamics of HTGRs, particularly concerning the development and validation of control rod systems.

Therefore, the work presented in this thesis mainly consists of three parts:

The first part involves the extension of the HCP code, primarily focusing on the development and validation of HTGR control rod systems. In HTGRs, the control rods and shutdown elements are located in the side reflector. These serve to regulate power and shut down the facility (reactivity control). For a precise description of power distribution within the core (e.g., equilibrium core) during normal

operation, as well as to describe core behavior during transients, control rods and KLAK (Small Ball Shutdown System) must be accurately modeled in neutron calculations. In the current HCP version, control rods and their movement can't be represented successfully. A "Flexible Curtain" control rod method is proposed by the article. In this approach, control rods are simulated by adding a strong neutron absorber, typically B-10, in the control rod regions. Control rods will be modeled using movable batch modeling from the fuel management module, allowing for free insertion and withdrawal of control rods during the simulation of the HTGRs. Finally, the establishment of the HTR-50 model, validated through comparison with the international code SERPENT, confirmed the effectiveness and accuracy of this functionality. This achievement enables HCP to simulate control rod behavior, thus laying the foundation for the long-term and short-term dynamic analysis of HTGRs.

The second part involves the establishment of fluid dynamics, core, and heat exchange models for the HTR-PM based on HCP, as well as short-term dynamic simulation of the core. Firstly, the neutron model of the HTR-PM was established based on HCP's MGT-N, dividing the core region into twenty axis meshes and forty radial meshes for simulation purposes. To facilitate comparison with Serpent, the core's filling factor was set to 0.6046. In this short-term scale benchmark test, the entire core was loaded with fresh fuel elements. The fuel and moderator temperatures were fixed at 900K, and the results were compared with SERPENT. Furthermore, a fluid dynamics model for the HTR-PM was established based on HCP's MGT-FD, coupled with the neutron model for calculation. Various short-term behaviors of the HTGR, such as control rod movement，and inlet temperature variations, were analyzed and simulated, validating the design safety of the HTGR.

The third part involves the simulation of multi-scenario fuel management, cycles, and long-term reactor operation for the HTR-PM based on HCP, followed by the evaluation of different scenarios. Firstly, descriptions of the SHUFFLE and TNT modules in HCP were provided. Then, two fuel management models for the HTR-PM, based on Seepage and Flowtube under SHUFFLE, were analyzed. Comparisons were made between the two refueling methods using the TNT burn-up program. Furthermore, simulations and analyses of the OTTO (once through then out) and multi-pass refueling scenarios for the HTR-PM were conducted, along with corresponding evaluations. Finally, by integrating long and short-term time scales using HCP, transient simulations and analyses of HTGRs under different lifetimes and fuel loading scenarios were performed.

2. Progress on development of HCP

HCP is one system code for HTGRs, serving as a crucial tool for analyzing the dynamic characteristics of HTGRs at multiple time scales. As mentioned earlier, HCP integrates various legacy codes that analyze different aspects of HTGRs using advanced programming techniques and concepts. It enables high-fidelity simulation of the full 3D core of HTGRs and comprehensive analysis of various core behaviors. However, in the past, the development of HCP was abruptly halted for various reasons, leading to the loss of some functionalities, a lack of systematic documentation for related code, and the absence of user and programmer manuals. Undoubtedly, this has caused significant inconvenience for users. Additionally, one of the core functionalities of HCP, the control rod system, remains undeveloped. This undoubtedly limits HCP's ability to perform safety analyses for HTGRs and to comprehensively analyze the short- and long-term dynamic characteristics of HTGRs.

In summary, the arrangement of this section is as follows: In the first part, this thesis will provide a detailed introduction to HCP, including its architecture, innovations compared to legacy codes, simulation capabilities, existing deficiencies, and comparisons with other codes. In the second part, this thesis will propose a control rod modeling approach based on changes in nuclide concentration called "Flexible curtain", and complete the development of relevant functionalities within HCP. This approach will utilize the nuclide proportions in mesh nodes within the MGT-N and MGT-FD modules, while incorporating the movable characteristics of nodes in the shuffle module. In the third part, the effectiveness of this method will be validated through steady-state and transient analyses of an HTR-50 model based on SERPENT and ATHLET.

2.1. Description of the HCP

HCP constitutes an integrated system of codes devised for the analysis of HTGRs. Serving as the foundational framework, HCP orchestrates the coordination of spatial coordinates while facilitating the uniform input, libraries, and output across different codes within the system. Each code within this ensemble is dedicated to modeling specific physical phenomena inherent to HTGRs. These codes, collectively termed HCP modules, empower the comprehensive simulation of HTGR operation and the simulation of critical safety-related accident scenarios.

As mentioned earlier, HCP currently consists of seven sub-modules: MGT-FD, MGT-N, TRISHA, TNT, SHUFFLE, STACY, and STAR. All modules are controlled through the main backbone. The backbone program executes all I/O operations, data flow, and controls the main program, as shown in Figure 12.

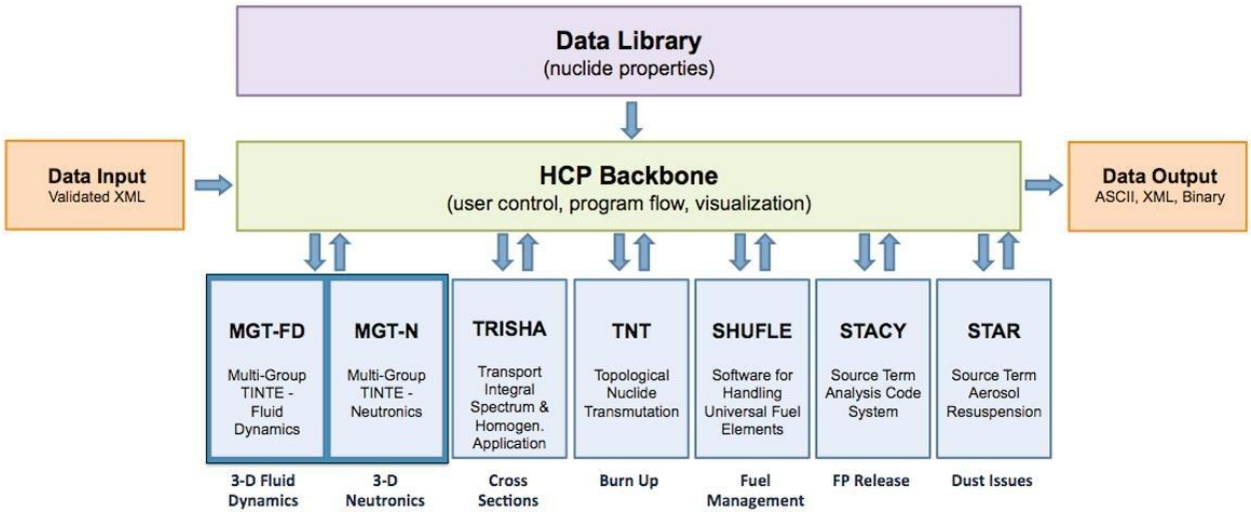

Figure 12 Structure of HTR code package [10]

2.1.1. Backbone

Integrating all modules into a unified code package requires managing an extensive volume of data previously scattered across multiple legacy systems. As the legacy data processing methods have reached their limitations, HCP adopts a modern data model built with C++ and its libraries to handle module data using an object-oriented approach. Physical entities are encapsulated as data objects, each with defined attributes and functionalities. The data model differentiates between two main categories of data classes. The first category includes classes that represent fundamental physical quantities, such as energy and temperature, at a basic level. On top of these foundational classes, more advanced reactor-specific classes are constructed to model higher-level data objects. Development of these advanced classes is ongoing, with input and output value classes being incrementally implemented. Concurrent testing ensures compatibility and the ability to replicate results from previous versions accurately. In the end, all modules will utilize the same set of input data, allowing for seamless data sharing across different code modules. This reduces the workload required for performing accident scenario analyses. Furthermore, this solution is less prone to errors since consistent input datasets are used to evaluate different physical aspects. In previous codes, different aspects were handled by multiple independent codes, requiring separate input files to be created for each. Adaptation of one aspect might necessitate adaptation of other aspects.

The HCP Backbone is implemented in C++, a versatile language capable of interfacing with codes written in the same language or accommodating functions and subroutines written in FORTRAN. Through the backbone, modules (or coupled codes) are seamlessly connected, enabling their coordination via a common algorithm within the backbone. This automation streamlines the simulation process. Within HCP, the data model is realized using an object-oriented approach. This model establishes a unified data structure, replacing the disparate data models and input structures of individual codes in their standalone versions. By serving as the platform for data exchange between code modules, the data model mitigates potential errors arising from manual data transfer. Moreover, the data model is conceptually designed, unrestricted by the previous input formats of legacy codes or the sequential requirements of modules. Consequently, it provides a standardized data platform for coupling codes in HTGR simulation, regardless of their original input formats. Furthermore, extensive

refactoring work has been undertaken to enhance the data and memory usage of codes integrated within HCP, adhering to high-quality standards. This technical effort holds significant value, particularly in ensuring precision, repeatability, and reproducibility across different operating systems and hardware configurations.

In the computational workflow of HCP (Figure 13), the process begins with HCP Control, which is responsible for initiating and concluding calculations, as well as coordinating steady-state and transient computations conducted by the MGT-N and MGT-FD modules. Subsequently, the HCP Backbone evaluates the necessity of the neutronics calculation module (MGT-N), with considerations such as pure thermo-fluid dynamics calculations leading to the exclusion of MGT-N. If HCP Control detects excessive variations in nuclear power production from neutronics calculations, it may adjust time steps to mitigate changes. The subsequent step involves dual evaluations within the backbone: firstly, determining the usage of the MGT-FD module, and secondly, assessing whether thermo-fluid dynamics calculations are warranted based on nuclear power production changes. Following these evaluations, HCP Control manages transient calculations or revisits step 2 for un-converged steady-state calculations, treating them as transient upon convergence. Finally, upon completion, HCP Control oversees data retrieval from the FORTRAN side, storing it in the data model and output.

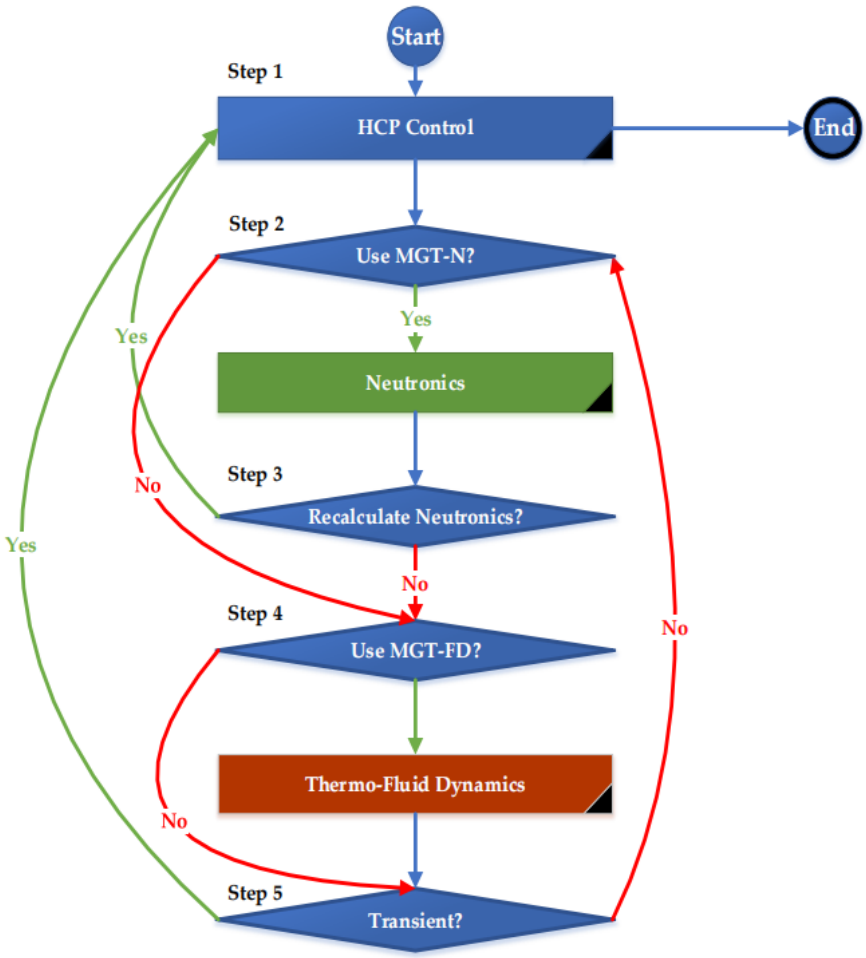

Figure 13 Workflow of Backbone [58]

2.1.2. Data library and Input/output

One of the most significant features of HCP is breaking down barriers between multiple sub-modules, achieving standardization of input languages, and enabling data sharing across different modules. Each input consists of four different files: Model.xml, DataSet.xml, Scenario.xml, and LibGen.xml, as depicted in Figure 14.

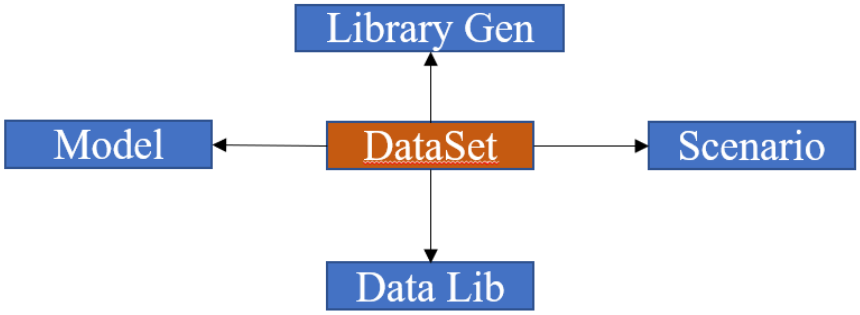

Figure 14 I/O structure of HCP

To standardize the input and output formats of different modules, HCP adopts a brand-new data file format based on XML (Extensible Markup Language) and binary. Such an approach facilitates the creation of elaborate input structures that align with the hierarchical nature of the object-oriented data model. XML validation schemes serve to ensure the coherence, accuracy, and entirety of the input data even prior to the initiation of the simulation. The elevated readability afforded by XML structures expedites and fortifies the modeling process, potentially mitigating maintenance overheads.

DataSet.xml serves as a linking file for different Model.xml and Scenario.xml files. The "DataSet.xml" file serves as the sole input provided by the user to the HCP executable file. Should the user fail to supply an argument, HCP prompts for this file immediately upon program initiation. This XML file is designed to encapsulate the simulation scenario by establishing links to other XML input files, while also encompassing a detailed case description and author information. Such an approach serves to mitigate the confusion arising from a disparate mix of input and output files, ensuring clarity regarding the specific combination of files utilized for executing the simulation.

In addition to DataSet.xml, another essential file is required to delineate the reactor's geometry, material composition, or pebble flow characteristics. This file is denoted as Model.xml. Within Model.xml, crucial details such as fuel element definitions and the arrangement and interplay of various fuel assemblies like cores and fuel casks are encapsulated. The content and size of the input model may vary substantially depending on the anticipated module, reflecting the diverse requirements and intricacies of each simulation aspect. As shown in the Figure 15, it is a structural presentation of some of the properties of the UO_2 material in a fuel sphere defining a typical spherical bed in Model.xml, where the density of the UO_2 layer is 10.4 g/cm3, the enrichment of U-235 is 8.3%, and the heat capacity and thermal conductivity of the material are also given.

```
<Material id="UO2">
  <Compound label="UO2">
    <Property type="Element" proportion="1"> U </Property>
    <Property type="Element" proportion="2"> O </Property>
  </Compound>
  <Properties type="Common">
    <Property type="Density" unit="g/cm^3"> 10.4 </Property>
    <Property type="Enrichment" nuclide="U-235" base="U" unit="w%"> 8.3 </Property>
    <!--in case no base, it refers to whole material -->
    <Property type="Impurity" element="B" base="U" unit="ppm"> 24.953 </Property>

    <Property type="HeatCapacity" kind="value" unit="Ws/cm3K" factor="1.0"> 3.526041 </Property>
    <Property type="HeatConductivity" kind="value" unit="W/cmK" factor="1.0"> 0.03163283 </Property>
  </Properties>
</Material>
```

Figure 15 Input scheme for fuel material in Model.xml

One another category of input data delineates the settings and temporal control parameters for a simulation case, cataloged within the file Scenario.xml. Each module execution is facilitated by a predefined set of default settings, delineating program parameters. Furthermore, a TimeLine element, comprising a sequence of Action elements, orchestrates the program flow and determines the order of module invocations.

A significant achievement in the HCP project involved the adoption of a unified nuclear data library across all physics code modules. This milestone was realized through a meticulous process: initially, the point-wise ENDF/B-VII data undergoes preprocessing using NJOY2012, as outlined by Kahler[24]. Subsequently, a specialized code, termed LibGen, is employed to construct the nuclear data library. LibGen facilitates the extraction and integration of data from the ENDF-6 data files generated by NJOY into the HCP data model. This sophisticated procedure necessitated the development of a dedicated code capable of populating nuclide data objects sourced from ENDF-6 raw files(Figure 16 [60]).

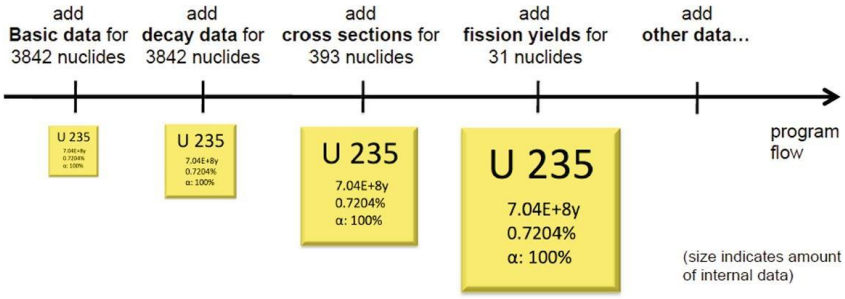

Figure 16 The process of generating a nuclear data library

A particular focus was directed towards accurately addressing the double heterogeneous nature of HTGR fuel. This entailed employing the Nordheim Numerical Method [26] within the NJOY calculation framework to handle resonance treatment. Consequently, a two-dimensional user-defined table, contingent upon fuel temperature and background cross sections, is generated, enabling interpolation for actual values during simulations. This process involves the generation of a comprehensive set of data, comprising 5 temperatures and 20 background cross sections as per the MUPO scheme utilized in previous iterations of the codes. To condense point-wise cross sections into fine-group cross sections via NJOY, a predefined HTGR weighting spectrum or a spectrum tailored to specific design criteria from another code must be applied, building upon the existing 43 energy group MUPO structure[25].

The HCP data library encompasses fundamental nuclide properties such as decay characteristics, reaction pathways, microscopic cross sections, as well as spontaneous and independent fission yields, accounting for up to three incident neutron energies or scattering matrices pertinent to graphite and H2O.

For each execution of an HCP module, a data library is requisite. Typically, this data is furnished through a serialized binary file (denoted by the file suffix ".bin"), previously generated by the HCP Library Generator (HcpLibGen). Alternatively, the data library can be composed in XML format. In this case, two distinct file types are necessary: a primary file (DataLibrary.xml) and a file containing data for each nuclide (Nuclide.xml). The main file encapsulates crucial information such as energy boundaries, temperatures, and a comprehensive nuclide list for the library. Each nuclide's data is specified in an individual file (e.g., U-235.xml). As XML is human-readable, it facilitates inspection of the data library's contents. However, due to the highly automated nature of the data library process, fundamental errors are rare. Consequently, reading the data library in XML format is no longer the default mode. Additionally, the large volume of data stored can impede the efficiency of parsing XML files, rendering binary format more favorable. Therefore, it is recommended to both write and read the data library in binary format.

Through the composition of these four files, the behavior of different reactor types under different transient conditions can be described, while also avoiding redundant modeling. This approach allows for an input structure that aligns with the object-oriented data model hierarchy. Beyond input concepts, new output concepts are also under development. This concept will enable HCP to output data in various formats such as standardized text, XML, and binary files, including options for graphical visualization.

2.1.3. MGT-N and MGT-FD

MGT-N is the neutron module, which is a refactored version based on the MGT-3D code and has been partially rewritten in C++. It is responsible for calculating the spatial neutron flux and the fission power distribution. The code is capable of performing both steady state and transient simulations of a 3-D reactor model modelled in cylinder coordinates.

In the simulation workflow shown in Figure 17, the process unfolds in sequential steps: initially, the fuel and moderator temperatures are extrapolated, either calculated by MGT-FD or set in the input, followed by temperature calculations for kernel layers or fuel and moderator temperatures using distinct methods by MGT-N. Then, a spectrum code computes cross-section using temperatures, leakage, and nuclide inventories, with options to switch between TRISHA and TISPEC for interchangeable 0D calculations. Subsequently, a neutron diffusion calculation generates the neutron flux distribution, alongside normalization, while the calculation of xenon concentration incorporates neutron flux distribution and fission cross-sections, crucial for larger reactors. Precursors of delayed neutrons and k-effective are then computed, initially for equilibrium and later adjusted with a correction factor for transient scenarios. Nuclear power production is derived from the neutron flux distribution, fission cross-sections, and xenon concentration, followed by the calculation of decay heat production and its spatial distribution to conclude the process.

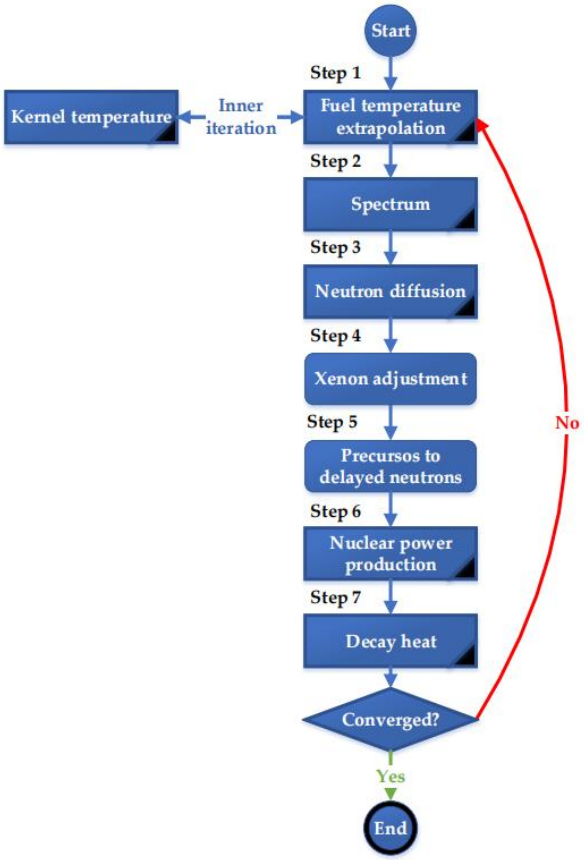

Figure 17 MGT-N workflow [58]

The spectrum codes utilized in HCP comprise TISPEC, integrated within the MGT-N module, and TRISHA. TISPEC, inherited from MGT-3D, is an adaptation of the MUPO code [27], primarily designed to compute and furnish nuclear macroscopic cross-sections to the neutron diffusion code. In contrast, TRISHA, a newly developed spectrum code, offers three distinct solvers: a diffusion code analogous to MUPO, a 0D transport code, and a 1D spherical transport code based on a collision probability method.

When simulating the behavior of a nuclear reactor, an essential task involves determining the neutron flux. This is often achieved through a diffusion approximation, which originates from the neutron transport equation and is applied within MGT-N. The neutron energy spectrum is divided into several discrete energy groups, represented by G. For the g-th energy group, the corresponding integral equation is formulated as shown below.

$$\frac{\partial}{\partial t}\int_{E_g}^{E_{g-1}}\frac{1}{v}\phi(r,E,t)dE-\nabla\cdot\int_{E_g}^{E_{g-1}}[D(r,E,t)\nabla\phi(r,E,t)]dE+\int_{E_g}^{E_{g-1}}\sum\nolimits_t(r,E,t)\phi(r,E,t)dE$$
$$=\int_{E_g}^{E_{g-1}}[\sum_{g'=1}^{G}\int_{E_{g'}}^{E_{g'-1}}\sum\nolimits_S(r,E'\to E,t)\phi(r,E',t)dE']dE+\int_{E_g}^{E_{g-1}}S(r,E,t)dE \quad (1)$$

In the neutron source term $S(r,E,t)$, contributions from various neutron sources are accounted for, including the fission neutron source as well as other sources like $(n,\ 2n)$, $(3,\ 3n)$, $(\gamma,\ n)$ reactions, and any external neutron sources. To solve the three-dimensional neutron diffusion equations in MGT-

3D, an iterative leakage method is employed, facilitating the computation of neutron flux distribution throughout the reactor core [28][29].

The total heat production within the reactor can be partitioned into two primary components: prompt heat E_p and decay heat E_d .

$$E_f = E_p + E_d \tag{2}$$

When considering the various contributions in detail, these two components can be specified as:

$$E_p = E_r + E_n + E_{\gamma p} \tag{3}$$

$$E_d = E_{\gamma d} + E_\beta \tag{4}$$

Where E_r denotes the rebound energy of the fission fragments, and E_n represents the kinetic energy of the prompt neutrons produced by fission. $E_{\gamma p}$, $E_{\gamma d}$ and E_β denote the prompt γ energy ,delayed γ energy and β decay energy respectively.

The prompt power density in the reactor is determined by the product of the fission rate and the prompt energy released per fission:

$$\dot{Q}_p''' = \sum_{i=1}^{G} \sum_f^i \phi_i E_p \tag{5}$$

The calculation of decay heat follows the DIN 25485 standard [30], which is applicable to all types of thermal reactors, including both HTGRs and LWRs. This approach relies on the power distribution of the fuel elements, segmenting the operational history into a sequence of time intervals T_j . The decay heat contributions from all preceding intervals, up to the present moment, are summed. The core idea of this method is depicted in Figure 18[59]. Calculating decay heat accounts for contributions from fission products, fertile isotopes, minor actinides, and heavy elements.

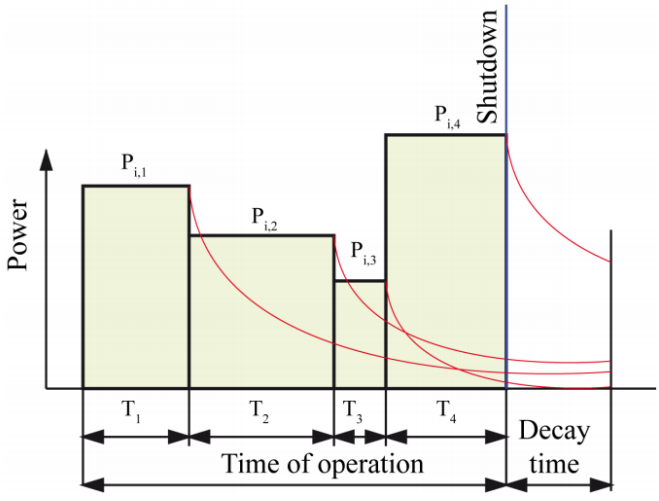

Figure 18 Power histogram and decay power [59]

Input data for each time interval include the average number of total fissions and details of fission types, which are typically supplied by burn-up codes like VSOP or Serpent. The time offset t_k is also considered in this calculation.

$$t_k = \sum_{j=k+1}^{m} T_j \tag{6}$$

the decay heat can be written as:

$$\dot{Q}_d = \sum_{l=1}^{30} \alpha_l' \sum_{k=1}^{m} F_k (1 - e^{-\lambda_l T_k}) e^{-\lambda_l t_k} \tag{7}$$

Here, l represents the 24 decay groups of fission products, along with 6 additional contributions from the actinides ^{239}U,^{239}Np,^{233}Th,and ^{233}Pa. F_k denotes the fission rates within the time interval T_k, while $a_l^{'}$ are the values selected to conform to the DIN standard. Consider different branches of decay heat:

$$\dot{Q}_{d,l} = \alpha_l' \sum_{k=1}^{m} F_k (1 - e^{-\lambda_l T_k}) e^{-\lambda_l t_k} \tag{8}$$

If the decay heat generated at the conclusion of the specified lifetime histogram is extended by a time interval Δ, assuming constant power during this period, it can be represented as follows.

$$\dot{Q}_{d,l}(t_0 + \Delta) = \dot{Q}_{d,l}(t_0) e^{-\lambda_l \Delta} + \alpha_l' F (1 - e^{-\lambda_l \Delta}) \tag{9}$$

This equation represents the solution to the time-dependent differential equation governing decay heat production.

$$\frac{d\dot{Q}_{d,l}}{dt} = \alpha_l' \lambda_l F - \lambda_l \dot{Q}_{d,l} \tag{10}$$

For steady-state reactor calculations, decay heat must remain constant as temperature approaches infinity ($T \to \infty$). In this scenario, the decay heat is incorporated into the effective energy per fission.

The total fission heat is given by:

$$E_f = E_p + (\frac{\dot{Q}_d}{F}) T \to \infty, t \to 0 = \frac{\dot{Q}_d}{F} \tag{11}$$

The fission reactions result in the liberation of energy in various forms, including kinetic energy exhibited by the fission fragments, β-radiation, high-energy neutrons, and γ-radiation. The kinetic energy carried by the fission fragments, constituting the predominant portion of the total energy released, is dissipated at the fission site through collisions with adjacent atoms. β-radiations, characterized by high-energy electrons, can be effectively attenuated by several millimeters of metallic shielding. Given that the dimensions of HTGR fuel kernels are on the scale of millimeters, it can be inferred that the energy from β-radiation is also localized within the immediate vicinity. Conversely, high-energy neutrons and γ-radiation lack electric charge and consequently possess the capability to traverse significant distances within the reactor core. Their energy deposition occurs both within the fuel and

moderator zones. Consequently, the heat generation can be partitioned into two distinct regions based on the localization of energy deposition.

1) The local heat source, emanating from the kinetic energy of fission fragments and β-radiation, may be characterized as follows:

$$\dot{Q}_l = \chi_p \dot{Q}_p + \chi_d (\dot{Q}_d - \dot{Q}_B) \tag{12}$$

χ_p and χ_d represent the ratios of local to total heat production for prompt and decay heat, respectively. $\dot{Q}_B$ denotes the breeding term of decay heat, regarded as non-local.

2) The non-local heat source encompasses neutron scattering interactions during moderation, neutron-γ reactions, and γ reactions.

MGT-FD is in charge of the thermo-fluid dynamics calculation in HCP. And similar with MGT-N, it is derived from MGT-3D as well. This module is responsible for computing the temperature, pressure, and flow velocity distribution within the core. Furthermore, the MGT-FD model encompasses specific chemical reactions occurring during transient events in the primary circuit, both within and outside the core, as well as a simplified secondary circuit represented through a network of 1D component simulations.

In MGT-FD, fluid mechanics calculations are divided into two main parts: homogeneous and heterogeneous calculations. The homogeneous calculation focuses on uniform meshes, including solid and porous media meshes, and involves gas flow, heat transfer, temperature computation, gas mixing, and corrosion analysis. Gas flow calculation determines pressure and mass flow rate across porous media meshes by solving mass and momentum conservation equations. Heat transfer in this calculation includes solid material and gas heat transfer, intertwined with heterogeneous heat transfer. Energy conservation equations are solved to find gas and solid temperatures using control volume discretization and leakage iteration methods. The heterogeneous calculation determines temperatures within each homogeneous mesh and assesses temperature rise in coated particles. It emphasizes fuel element surface temperature, average moderator temperature, and fuel kernel temperature crucial for nuclear reactions. Accurate temperature distribution within fuel elements is essential, with heat primarily conducted in solid construction but thermal radiation also contributing across particle gaps.

The fluid mechanics calculations of reactors are governed by three fundamental conservation laws: conservation of mass, momentum, and energy.

For the gas phase:

$$\frac{\partial \rho_g}{\partial t} + \rho_g \Delta \nu = S \tag{13}$$

Where the ρ_g denotes the gas density, ν is the velocity and S is the gas source.

$$\frac{\partial \rho_g \nu}{\partial t} + \nabla \bullet \rho_g \nu\nu - \nabla \bullet \overline{\overline{\tau}} = -\nabla P + \rho_g g + \nu S \tag{14}$$

Where the $\nu\nu$ is the dyadic product of two vectors, $\overline{\overline{\tau}}$ is the viscous stress tensor, P denotes the pressure and g is the gravity vector.

$$\rho c_p \frac{\partial T_g}{\partial t} + \rho_g c_p \nabla \bullet (v T_g) = \nabla \bullet (k \nabla T_g) + q_g''' \tag{15}$$

Where the T_g is the gas temperature, c_p is the heat capacity, and q_g''' denotes the heat source

For the solid phase:

$$\rho_s c_p \frac{\partial T_s}{\partial t} = \nabla \cdot (k \nabla T_s) + q_s''' \tag{16}$$

Where k is the thermal conductivity, q_s''' is the total heat source.

The computational process involves several steps as shown Figure 19 [58]. Initially, data undergo preprocessing, encompassing tasks such as defining coarse mesh temperatures, adjusting values via solid material ramps, and acquiring nuclear power density per mesh from MGT-N. Coarse mesh temperatures serve as either initial values or are derived from preceding MGT-FD computations, with only coarse mesh data existing at this stage. Subsequently, fluid dynamics and chemistry calculations occur concurrently, iterated together to ensure mutual feedback and refinement. Thermodynamic computation follows, utilizing fluid dynamics data to determine global and heterogeneous temperatures. Iterations continue until convergence, defined by specific temperature differentials and fluid density criteria. Upon convergence, a heat balance calculation is executed, extrapolating temperature changes over time to inform subsequent computational steps. Finally, the code returns to the HCP Backbone for further evaluation and decision-making.

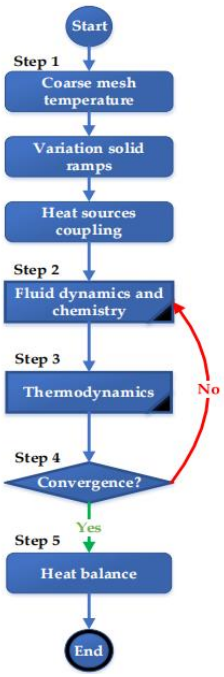

Figure 19 The MGT-FD workflow

2.1.4. New Spectrum code TRISHA

The spectrum code TISPEC originates from the 0D MUPO code, which is founded on neutron diffusion theory [31]. TISPEC discretizes the energy domain into 43 energy groups, following the MUPO energy structure [32], and employs the Gauss-Seidel method [33] for numerical solution. Similar to TOTMOS and other previously developed codes, TISPEC uses its own format for the neutron cross-section data library. Different library versions may include varying quantities of resonant isotopes and scattering matrices, often utilizing different versions of the ENDF raw data, and sometimes incorporating mixed data sources. Furthermore, the generation process and authorship of some libraries remain unclear. This divergence from the goal of the HCP, which aimed for a unified and consistent shared data library across its code package modules, poses a challenge.

TRISHA was created to transition from the MUPO library (TISPEC), which was utilized in MTG-3D, and address the limitations associated with its MUPO-like spectrum code TISPEC. The new HCP spectrum code harnesses the potential of the updated data library generator and employs a modern object-oriented approach to provide users with complete control and a well-defined process for generating and utilizing nuclear cross-section data. Unlike TISPEC or TOTMOS [34], which treat the double heterogeneity based on empirical experience, TRISHA uses small (particle + graphite) and big (pebble + gas) unit cells for the coated particles and the fuel pebbles. The unit cells are automatically updated to account for spatial and time-dependent changes in nuclide concentrations or variations in the coolant gas surrounding the fuel. This eliminates the need to manually define different unit cells, as is necessary in VSOP, for instance, when shuffling a core partially filled with graphite-only pebbles or during a water ingress event.

TRISHA was initiated to address several limitations of the previous MGT-3D spectrum code, TISPEC. Key objectives included leveraging a more comprehensive and efficient neutron data library, improving treatment of neutron resonances particularly in addressing the double heterogeneity issue, eliminating dependencies on spectrum code, and incorporating the latest capabilities of modern programming languages such as C++. The implementation of the new spectrum code within the HCP framework was demonstrated in this study, highlighting its integration with diffusion and burn-up code modules.

TRISHA has been fully implemented in HCP and is the preferred spectral program, and the calculation scheme is shown in Figure 20 [37]. TRISHA provides two solvers, a diffusion code similar to MUPO and a 0-D B1 transport code. Two different analytical methods are employed to compute Dancoff factors, each beginning with the geometry of the pebble, the quantity of coated particles per pebble, the ratio between dummy and fuel pebbles, and the gas mixture within the cell. The first method relies on first-flight escape and transmission probabilities, as outlined by Bende et al [35]. Conversely, the second method is grounded in the chord method, as proposed by Ji and Martin [36].

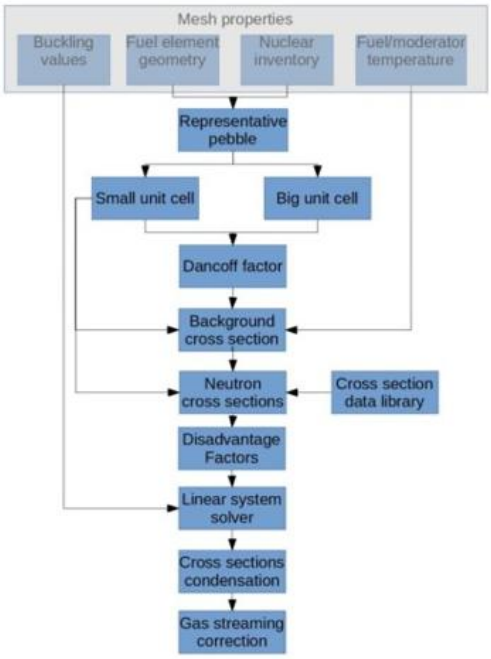

Figure 20 General flow chart of the spectrum code[37]

The 0-D diffusion module has been tested in benchmark calculations and shows good consistency with Serpent. Currently, the 1-D transport [13] code is still under development and its functionality has not yet been fully tested. It is worth noting that TISPEC is also integrated into HCP, so MGT-3D calculations can be performed within HCP. However, when it comes to complex modelling, the computational speed of TRISHA is not satisfactory and there is still considerable space for optimization in this respect. If the operational scenario is calculated by introducing burn-up (TNT) and shuffling (SHUFLE), the HCP spectrum code to be used to obtain the correct nuclear data is TRISHA rather than TISPEC.

2.1.5. SHUFLE

One of the primary advantages of a pebble-bed high-temperature gas-cooled reactor is the ability to replenish fuel in the reactor core during normal operation. Accurately describing the location of materials within the core is a critical issue, especially in the pebble-bed HTGR. Therefore, a new code module named Software for Handling Universal Fuel Elements (SHUFLE) was developed in the previous work. This includes two fuel management modules: as is shown in Fig. 2[16], one is called the Seepage model, and the other is called the Flowtube model. The Seepage model was the first to be developed. It divides the fuel into the same grid as fluid dynamics and neutron modules. When the fuel pebbles are discharged from the bottom of the pebble bed, a gap forms at the lower part of the core. During this period, although the fuel pebbles above the gap can remain stable for a short time, they will gradually start to flow to fill the gap below. Consequently, the gap gradually moves upwards, and when it reaches the surface of the pebble bed, one iteration is completed. This fuel management model has been successfully integrated into HCP and has undergone relevant testing. However, most of the legacy code was based on the Flowtube model. To ensure compatibility with the old code and retain existing models in HCP, the Flowtube model has been incorporated into SHUFFLE. This model approximates the core by dividing it into different flow channels, each further divided into nodes with equal geometric volumes, and it approximates the movement of larger volumes at discrete time points. The VSOP

geometric preprocessing tool, BIRGIT, which is essential for the Flowtube model, has been reimplemented with updated code and enhanced with additional features. The Flowtube model in SHUFLE now accommodates a filling factor distribution, includes a discharge tube and conical pile at the lower end, and supports full 3-D shuffling. Additionally, a more user-friendly and reliable input scheme has been developed.

The flow tube model approximates the movement of spheres as the transfer of contents between larger volumes at discrete time points. These volumes are divided into flow channels and nodes, where pebbles are treated as an incompressible fluid passing through well-defined boundaries. During fuel management steps, contents of each node are shifted downward, with the number of nodes affecting the flow velocity. While an irregular node grid is used for this purpose, Cartesian or cylindrical mesh grids are employed for fluid dynamics and Neutronics calculations, necessitating data mapping between grids. Shared volumes, as shown in Figure 21 [38], fully within one mesh and one node, are identified to aid in this process. In the legacy code, BIRGIT determines node grid layout and shared volumes through an indirect approach involving overlay meshes. These overlays are temporarily added to grids, with shared volumes determined by overlay mesh centers assigned to both the same mesh and node. Selecting an appropriate number of small meshes is crucial for accurate shared volume calculations.

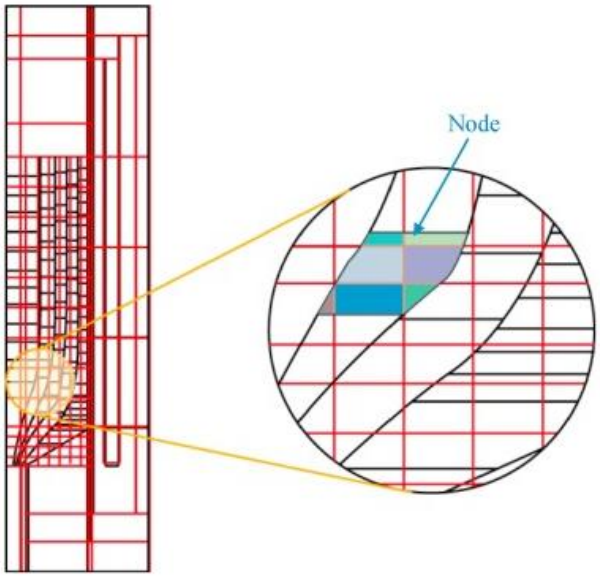

Figure 21 Shared volunmes for one single node[38]

Compared to the past, the SHUFLE module in HCP has new features:

1） The fuel management module now has a more flexible layout of node grids. The legacy code defines flow channels in pebble-bed reactors based on node numbers, inner and outer flow curves, and radial limitations. It also includes outer and potentially inner cones in angular core configurations. Triangular cross-sectional views are utilized, allowing the modeling of pebble beds as cylinders with conical chutes. The discharge tube, however, cannot be explicitly represented within the original node grid. In more refined fluid dynamics simulations, the pebbles inside the discharge tube are modeled in the same manner as those in the primary section of the pebble bed but fall outside the scope of fuel management. Instead, fuel removal occurs at the lower boundary of the main pebble bed region. In the HCP model, the node grid layout is more flexible, subdividing

the cross-sectional area into channels. This allows even volumes occupied by cones or parts of the reflector to be modeled as channels, although their contents are non-movable. These channels are constrained by user-defined flow lines, offering flexibility in defining their contours and enabling the inclusion of geometric details like the discharge tube without artificial adjustments for fuel residence time.

2） It is capable of implementing spatial distribution of filling factors. The legacy codes have limitations in handling pebble-bed reactors with a homogeneous filling factor, as seen in the VSOP fuel shuffling model. These codes assume equal geometrical volume for each node during execution, restricting shuffling to nodes with equal filling factors. While a 61% filling factor is typically assumed, the actual distribution varies spatially and may change over time, affected by factors like seismic events. This spatial variation affects coolant flow rates and power release. The HCP model addresses this by allowing for spatially dependent filling factors, managed through a geometry pre-processing tool. By subdividing flow channels into nodes of equal solid volume, individual filling factors can be considered. Users can define node-wise or mesh-wise filling factors, with node-wise definitions requiring fewer steps. However, mesh-wise definitions require iteration between pre-processing and main steps due to shared volumes. Currently, the filling factor distribution remains constant over time, but a simple modification could enable time-dependent distributions, facilitating simulations of seismic events and related effects on reactivity and coolant flow.

3） It can simulate the surface of the pebble bed. Users can define a flow channel-specific axial starting point in geometry pre-processing to approximate the shape of the conical pile using a step curve.

4） It can perform 3D pebble flow modeling. HCP introduces capabilities for full 3D modeling, with options for cylindrical or pseudo Cartesian coordinates. Initially, SHUFLE introduces a "2.5 dimensional mode" for fuel management, dividing the reactor core into rz-layers where independent flow patterns can be defined for each layer. However, the sub-division of channels into nodes of equal solid volume is done separately for each channel, limiting movement to within the same channel in box-wise shuffling due to interdependent node volumes. While individual flow patterns can be defined for each layer, there's no movement in the azimuthal direction. Additionally, HCP now offers full 3D pebble flow, allowing for pebble drift in the azimuthal direction, beneficial for designs with non-central discharge tubes, where pebbles flow distinctively around the annular core circumference

2.1.6. STACY

In the context of high-temperature reactor safety assessments, estimating fission product release rates is crucial for both normal operation and accident scenarios. Modern HTGR fuel elements incorporate TRISO coated particles (CP) designed to retain fission products, primarily through the use of a silicon carbide (SiC) layer. However, given potential uranium contamination in the outer pebble shell and the inherent probability of particle failure, a small fraction of isotopes may still escape the fuel and enter the coolant gas. To address this, the STACY (Source Term Analysis Code System) module is employed for calculating fission product source terms. Within STACY, fuel elements are represented by tracer pebbles, each with a distinct position [39]. Unlike in VSOP, these tracer pebbles remain separate and are not mixed with others at the conclusion of each core pass. Instead, their new radial positions are determined using a random number generator.

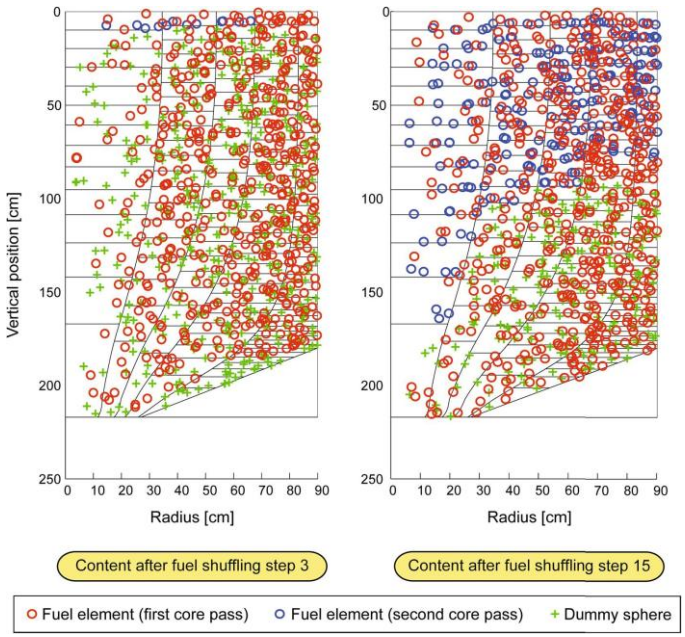

Figure 22 Tracer elements at two different core status of a typical HTGR core [39]

The computational programs FRESCO-I, FRESCO-II, and PANAMA have been integrated into the computational module STACY, which is not yet incorporated into HCP. This module was designed for calculating spatially high-resolution release of fission products from spherical or block-shaped fuel elements. It simulates individual particle breakage fractions and fission product release rates for a representative number of fuel elements. The trajectories of several thousand "tracer fuel elements" through the core are tracked in detail. A module-specific calculation of convective and diffusive transport of fission products allows for the simulation of the redistribution of fission products with the coolant. During the subsequent core heating phase in a pressure relief accident, fuel temperatures in the reactor core rise due to reduced cooling. STACY enables quantification of fission product release due to increasing particle breakage fractions and faster diffusive transport through the coating of intact particles. STACY has been provisionally coupled with HCP, and its integration as a fully integrated module is yet to be implemented.

2.1.7. TNT

The computational tool HCP employs a novel depletion module called TNT to calculate nuclide densities and energy release in nuclear systems. TNT, rooted in the established algorithms of the ORIGEN depletion code, implements these algorithms efficiently through graph theory. By considering individual reactions, TNT offers a more precise modeling of spatial power distribution within reactor cores during normal operation and accident scenarios. Unlike fixed depletion chains, TNT's dynamic depletion chain adjusts spatially and temporally, dependent on the nuclear data library and existing nuclides. With current data libraries containing thousands of nuclides, TNT enables accurate depletion calculations and analysis of radiologically significant nuclide inventories in a single simulation step, facilitating precise quantification of fission product release from fuel. Moreover, TNT allows decay power calculation on a nuclide-by-nuclide basis, supplementing the traditional DIN 25485 method.

Physically, TNT introduces significant enhancements over ORIGEN burn-up codes in two aspects: physics and programming techniques. It enables the input of problem-specific neutron energy spectra

and cell information for real-time generation of broad group cross sections for all nuclides and burn-up time steps. This eliminates reliance on precompiled cross section sets, allowing users to input internal information derived from spectrum codes. TNT also separately calculates nuclear power for decay, fission, and capture processes, distinguishing between local and non-local heat generation. Unlike traditional methods, TNT utilizes recent nuclide vectors and distinct Q values for all capture processes available in the data library, incorporating energy-dependent fission yields from ENDF/B-VII.0 files.

TNT's development as a new code from scratch, adopting an object-oriented paradigm implemented in C++, ensures flexibility and clarity. Problem-specific data types such as Nuclide, NuclideVector, Reaction, ReactionHandler, and CrossSectionSet improve code readability by encapsulating irrelevant implementations and segregating data handling routines from algorithms. Additionally, an object-oriented data model tailored for nuclear simulation facilitates basic nuclear data generation and storage, encompassing decay data, cross sections, independent fission yields, scattering matrices, and fission spectra for each nuclide. This library, typically sourced from ENDF/B-VII, undergoes automatic generation, serialization into a binary file, and swift loading into main memory, ensuring efficient utilization during simulations.

2.1.8. STAR

During operation, contaminated dust generated can contribute significantly to the radiological source term in the event of a design-exceeding accident. In a pressure relief accident, high velocities in the primary circuit occur due to the high pressure difference between the primary circuit and the reactor building. As a result, some of the dust deposited during normal operation can be resuspended, and a discharge from the primary circuit occurs at the leak. To quantify the dust release during the accident, the currently separate computational module STAR calculates the deposition of carbon dust in the primary circuit during operational mode. The temporal evolution of the dust release can be used, for example, as a source term in subsequent dust transport calculations with COCOSYS. STAR is still not implemented now.

2.2. Rod motion model

In an HTGR, control rods and small absorber spheres are normally located in the side reflector region, and their role is to regulate power and shut down the reactor. Therefore, accurate modeling of control rods and small absorber spheres is crucial for the safety assessment of HTGRs. This enables HCP not only to accurately describe the behavior of the core under steady-state and transient conditions but also to analyze reactivity accidents, such as rod stuck or ejection accidents, thereby enhancing HCP's capability for safety-related analysis. In the legacy codes, MGT-3D had simplified control rod modeling capabilities but was not successfully coupled with HCP. Therefore, to enable HCP to accurately describe the core behavior with rod insertions, this thesis proposed a "Flexible Curtain" control rod modeling method.

For modeling HTGRs, it's challenging to directly represent axial control rods in a 2D axisymmetric context, and many models are used to overcome this issue. The earlier MGT-3D employed a method known as the "gray curtain" model. This approach allows for the simulation of continuous control rod movements by modifying the neutron poison concentration within a designated material. A notable limitation of this method lies in the difficulty of determining the neutron poison concentration—and by extension, the rod efficiency—based on the control rod's geometry and composition. However, if the rod efficiency is predetermined, the model can be implemented straightforwardly by utilizing overlaid cross-section sets. Typically, two cross-section sets are used: one corresponding to the fully inserted

control rod and the other to the withdrawn control rod, within the same material mesh. To apply this method, each material mesh containing control rods must be assigned a distinct material with the appropriate overlaid cross-section sets. This method does not show the true geometric shape, material, and density of the control rods but approximates their effect through strong neutron absorbers. Additionally, this modeling approach only allows for the complete insertion of control rods into a specific grid cell, while the intermediate positions of the grid cannot be reflected.

However, due to certain internal issues within HCP, past developers have not successfully rewritten and deployed the control rod movement model based on the "gray curtain." The current version of HCP does not have the capability to simulate control rods and absorbers. Therefore, this thesis proposes an optimization of the gray curtain model based on the internal structure and operational logic of HCP, using the concept of "overlay compositions" to introduce a flexible curtain method for modeling control rod systems. In this method, users can not only directly add strong neutron absorbers (such as B-10) to simulate the effects of control rods, as in the past MGT-3D's "gray curtain" method, but also define and simulate control rods through user-defined geometric shapes (currently extended to cylindrical structures with circular or equilateral triangular cross-sections), materials, and densities. The effectiveness of this method is validated using the HTR-50 model, verified through the international Monte Carlo code SERPENT. Since the impact of control rods is nonlinear and depends on the insertion depth, the results from SERPENT can also serve as calibration for this reactor type and experiment.

2.2.1. Control rod and shut-down system

The reactivity control and shutdown system in a nuclear reactor is essential for safely managing reactor operations, responding to various operational scenarios, and ensuring reactor shutdown during emergencies. Its primary functions include facilitating reactor shutdown in normal and emergency situations, maintaining the reactor in a cold subcritical state for extended periods, and enabling control over reactor power output, including partial load operation. Additionally, the system may be utilized to regulate the radial temperature profile within the reactor core. It plays a crucial role in mitigating accidents such as water ingress into the core or malfunctions within the shutdown system itself. Modern reactors typically feature two independent and diverse shutdown systems to ensure redundancy and reliability. Table 2 provides detailed technical information and aspects related to the design and operation of shutdown systems.

Table 2 control and shut down systems of HTGR

System	Function	Large HTGR(THTGR)	Small MHTGR
Shut down system	Fast shut down, Control of power	Reflector rods	Reflector rods
Shut down system	Longtime cold shut down; Trimming processes	Core rods	Absorbers in reflectors

All high-temperature reactors exhibit a significant negative temperature coefficient, primarily due to the resonances of U^{238} or Th^{232}. This inherent physical property results in the reactor ceasing operation

if the heat removal systems fail, leading to a rise in core temperature. The negative reactivity change associated with a temperature increase is expressed by

$$\Delta k = \Gamma \cdot \Delta T \tag{17}$$

where Γ represents the negative temperature coefficient. By applying a value of $\Gamma = -10^{-4} K^{-1}$, a temperature change of 100°C in the fuel compensates for a 1% change in reactivity. Ensuring long-term cold subcriticality of the core requires compensating not only for the temperature difference between hot operational states and cold conditions (typically 50 to 100°C in the fuel) but also for reactivity gain resulting from the decay of Xenon and Protactinium. These factors are significant during extended shutdown periods for inspection and repair.

It's essential to clarify the requirements for reactivity compensation due to various effects and the importance of the shutdown system. The primary shutdown system typically comprises rods, which are inserted into borings in the side reflector. This system must address several reactivity factors, including those arising from accidents, hot standby conditions (temperature equalization), temperature reduction for control purposes, and additional considerations for uncertainties.

As Figure 23 shows, The MHTGR, presented here as a representative example of other modular HTGRs, features two independent and diverse shutdown systems, both located within the side reflector. Gravity is solely relied upon to position the shutdown elements optimally during accidents. The first system is activated by the reactor protection system, while the second is manually controlled. This second system is specifically used for cooling the reactor core to room temperature and ensuring long-term subcriticality. In all scenarios, the modular HTGR benefits from a strong negative temperature coefficient, ensuring nuclear stability under both normal operating conditions and accident situations. Operating between 50% and 100% part load, the first system also serves the purpose of control. A minimal excess reactivity is intentionally included for this purpose, eliminating the need for excess reactivity for burn-up compensation due to the continuous loading and unloading of the pebble bed reactor during normal operation, a significant safety advantage.

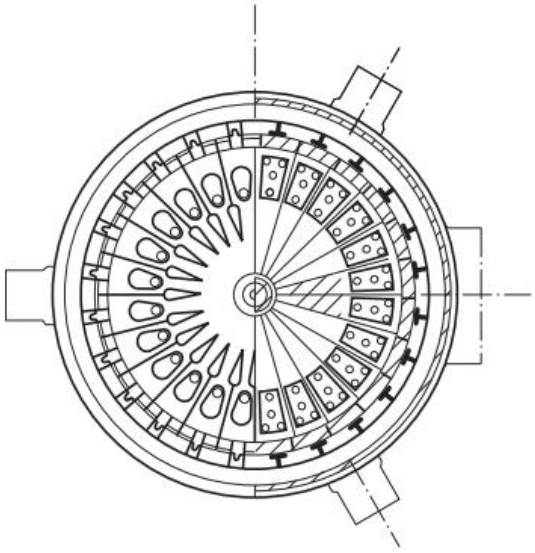

Figure 23 Position of the elements of the shut-down system in side reflector (MHTGR)[42]

Figure 24 shows the components of the first shut-down system. The rods comprise individual pieces interconnected by joints, with ceramic B_4C-rings serving as absorbing material nestled between metallic

tubes. Cooling of the absorber system is facilitated by a cold helium bypass. Rod drives are seamlessly integrated into the reactor pressure vessel, housing an electric motor, planet gear, and chain. Rod position is monitored by a dedicated device. In the event of a scram, motor energy supply is cut off, allowing the rod to descend solely under the influence of gravity to its lowest position.

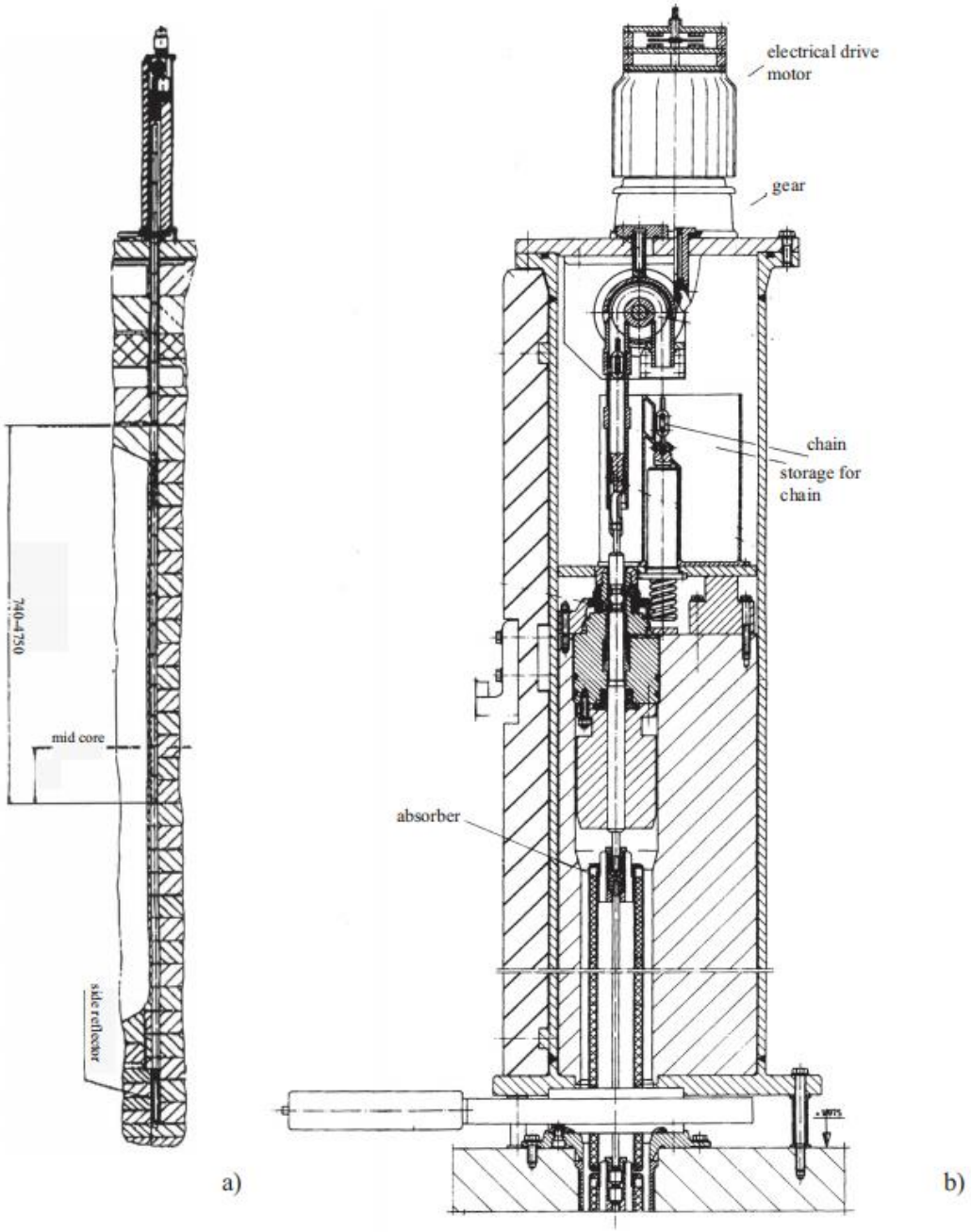

Figure 24 First shut-down system of MHTGR [42]

Figure 25 illustrates the technical design of the second shut-down system. These systems ensure ample shutdown reactivity, even in the event of a malfunction in one position of the second system. Moreover, there exists the option to shut-down the reactor using boron balls, which are loaded by the standard fuel element loading system.

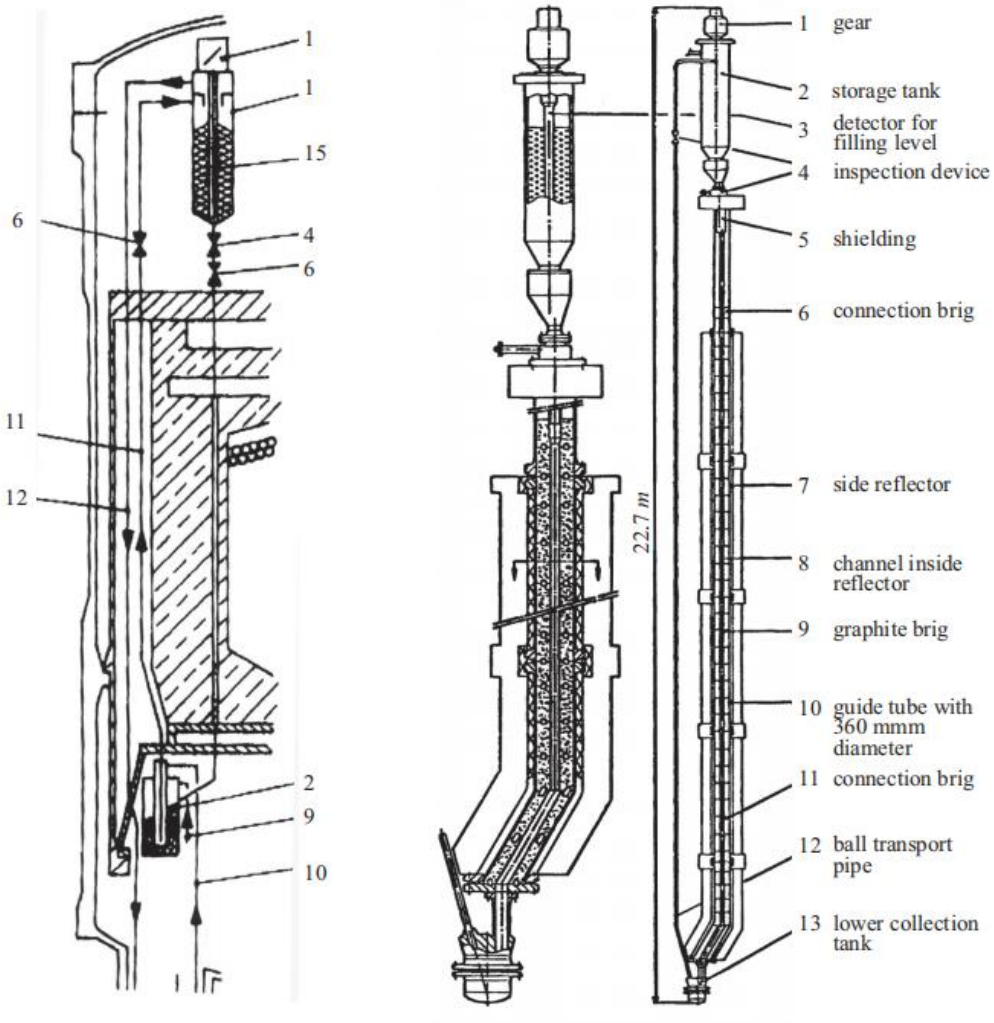

Figure 25 Second shut-down system [42]

2.2.2. The Calculation domain

For the "Flexible Curtain" method, changes in the internal nuclide concentrations in different computational domains lead to alterations in the homogenized multi-group cross-sections, thereby effectively simulating the effects of control rods. As illustrated in the Figure 26, within HCP, different types of physical calculations are performed by dividing the corresponding regions into various computational domains such as Fuel, Void, Nuclear, Fluid, Solid, Rod, etc. The settings of these domains delineate specific areas for different types of physics calculations. For instance, the Solid and Void domains represent calculations related to solid materials and gas flow, respectively, without further elaboration here. The variation in nuclide concentrations is controlled by the Nuclear computational domain. In the domain setting framework, each nuclear material block is associated with a specific nuclear material, and it's possible for a material to be assigned to multiple blocks. Within this structure, each material possesses a distinct set of cross-section polynomials and maintains a historical record of operation and fission rate fractions for heat production calculations. These material parameters are provided by the user and are integral to the accurate simulation of nuclear processes within the system.

```
<CalcDomainSettings>
  <CalcDomainGrids>
    <CalcDomainGrid type="Fuel" ids="7" label="pebble bed" />
    <CalcDomainGrid type="Void" ids="8" label="void" />
    <CalcDomainGrid type="Nuclear" ids="2 3 7 8" label="pebble bed, reflector" />
    <CalcDomainGrid type="Fluid" ids="1 2 3 7 8" label="whole calculation domain" />
    <CalcDomainGrid type="Solid" ids="0 1 2 3 7 8" label="whole calculation domain" />
    <CalcDomainGrid type="Rod"   ids=" 5 " label="control rod"/>
  </CalcDomainGrids>
</CalcDomainSettings>
```

Figure 26 Calculation domains setting of HCP

Currently, HCP utilizes a nuclide module similar to MGT-3D, which models using two-dimensional axisymmetric coordinates. The development of a full 3D computational scheme is underway. Therefore, to ensure the correctness of computational results, the HCP extensions and reactor calculations mentioned in this thesis are all based on a two-dimensional axisymmetric modeling approach. A structured rectangular mesh, as illustrated in Figure 27, is employed throughout the computational framework, with multiple meshes delineated within the overall computational domain. While these meshes share a common geometry, their distinction is essential for facilitating the mapping of values between different locations. The defined meshes include: the nuclear material mesh, encompassing all nuclear properties and solutions; the nuclear iteration mesh, tailored for neutron flux calculations and potentially aggregating material blocks to enhance computational efficiency; and one-dimensional (1D) iteration meshes in the radial, axial, and azimuthal directions, featuring fine sub-meshing to support specific calculations such as radial leakage iterations. These meshes collectively contribute to the comprehensive modeling of the reactor system while optimizing computational performance.

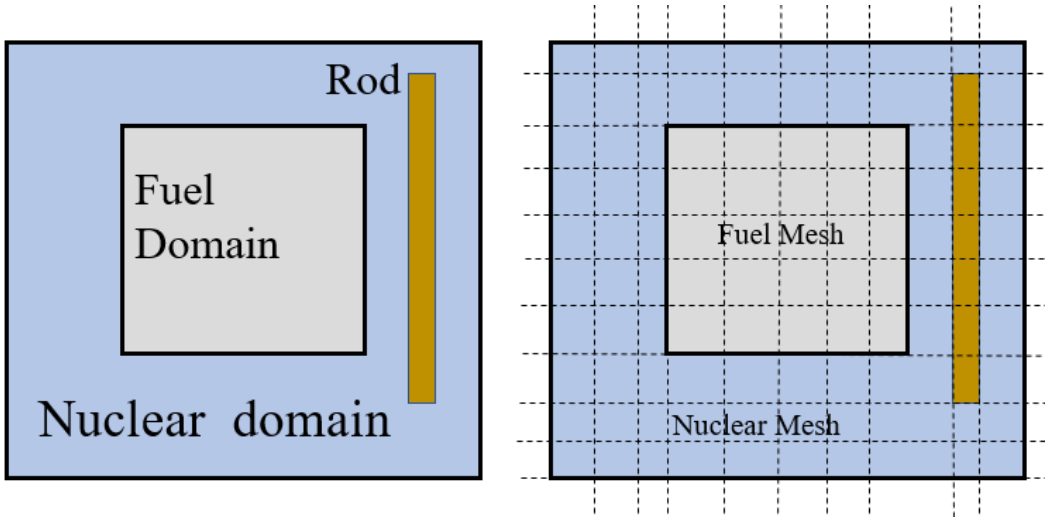

Figure 27 Calculaiton Domain of HCP

2.2.3. Cross section calculation

In HCP, neutron energy group modeling is realized through two distinct methods: the two-group method derived from TINTE and the 43-group method from MGT-3D. The approach stemming from TINTE employs a simplified representation with only two energy groups, delineated as thermal and fast groups. Here, cross-section calculations for core materials are pre-calculated and stored in a table, allowing for

polynomial fit interpolations during the main simulation instead of computing them at each time step. Conversely, MGT enables the utilization of up to 43 broad energy groups, necessitating numerical solution of a banded matrix. This method allows for inline spectrum calculations for cross-section determination at each time step and location within the reactor, offering enhanced computational flexibility and accuracy. Due to the use of different cross-section calculation methods, there may be some slight errors in the results. However, the average deviations in the results are within an acceptable range [41]. Therefore, in this section, we illustrate the cross-section calculations using a two-group neutron energy spectrum as an example.

The cross sections are presented in two-group diffusion method by a series of N order polynomials of the form shown:

$$\begin{aligned}&\Sigma\left(T_f, T_m, Xe, C_{N_2}, C_{H_2}, G_g\right) = \Sigma_0 \\ &+\left[a_1(T_f - T_0) + a_2(T_f - T_0)^2 + ... + a_m(T_f - T_0)^m\right] \\ &+\left[b_1(T_f - T_0) + b_2(T_f - T_0)^2 + ... + b_m(T_f - T_0)^m\right]\end{aligned} \tag{18}$$

Where,

T_f =fuel temperature/K(unit);

T_m =moderator temperature/K;

T_0 = Initial fuel temperature/K;

Xe = xenon concentration/atoms.barn^{-1}.cm^{-1};

C_{N_2} = nitrogen concentration/mol.m^{-3};

C_{H_2} = hydrogen concentration/mol.m^{-3};

G_g =Graphite burn-up/mol.m^{-3}

Each term in the polynomial depends exclusively on a single parameter, with coefficients specified for each material. The reference value, Σ_0, represents the macroscopic cross section under standard operating conditions within the reactor's relevant region. The subsequent coefficients (e.g., Ai, Bi) are designed to reflect variations in the reactor's operating conditions. These coefficients are typically pre-determined using steady-state results obtained from VSOP 99 or prior HCP simulations, encompassing a range of assumed operating scenarios. While this approach ensures precise cross-section calculations near the reference conditions, accuracy tends to decline as deviations from these conditions increase. In HCP, macroscopic cross sections for specific operating states are pre-calculated using the TISPEC/THISHA spectrum code. Each nuclear material mesh is assigned a unique set of cross sections, computed based on factors like temperature, buckling, and other relevant parameters within the mesh at the start of each nuclear time step. For steady-state analyses, these parameters are propagated from the results of the preceding iteration. The computed cross sections and nuclear parameters include:

- Fast(Σ_{tr1}) and thermal(Σ_{tr2}) macroscopic transport cross sections;
- Fast(Σ_{a1}) and thermal(Σ_{a2}) macroscopic absorption cross section (including fission);
- Fast($\nu\Sigma_{f1}$) and thermal($\nu\Sigma_{f2}$) macroscopic nu-fission cross section;

- Fast (Σ_{f1})and thermal(Σ_{f2}) macroscopic fission cross section;
- Fast (Σ_{r1})and thermal(Σ_{r1})l macroscopic removal cross section;
- Fast($1/v_1$) and thermal ($1/v_2$)group reciprocal mean neutron velocity;
- ^{135}Xe(σ_{Xe5}), ^{149}Sm(σ_{Sm9}), ^{151}Sm(σ_{Sm1}) and ^{157}Gd(σ_{Gd7}) thermal group microscopic cross sections;

The diffusion constants equation is given $D = \frac{1}{3\Sigma_{tr}}$ .In scenarios involving cavity regions and pebble-bed-type cores, special considerations are required to address neutron streaming phenomena. This is addressed by incorporating distinct diffusion constants in the radial, axial, and azimuthal directions. Directional diffusion coefficients are established using correction factors specific to each direction. The directional macroscopic transport cross section can be expressed as:

$$D_r = c_r D \tag{19}$$

$$\begin{aligned}
\Sigma_{tr}^r &= \frac{\Sigma_{tr}}{c_r} = \frac{\Sigma_{tr,0}}{c_r} \\
&+ \left[\frac{a_1}{c_r}(T_f - T_0) + \frac{a_2}{c_r}(T_f - T_0)^2 + \ldots + \frac{a_m}{c_r}(T_f - T_0)^m \right] \\
&+ \left[\frac{b_1}{c_r}(T_f - T_0) + \frac{b_2}{c_r}(T_f - T_0)^2 + \ldots + \frac{b_m}{c_r}(T_f - T_0)^m \right] + \ldots \\
&= \frac{\Sigma_{tr,0}}{c_r} + \left[a_1^r (T_f - T_0) + a_2^r (T_f - T_0)^2 + \ldots + a_m^r (T_f - T_0)^m \right] \\
&+ \left[b_1^r (T_f - T_0) + b_2^r (T_f - T_0)^2 + \ldots + b_m^r (T_f - T_0)^m \right] + \ldots
\end{aligned} \tag{20}$$

where D_r represents the radial diffusion coefficient and c_r remains constant throughout the calculation for the given material. For nuclear material, New polynomial coefficients $a_i^r = \frac{a_i}{c_r}, b_i^r = \frac{b_i}{c_r}$ may be defined.

The ability to adjust material compositions dynamically within the reactor model is particularly useful for scenarios such as introducing neutron poisons or adding extra moderator material. This feature is implemented using overlaid cross sections, which allow multiple cross-section sets to be assigned to each nuclear material. The cross-section values employed in the diffusion calculation for the nuclear material mesh are derived by fractionally combining the cross sections calculated using the polynomial expansions outlined in the relevant equation:

$$\Sigma = (1 - w_1 - w_2 - w_3 - \ldots)\Sigma_A + w_1\Sigma_B + w_2\Sigma_C + w_3\Sigma_D + \ldots \tag{21}$$

Where, $w_i, i \in R$ is calculated by HCP backbones based the parameters given by users.

2.2.4. Method for the rod motion simulation

Currently in HCP, both neutron and thermal-hydraulic calculations are performed using the same mesh grid partitioning. To successfully couple the control rod system with HCP and accurately describe control rod behavior in neutron calculations, the same grid partitioning as in MGT-N and MGT-FD is adopted. Control rods are represented by axially subdivided, homogenized annuli positioned radially at the correct locations of the neutron absorbers.

In this approach, the actual geometric shape of control rods is abstracted, and control rods are simulated by adding the material compositions of the control rods within the control rod volume region. Subsequently, any errors caused by the geometric shape of control rods can be compared and calibrated against experimental results or high-fidelity (Monte Carlo) calculations.

As shown in Figure 30, control rods are modeled through the discretization of the MESH grid.

The mesh serves as a crucial component of the cylindrical mesh grid defined in Model.xml within the reactor model. It encompasses various essential data and facilitates both nuclear and fluid dynamics calculations performed by HCP code modules such as TRISHA, MGT-N, MGT-FD, TNT, and STACY. When the node and mesh grid do not align, as in scenarios involving reactors with non-standard geometries like cones, the mesh maintains pointers to different batch fractions associated with it. Moreover, the mesh grid forms the foundation for data exchange between the HCP backbone in C++ and Fortran, particularly concerning modules like MGT-N and MGT-FD. Except for the last mesh, the control rod is fully inserted into each mesh, where the material density of the control rod is uniform. In the last mesh, where the control rod is not fully inserted, the density is calculated using interpolation as follows [40]:

$$n^*(l) = \frac{\ln\left(1-\frac{l}{L}S\right)}{\ln(1-S)} * n, \qquad 0 \le l \le L \tag{22}$$

Here, n represents the nuclide concentration in the rod region when the rod is fully inserted, while $n^*(l)$ denotes the nuclide concentration when the rod is partially inserted into the region over a length l. l and L refer to the insertion length of the rod and the axial height of the rod region, respectively. S is the interpolation factor used in the special exponential interpolation scheme for the linear rod movement model, with a value always between 0 and 1.

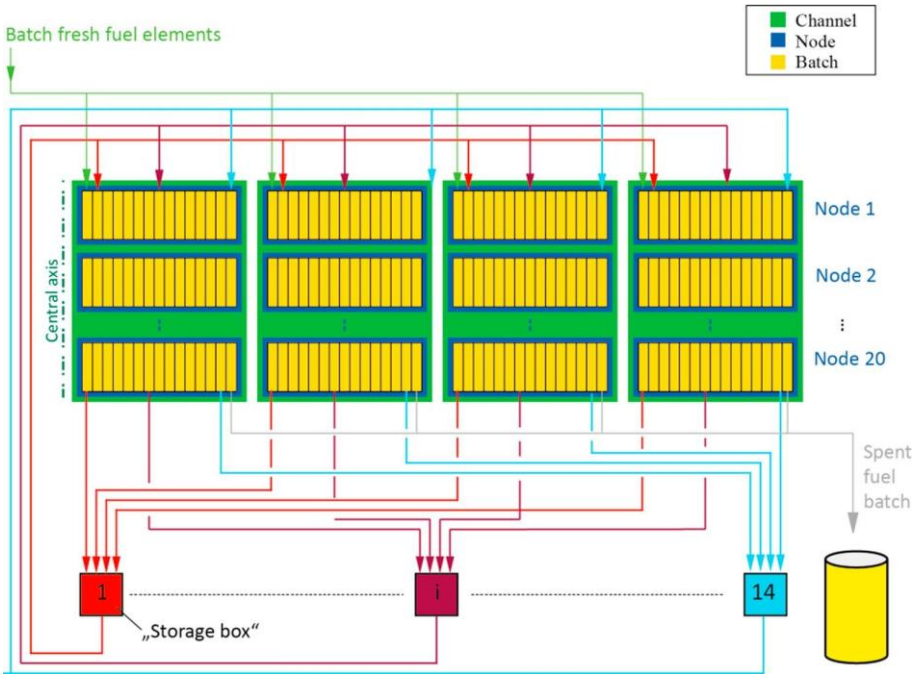

Figure 28 Batch, Node and Channel concept in HCP [38]

The "Flexible Curtain" method is implemented through batches in the SHUFLE module as the smallest computational units. Utilizing the functional functions within other modules not only reduces program complexity but also facilitates better coupling with other modules during subsequent program expansions. The batch in the context of HCP represents a virtual volume encompassing homogenized nuclide inventories within a specified node, delineating various burn-up states or fuel elements. It serves as the smallest unit volume managed by the HCP fuel management code SHUFLE. Batches are categorized as either solid or fluid, with the potential for mobility depending on whether they are designated as movable. For immovable batches, SHUFLE cannot relocate them between different nodes. Each batch is associated with a reference fuel element, encapsulating all its properties, and maintains information regarding the recent number of core passes, particularly relevant for shuffling schemes, as shown in Figure 28.In the HCP framework, a node represents a distinct component of the reactor model's node grid as specified in the Model.xml file. It constitutes a defined volume housing multiple batches and is integral to the flow of the reactor system. Typically, a node may accommodate a combination of solid and fluid batches, delineating between stagnant and non-stagnant gas regions. Within these batches, the nuclide inventory is defined, detailing the composition of materials present. The node grid, established by flow lines, subdivides the reactor into distinct flow channels comprised of nodes. Additionally, the movement of batches within the reactor grid is orchestrated by the HCP module SHUFLE.

As shown in Figure 29, when explicit flow lines are not defined, the nodes and mesh grid coincide. However, when flow lines are explicitly defined, regions in the node belonging to different meshes are separately calculated within their respective regions.

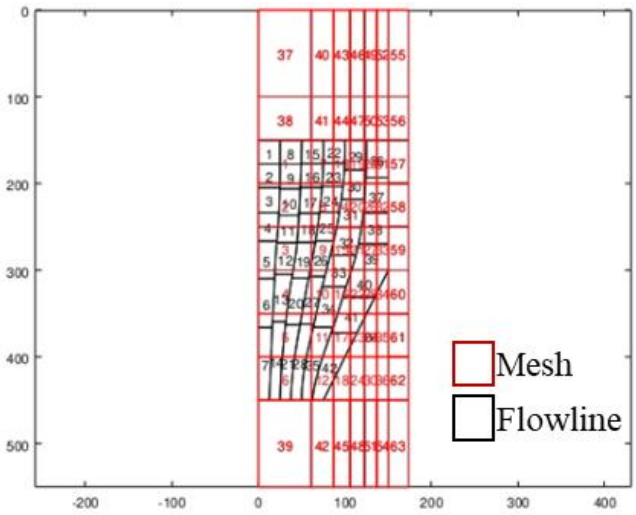

Figure 29 Flowline in HCP

If a node belongs to the reflector, it typically consists of one batch symbolizing the solid material. For nodes that include boreholes, an additional batch representing the coolant may also be included. In regions with control rods, nodes might encompass as many as three batches: one for the graphite in the reflector block, another for the control rod, and a third for the coolant. Nodes situated in the pebble-bed region can house several batches to account for distinct fuel types or different burn-up levels of the same fuel type. The batches throughout the core are homogenized over the node's volume.

The flexible curtain algorithm is developed and implemented in HCP using the C++ language. It is modeled through the movement and non-movement of batch in the SHUFLE fuel management. Each mesh in the control rod region is composed of three batches: two solid batches representing the immobile reflector (batch_1) and the control rod about to be inserted (batch_2), and one fluid batch (batch_3) representing the remaining cavity space.

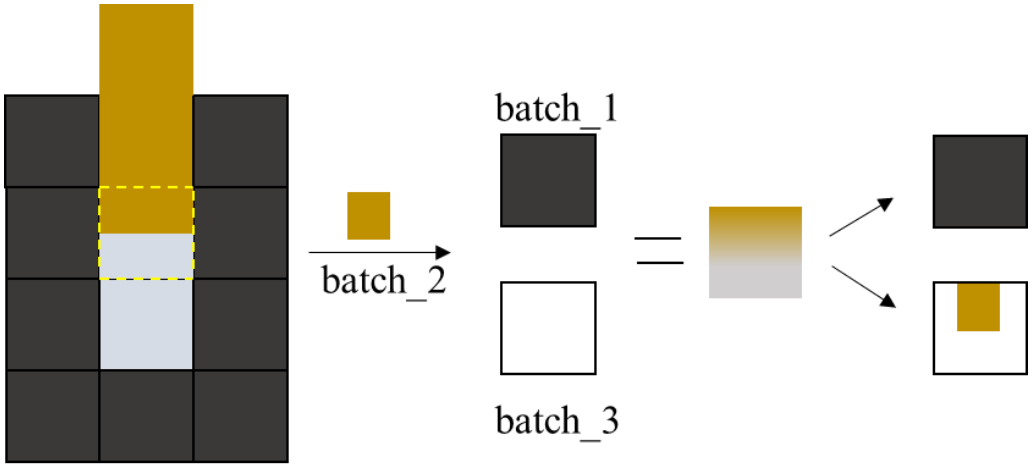

Figure 30 The process of control rod insertion

After insertion, the immovable batch_1 remains unchanged, and the properties of the movable batch_2 are replaced with updated properties such as control rod volume and isotope densities. The control rod

volume is calculated based on specific control rod attributes defined in model.xml, and the calculation formula is as follows:

$$V_{rod} = num * A_{rod} L \tag{23}$$

Where the V_{rod} and A_{rod} denote the volume and cross-sectional area of the control rod, respectively, and the num is the number of the control rod bundle. Currently, the volume calculation method for control rods with triangular and circular cross-sections has been integrated into HCP. For irregular cross-sections or other types of shapes, users can input the volume of a single control rod for insertion or withdrawal through custom-defined methods, and then utilize HCP for calculations. In this scenario, the formula for calculating the volume of the control rod is as follows:

$$V_{rod} = num * V_{usrod} \tag{24}$$

Where， V_{usrod} denotes the user defined volume inserted.

The volume of batch_3 will also be recalculated based on the updated volumes of batch_1 and batch_2 as follows:

$$V_{batch\_3} = V_t - V_{rod} - V_{batch\_1} \tag{25}$$

Where V_t denotes the total volume of the rod nodes, V_{batch_1} is the immovable volume of the rod region. When defining the volume of control rods, the following relationships should be satisfied:

$$\begin{aligned} &V_t \geq V_{rod} \\ &V_t \geq V_{batch\_2} \\ &V_t - V_{batch\_1} \geq V_{batch\_2} \geq V_{rod} \end{aligned} \tag{26}$$

Where, V_{batch_2} is the defined control rod volume to be replaced by users.

When defining control rods, it's important that the materials and densities for different types of control rods match the real-world conditions. Additionally, the volume definition of control rods should align with the requirements of the computational model to ensure the accuracy and reliability of calculations in HCP.

After iteration, HCP will have updated isotope densities within each mesh in the control rod region. Subsequently, these values will flow through the backbone and be passed to MGT-N and TRISHA for new neutron calculations. These updated calculations will then participate in calculations with other modules based on the defined computational scenarios.

2.2.5. Control rod calculation

In the latest version, the model.xml file has been enhanced to allow for the definition of various parameters related to control rods, including their position, quantity, radius, and borehole radius. These updates provide a flexible framework that can accommodate the modeling requirements of most high-temperature gas-cooled reactor control rod systems. With these improvements, the updated HCP version is better equipped to handle the modeling tasks associated with control rods in different reactor designs. The flexible curtain control rod modeling method described above has also been incorporated into HCP.

Users can perform control rod insertion or withdrawal actions for the HTGR control system in Scenario.xml using XML syntax.

To provide a user-friendly and precise description of control rod actions, two different description methods have been implemented. In the first method, users can directly modify the nuclide concentrations at specific nodes to simulate the process of control rod insertion and withdrawal. As illustrated in Figure 31, users are required to define the time duration, nodes and nuclide vector for control rod insertion.

```
<Action begin="2.0" end="2.0" unit="s">
     <Calculation type="Stationary" mode="manual">
       <Ramp type="NuclideConcentration">
         <NuclideConcentration node="47">
           <Amount nuclide="B-10" unit="1/barn/cm"> 6.72877E-04 </Amount>
           <Amount nuclide="B-11" unit="1/barn/cm"> 2.70841E-05 </Amount>
         </NuclideConcentration>
       </Ramp>
     </Calculation>
   </Action>
```

Figure 31 control rod input scheme 1

The "Flexible Curtain" method has been incorporated into HCP as a specialized action type. Within HCP, an action encompasses a series of commands delineated within the Scenario.xml file's timeline, defining either a specific time interval or duration. Moreover, actions specify the type of calculation to be executed. Thus, when employing this method to simulate control rod behavior, the entire control rod operation can be handled as a scenario within HCP.

A simulation scenario may encompass numerous actions (Figure 32), each involving various transient calculations. Additionally, for transients or sequences of steady states, an action may include details about alterations and new boundary conditions, known as ramps in HCP. These actions are interpreted by HCP Control, which configures the requisite data to initiate either a steady state or transient calculation, incorporates ramp information, and facilitates coordination between MGT-N and MGT-FD. Upon completing the action, HCP Control forwards this information to HCP Backbone, prompting another action if necessary. Once all actions are processed, HCP concludes the calculation process. A ramp defines a user-defined change in one or more parameters of the reactor model. It can be an instantaneous change or a change over time. A ramp is always located inside of an Action within the time line. Typical ramps are steady state commands, burn up or fuel management ramps. The approach of ramps is based on the code MGT but have been extended for the application in HCP.

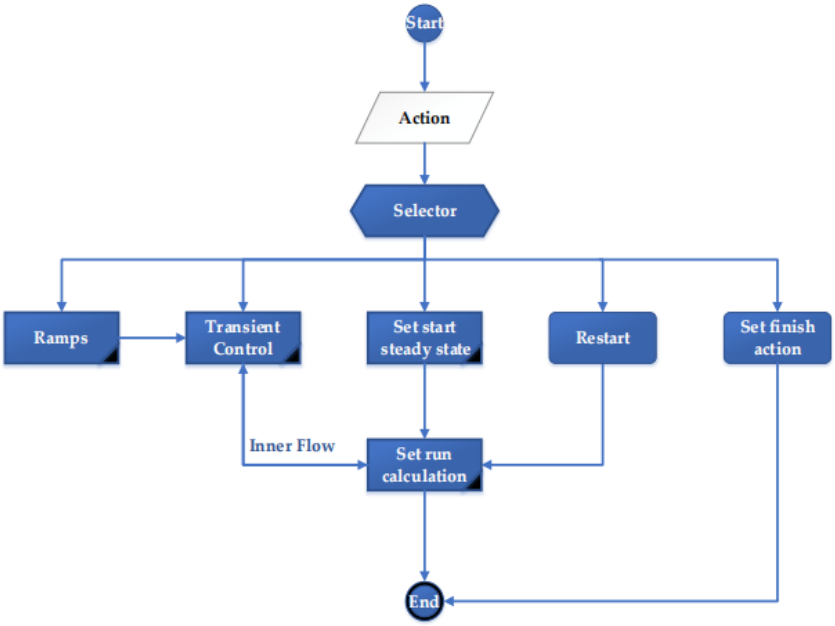

Figure 32 Action control logic[58]

The steady-state calculation in HCP mirrors a long-term transient scenario with constant boundary conditions, encompassing factors such as nuclear power production, nuclear inventory, mass flow source, reference pressure, and boundary temperatures. During this process, the calculation loop within MGT-N and MGT-FD adopts a semi-implicit approach. Critical data such as k-effective, temperature, and pressure fields are determined during the steady-state calculation, as these values serve as crucial inputs for subsequent transient simulations. Achieving convergence for a specified time point in the distant future, necessitates adherence to stringent convergence criteria. Consequently, numerous iterations may be necessary to ensure convergence during steady-state calculations.

The ramps refer to changes introduced in the model during a steady state or transient calculation. In this context, during steady-state calculations, changes in the isotopic concentrations are introduced using ramp instructions, followed by transient calculations. As mentioned earlier, the changes in concentration are based on batches within nodes. These nodes should belong to the rod calculation domain within the nuclear module.

As shown in Figure 32, when the program initiates the ramp instruction, corresponding to the control rod action, HCP executes the transient process. In the flexible curtain method, the transient process primarily considers neutron behavior and thermal-hydraulic calculations, which are respectively handled by MGT-N and MGT-FD. For the transient calculations of the relevant modules, they do not use the same time steps; instead, they solve with time steps based on their respective conditions. However, to ensure consistent data, both calculations must provide results at the same time points. Therefore, the coordination of both time steps is necessary.

The time step calculations in HCP are based on semi-empirical approaches combined with corrections to improve both performance and numerical stability. Neutronics calculations are prioritized at the start, followed by integration with thermo-fluid dynamics and rod movement simulations. Each step imposes limits on the time step size, which are influenced by user-defined settings, physical parameters used in correction techniques, and the time spans of ramps. Additionally, default limits are imposed to ensure a

maximum and minimum time step value. These collective constraints ensure efficient and stable time step calculations in HCP.

Through this approach, users can flexibly simulate control rod behavior, even when multiple control rods are inserted simultaneously in different regions. By incorporating these features, the updated HCP framework can provide increased flexibility for the new design of pebble bed reactors. Additionally, this approach offers a high degree of flexibility. Users can utilize this functionality not only to simulate control rods or absorber pebbles but also to introduce arbitrary isotope concentrations in other non-control rod regions to simulate different operating conditions and scenarios.

To streamline control system modeling and make it more efficient, control rod automation modeling has been integrated into the backbone of HCP. Scheme 2 is designed for traditional pebble bed reactor control rod adjustment scenarios. As is shown in Figure 33, users only need to input the starting and ending rod positions, insertion speed, and control rod composition. The program will automatically perform steady-state or transient calculations. In this mode, users can conveniently and efficiently configure the control rods for the reactor, enabling streamlined control rod setup and analysis. The built-in algorithms calculate the control rod position based on the insertion rate and node height.

```
<Action begin="0.0" end="100.0" unit="s">
  <Calculation type="Transient">
    <Ramp duration="100.0" unit="s" type="Nuclear">
     <Nuclear type="ControlRod">
        <ControlRod conservative="0" value="0.0" unit="cm"/>
      </Nuclear>
    </Ramp>
  </Calculation>
</Action>
```

Figure 33 control rod input scheme 2

2.3. Verification and Validation

The introduced control rod related code still requires further verification and validation. To ensure the integrity of the new code and the correctness of the overall HCP computations, HCP needs to undergo verification under the new control rod insertion and withdrawal operating conditions. For these cases, HCP was mainly benchmarking with the Monte Carlo code SERPENT and nuclear system code ATHLET. In this section, the thesis utilizes the updated HCP to create a simplified version of the HTR-50 reactor. It then compares and validates the steady-state and transient calculation results after control rod movement with results from SERPENT and ATHLET. Selected representative validation results are presented for analysis.

2.3.1. Simplified reactor model HTR-50

This thesis utilizes a simplified HTR-50 as a model for benchmark testing, and the primary parameters of the HTR-50 are presented in Table 3.

Table 3 Primary parameters of HTR-50

Parameter	Value	Unit
Reactor Power	50	MW
Active core diameter	3.0	m
Active core height	3.0	m
Reflector thickness	0.23	m
Helium pressure of the primary loop	30	bar
Helium mass flow rate	25	kg/s
Inlet/Outlet helium temperature	250/635	℃
Fuel element diameter	60	mm
Pebble-bed core porosity	0.3954	-

The reactor core is a cylindrical loose pebble bed, consisting of approximately 113,097 pebbles within an active region of approximately 21.206 cubic meters. Each pebble contains an inner core with a radius of 2.5 centimeters, housing approximately 15,000 TRISO-coated fuel particles dispersed in a graphite matrix. These TRISO fuel particles, with a diameter of nearly 1.0 millimeter, consist of a 0.5 millimeter diameter UO_2 kernel surrounded by three layers of PyC (Pyrolytic Carbon) and an outer layer of SiC (Silicon Carbide).

The enrichment level of U-235 in each fuel pebble is approximately 8.3%, and each fuel pebble initially contains 9 grams of heavy metal. The filling factor is 0.6046. The graphite reflector surrounds the core, and there is a 0.5-meter void space located above the fuel region and the upper graphite reflector. Six control rod clusters with a radius of 2 centimeters are positioned within the side reflector region.

2.3.2. Model based on HCP

Building the HCP model for HTR-50, as shown in Figure 34, involves dividing the fuel region into a grid of 6x6 nodes, each with 9 sub-grids. The core is encased in a graphite reflector, while helium gas enters from the top of the pebble bed. As the gas flows through the fuel region, it absorbs heat before exiting at the bottom. Both the fuel and moderator temperatures are maintained at a constant 900K. Neutron diffusion calculations are conducted using two energy groups, with the Xenon equilibrium calculation disabled. The heat is produced by the MGT module rather than TNT.

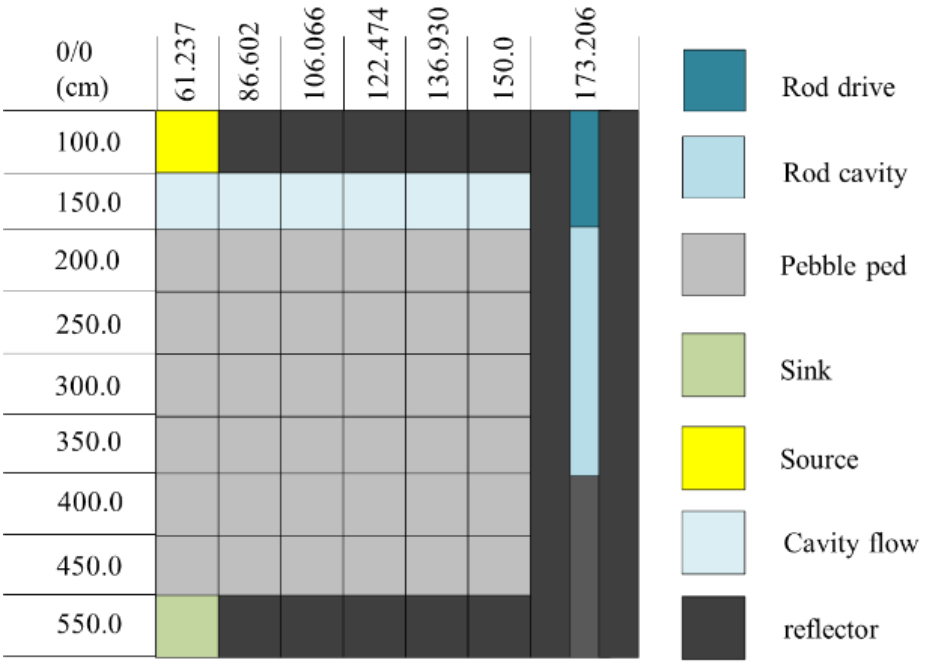

Figure 34 model for the HTR-50

2.3.3. Model based on Serpent

Serpent is an advanced 3-D continuous-energy Monte Carlo code designed for reactor physics and burnup calculations. It was developed by the VTT Technical Research Center of Finland. Built upon the universally constructive solid geometry model akin to MCNP and Keno-VI, Serpent offers comprehensive capabilities for simulating reactor physics, neutron transportation, and burnup processes across various reactor types, including LWRs and HTGRs. Its versatile functionality extends to the calculation of parameters at the fuel pin, fuel assembly, and core levels, making it a valuable tool for nuclear reactor analysis and design. Monte Carlo methods, broadly speaking, are computational algorithms that use random sampling to obtain numerical results. In the context of SERPENT, these methods are employed to simulate the behavior of neutrons in complex geometries, such as nuclear reactors.

The primary function of SERPENT is to simulate the transport of neutrons through a system, tracking their interactions with materials and the production of secondary neutrons as well as other reaction products. This simulation is essential for a variety of purposes, including:

- Reactor Design and Analysis: SERPENT can be used to simulate the behavior of different reactor designs, aiding in the optimization of fuel configurations, safety analysis, and performance evaluation.
- Nuclear Fuel Cycle Analysis: By simulating the behavior of neutrons in nuclear fuel cycles, SERPENT can help in evaluating the efficiency of fuel usage, isotopic compositions, and the production of nuclear waste.
- Shielding Design: Neutron shielding is crucial for the safety of personnel and equipment in nuclear facilities. SERPENT can be used to optimize shielding designs by simulating neutron interactions with various materials.
- Radiation Dosimetry: Understanding the distribution of neutron flux and energy spectra is important for assessing radiation doses to personnel and equipment in nuclear environments.

SERPENT can provide detailed information on neutron transport characteristics for dosimetry studies.

In Serpent, the detailed HTGR geometry model obtains the coordinates of fuel particles or pebbles directly from a separate input file. The geometry is constructed exactly as specified, avoiding any approximations. This model functions across various levels, such as particles within a pebble and pebbles distributed throughout the core, guaranteeing precision and realism in simulations. Extensive testing has been conducted on realistic double-heterogeneous reactor configurations to validate the model's performance and reliability.

Since the neutron transport is not directly solved in ATHLET, a point kinetics model has to be implemented to describe the neutron behavior and the temperature feedback effect during the transient. The neutron transport code: Serpent, developed at VTT Technical Research Centre of Finland since 2004, is used in this work to generate the necessary parameters for the point kinetics model. In order to make the models in HCP and ATHLET comparable, the consistent geometry is applied as shown in Figure 35, and the ENDF/B-VII library is used in both codes to ensure the consistency of the nuclear data. Also, Serpent's modeling can verify that the HCP can accurately calculate the introduction of reactivity after insertion of the control rods.

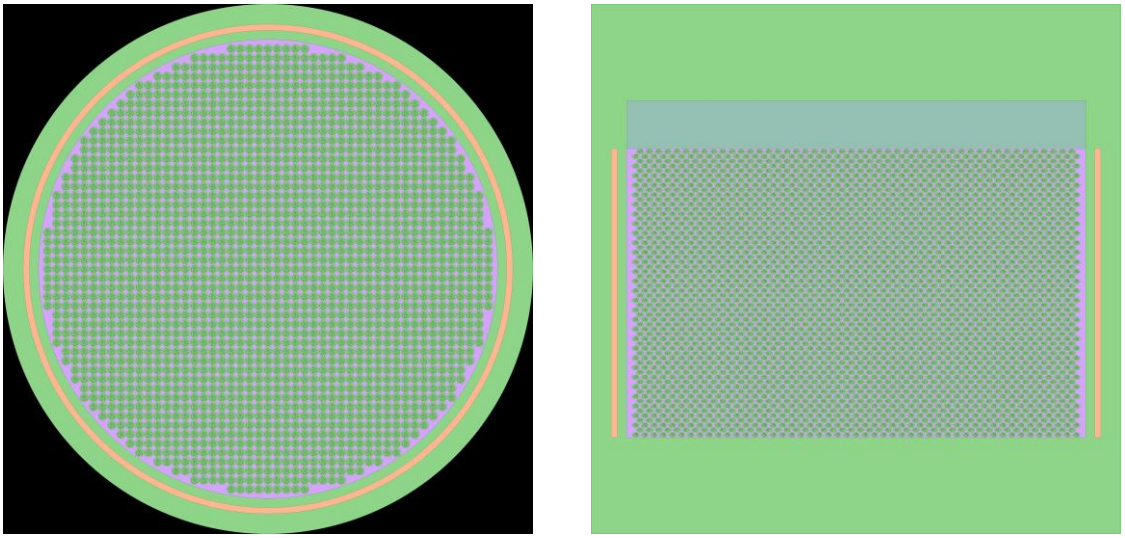

(a) Cross-section (b) Profile

Figure 35 Geometry of HTR-50 in Serpent

2.3.4. Model based on ATHLET

ATHLET (Analysis of Thermal-Hydraulics of Leaks and Transients) is a best-estimate system code developed by the Gesellschaft für Anlagen- und Reaktorsicherheit (GRS) mbH in Germany. It is primarily used for the simulation and analysis of thermal-hydraulic behavior in nuclear power plants, particularly during accidents and transients.

The function of ATHLET revolves around providing a comprehensive simulation environment for understanding the behavior of nuclear reactor systems under various operational and accident conditions. Some of its key functions include:

- Accident Analysis: ATHLET can simulate a wide range of accident scenarios, including loss-of-coolant accidents (LOCA), steam generator tube ruptures, pump failures, and control rod

malfunctions. It calculates the behavior of coolant flow, temperature distribution, pressure evolution, and other relevant parameters during these accidents.

- Transient Analysis: Apart from accidents, ATHLET can also simulate operational transients such as power changes, load variations, and control system manipulations. This capability allows for studying the dynamic response of the reactor system to different operational conditions.
- Coolant System Behavior: ATHLET models the behavior of coolant systems, including primary and secondary loops, heat exchangers, pumps, valves, and other components. It accounts for phenomena such as single- and two-phase flow, heat transfer, mass transfer, and hydraulic instabilities within the system.
- Safety System Response: The code includes models for safety systems such as emergency core cooling systems, containment systems, and reactor protection systems. It evaluates the effectiveness of these systems in mitigating accidents and ensuring reactor safety.
- Severe Accident Analysis: ATHLET has capabilities to simulate severe accident scenarios, including core degradation, hydrogen production, containment pressurization, and fission product release. This is crucial for assessing severe accident management strategies and improving reactor safety.
- Validation and Uncertainty Analysis: ATHLET is extensively validated against experimental data from various facilities, including integral test facilities and separate effect test facilities. Additionally, it provides tools for uncertainty analysis to quantify the uncertainty associated with model predictions.

To create a corresponding model in ATHLET based on HTR-50 parameters, it's important to note that ATHLET cannot precisely map the multilayer material relationships in fuel pebbles. Therefore, for simplicity, a two-layer spherical fuel element model composed of UO_2 and graphite is used. The radius of UO_2 can be calculated as an equivalent volume based on the presence of 15,000 TRISO-coated fuel particles dispersed in the graphite matrix. The calculation formula is as follows:

$$N * \frac{4}{3}\pi r_c^3 = \frac{4}{3}\pi r_a^3 \tag{27}$$

Where N denotes the number of TRISO coated particles, r_c is the radius of the UO_2 layer within the coated particle, and r_a is the fuel radius within the spherical heat structure in ATHLET.

The reactivity is primarily composed of control rods and feedback, as shown in Equation (28). The feedback of reactivity in this thesis is based on the reference [61]and the programmer manual of ATHLET. This study mainly considers the temperature feedback of the moderator and fuel while neglecting the temperature and density feedback of the helium. All the temperature reactivity coefficients are calculated by the HTR-50 model in Serpent.

$$R_{Tc}(t) = \frac{1}{\sum_{i=1}^{NS} V_{S,i}} \cdot \sum_{i=1}^{NS} \left[R_{Tc,i}(t) \cdot V_{S,i} \right] \tag{28}$$

$$R_{Tc,i}(t) = C_f \cdot (\sqrt{T_{c,i}(t, V_{S,i})} - \sqrt{T_{c,ref}}) + (\alpha_r + \alpha_m)(T_r - T_{r,ref}) \tag{29}$$

Where R_{Tc} denotes the reactivity contribution if the core temperature, and $V_{S,i}$ denotes the Volume of fuel rod segment i. C_f are the Reactivity coefficient for fuel temperature. The $T_{c,i}(t, V_{S,i})$, $T_{c,ref}$, T_r and

$T_{r,ref}$ denote the core temperature in rod segment *i* at problem time *t* ,the reference core temperature, the reflector temperature and reflector reference temperature. α_r, α_m is the temperature reactivity coefficients of the reflector and moderator respectively.

The expansion coefficient of graphite is dependent on the temperature, a conservative value of -4.0×10^{-6}K^{-1}is selected for the calculation of temperature feedback coefficient in the Serpent model.

2.3.5. Steady state verification

Based on the constructed HTR-50 model, the steady state calculation results are validated for the working conditions when the depth of the inserted rod is 50cm, 80cm, and 100cm, respectively. Typically, control rod materials are composed of indium-silver-cadmium alloys. However, for computational convenience, an equivalent neutron absorber B-10 with a density of 0.01119g/cm^3 (insert the specific value) has been introduced.

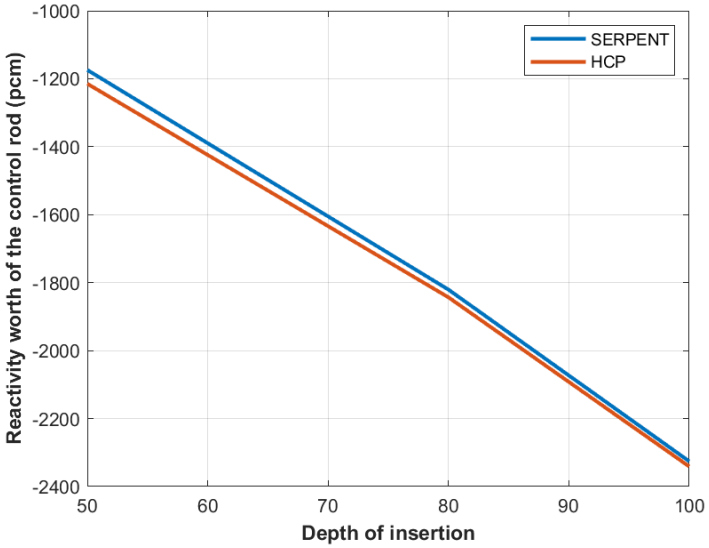

Figure 36 Reactivity of the HTR-50 during control rod inserting process

As shown in Figure 36 and Table 4, after the control rod is inserted 50 cm, the SERPENT and HCP calculations show a negative reactivity insertion of 1214.7 pcm, and1174.3 pcm, respectively, with an error of approximately 3.3%. When the control rod is inserted 80 cm, the calculated negative reactivity insertion is 1843.3 pcm, and 1820.6pcm, respectively, with an error of about 1.23%. The error is calculated by follow equation:

$$E = \frac{Rho\_HCP - Rho\_Serpent}{Rho\_Serpent} * 100\% \tag{30}$$

After the control rod is inserted 100 cm, the SERPENT and HCP calculations indicate that negative reactivity is introduced, with a minimal error of just 0.65%. The two codes show good consistency. The comparison with SERPENT results demonstrates that the HCP control rod insertion method based on the flexible curtain approach can accurately map the reactivity changes due to control rod insertion and withdrawal, effectively reflecting neutron behavior.

Table 4 Reactivity comparison of HTR-50 control rod insertion process

Rod Depth(cm)	R_HCP(pcm)	R_SERPENT(pcm)	Error%
50cm	-1174.3	-1214.7	3.33%
80cm	-1820.6	-1843.3	1.23%
100cm	-2325.9	-2341.1	0.65%

2.3.6. Transient verification

The transient results after insertion of the control rod at 50 cm are compared with the transient results based on ATHLET. After the introduction of negative reactivity at 100s, more neutrons will be absorbed by the absorber isotope introduced by the control rod. At this point the reactor power will decrease, and the outlet temperature of the helium will decrease until a new equilibrium is reached.

Due to the differences in the thermohydraulic and neutron kinetic models between ATHLET and HCP, as shown in Figure 37, there are slight variations in the internal temperature distribution during the initial steady-state condition, with an outlet temperature difference of about 1℃. The power of HTR-50 based on HCP and ATHLET reaches its minimum at 109.5 seconds and 101 seconds, with values of 66% and 70%, respectively, after the control rod is inserted at 100 seconds. The power then gradually increases to the same new steady state point of 93%. The outlet temperatures finally stabilize at 608℃ and 609℃ with an error of only 0.16%. The results demonstrate that HCP can accurately predict the system responses after introducing reactivity.

The significant differences in transient behavior can be attributed to two main reasons: first, HCP uses a full 3D core modeling approach, while ATHLET employs a point reactor model for neutronics, with simplifications in the thermal-hydraulic domain. Even though accurate parameters from SERPENT were employed, there are still inherent discrepancies due to modeling approaches. At the same time, AHTLET is unable to accurately model the fuel spheres of TRISO Particles dispersed in the carbon matrix. Therefore, in this thesis, an equivalent volume approach is used, which inevitably reduces the heat transfer area and causes the transient process to change temperature more slowly than the actual process, which is in agreement with the results obtained. Secondly, we derived C_f and α_m in detail using Serpent, but did not calculate specific reflector temperature feedback coefficient α_r. Instead, we directly referenced results from other literature [43]. Different parameters of HTGRs have varying α_r values, so this simplification could potentially introduce errors. Nevertheless, the result shows a good agreement in the transient results between the two codes in a general way.

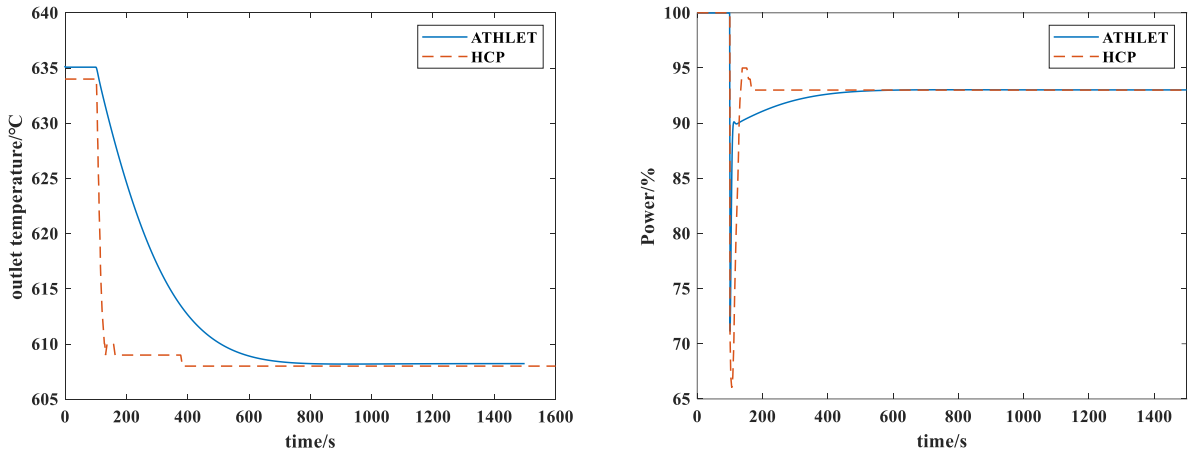

a) Outlet temperature b) Power

Figure 37 Outlet temperature and power of the HTR-50 during the rod insertion transient

3. Neutronics and Fluid dynamics Scenarios of HTR-PM

Analyzing HTGR behavior across various time scales is imperative for comprehensive understanding and ensuring safe, reliable operation. Short-time scale analysis (seconds to minutes) is crucial for assessing transient responses and optimizing startup and shutdown procedures. Medium-time scale analysis (minutes to hours) enables evaluation of load-following capabilities and accident mitigation strategies. Long-time scale analysis (hours to days) is essential for studying coolant transients and fuel integrity over extended periods. Lifetime analysis (years to decades) is necessary for evaluating material degradation and ensuring long-term safety and performance. By conducting analyses across these time scales, operators and designers can effectively manage risks, optimize operational procedures, and ensure the integrity of HTGRs throughout their lifespan.

After the expansion of the control rod functionality in HCP, it is now more suitable than historical codes for analyzing the behavior of HTGRs across different time scales. Specifically, it can analyze and simulate various behaviors of HTGRs across different time scales using the same model. Additionally, it can handle complex scenarios, encompassing both long-term and short-term dynamic behavior simulations.

This thesis will use the currently operational commercial Advanced High-Temperature Gas-cooled Reactor (HTR-PM) system as a case study to establish a relevant physical thermal-hydraulic model using HCP. Leveraging the SERPENT model of HTR-PM as a reference, a code-to-code comparison validation of the HCP model was conducted to ensure the quality of the code and the correctness of the results. Based on the established model of HTR-PM, short-term scale simulations of thermal-fluid behavior under equilibrium core conditions were performed using HCP. The critical thermal-fluid parameters design of HTR-PM was evaluated by comparing it with models based on ATHLET and literature.

In this section, the focus is on the steady-state and transient responses of the HTR-PM at short time scales, primarily handled by HCP's MGT-N and MGT-FD modules. The main exploration in this section includes the following steady-state and transient scenarios:

1） Firstly, steady-state thermal-fluid analysis of the HTR-PM model, coupled with HCP's neutron (MGT-N) and fluid dynamics (MGT-FD) modules, is conducted. Simulation results are compared and validated against SERPENT models and literature findings.
2） Secondly, simulations and analyses of various transient scenarios at multiple short time scales were conducted based on the model. These scenarios include changes in helium inlet temperature, insertion and withdrawal of control rods, and variations in helium flow rate. Simulation results were compared and validated against models based on ATHLET and selected literature.
3） Finally, based on the established model, the PLOFC accident is simulated and analyzed by combining short-term and mid-term core behaviors. The results are compared with the selected reference literature, demonstrating the inherent safety of HTR-PM under this accident scenario.

3.1. HTR-PM model

As mentioned in part 1, the HTR-PM is a pioneering nuclear energy project based in China, representing a significant advancement in high-temperature gas-cooled reactor (HTGR) technology. Spearheaded by China Huaneng Group, China National Nuclear Corporation (CNNC), and Tsinghua University, the HTR-PM project aims to demonstrate the feasibility, safety, and commercial viability of this innovative reactor design for electricity generation and various industrial applications [44]. At the heart of the

HTR-PM concept lies a novel modular reactor configuration. Each HTR-PM unit comprises two 250 MW high-temperature gas-cooled reactors, coupled with a steam turbine system to produce electricity. The use of a modular design enables scalability and flexibility in deployment, allowing for the construction of multi-unit plants tailored to meet specific energy needs. the HTR-PM represents a transformative approach to nuclear energy, offering inherent safety, high efficiency, and versatility in application. By harnessing the potential of pebble-bed reactor technology and helium-cooled systems, the HTR-PM project paves the way for a sustainable and resilient energy future, driving innovation and progress in the field of nuclear.

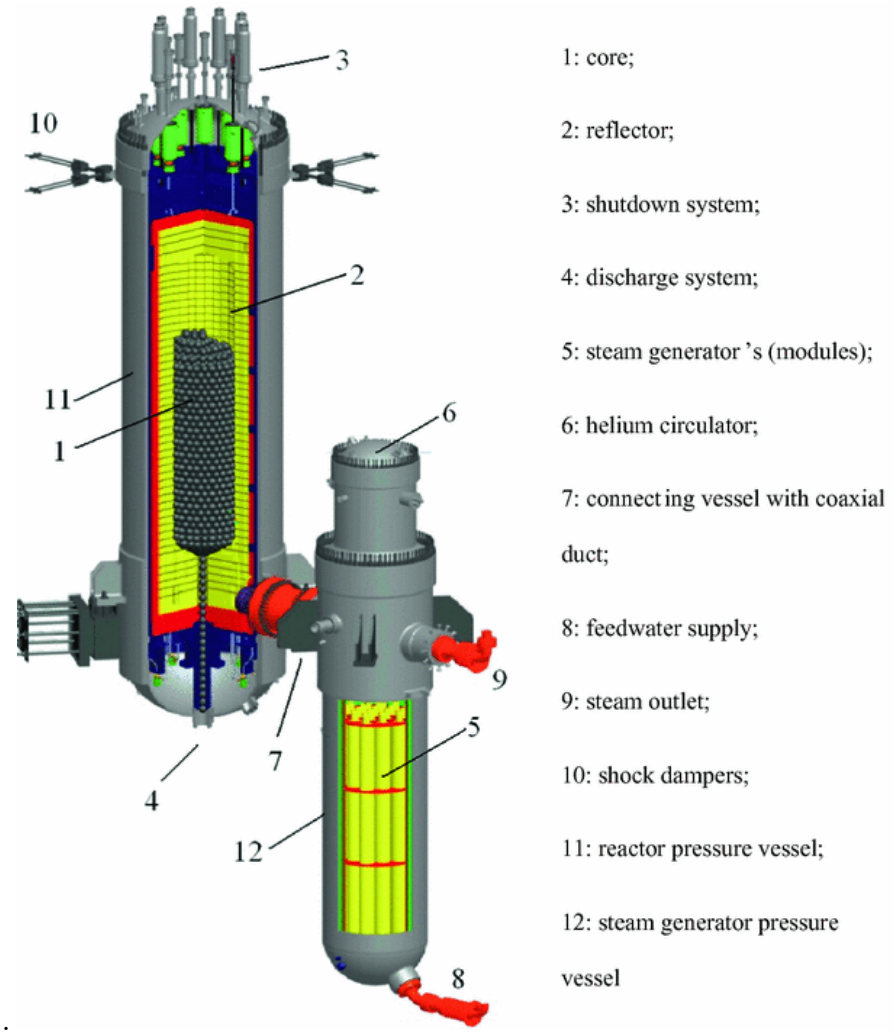

Figure 38 Overview on a module of the HTR-PM[42]

The HTR-PM demonstration plant is equipped with two standard nuclear steam supply system (NSSS) modules, each interlinked with a conventional steam turbine generator. As depicted in Figure 38, each NSSS module primarily consists of a pebble bed reactor, a steam generator, a helium circulator, and a hot gas duct. A horizontal hot gas duct connects the reactor pressure vessel (RPV) and the steam generator pressure vessel, arranged side by side, thereby establishing the primary pressure boundary for one NSSS module. Notable design parameters are detailed in Table 5[45].

Table 5 Primary parameters of HTR-PM

Parameter	Value	Unit
Reactor Power	250*2	MW
Thermal power	458	MW
The load factor	85	%
Active core diameter	3.0	m
Active core height	11.0	m
Reflector thickness	0.75	m
Diameter of central graphite	220	cm
Helium pressure of the primary loop	70	bar
Helium mass flow rate	96	kg/s
Inlet/Outlet helium temperature	250/750	℃
Number of control rods	24	
Number of absorber ball units	6	-
Maximum fuel temperature	1055	℃

The reactor core is composed of a cylindrical loose pebble bed consisting of approximately 420,000 pebbles. Each pebble contains an inner core with a radius of 2.5 centimeters, housing around 12,000 TRISO-coated fuel particles dispersed in a graphite matrix. These TRISO fuel particles have a diameter of approximately 1.0 millimeter and are made up of a 0.5-millimeter diameter UO_2 kernel surrounded by three layers of PyC (Pyrolytic Carbon) and an outer layer of SiC (Silicon Carbide). The fuel pebbles contain approximately 8.5% U-235 enrichment and 9 grams of heavy metal each. The filling factor is 0.61. The graphite reflectors contain 30 coolant channels, 24 control rod channels, and 6 small absorber ball channels. The average designed burnup is 90 GWd/tU, with a maximum fuel burnup of 100 GWd/tU not to be exceeded[44].

The selection of a core diameter around 3 meters facilitates the natural dispersion of decay heat to the surroundings. This dimension ensures effective heat dissipation. Moreover, by constraining the thermal power to 250 MW, the reactor can maintain fuel temperatures below 1600°C even under conditions of "total loss of active cooling." Additionally, accommodating all control and shutdown elements within the side reflector enables efficient operation of both primary and secondary systems. Within the reactor, helium undergoes heating from an initial temperature of 250°C to an average of 750°C. Operating at a pressure of 7 MPa helps mitigate the effects of pressure drop within the relatively large core on the overall pressure within the helium circuit. The first shutdown system entails control rods with electrical drives, ensuring precise and rapid response during emergencies. As a complementary measure, the

second shutdown system employs small absorber balls that descend under gravity into borings within the reflector. Though not required to act swiftly for safety reasons, this system serves as a backup mechanism. Furthermore, akin to practices observed in AVR and THTGR, the reactor can be rendered subcritical over an extended period by removing fuel elements from the core, offering an additional layer of safety and control.

The journey of the cold helium commences with its propulsion by the helium circulator into the RPV, where it descends along the annular space between the core vessel and the RPV. Within the RPV lower cavity, a fraction of the helium is directed towards the fuel elements via the fuel discharging tube. This portion of the coolant subsequently converges with the hot helium plenum, situated within the bottom reflector. Meanwhile, the remaining coolant traverses the bottom steel structures before ascending through the 30 coolant channels within the side reflector. Upon completion of this upward journey, the coolant is gathered within the cold helium plenum positioned in the top reflector. Within the control rod channels, a small segment of the coolant serves the purpose of cooling the control rods before eventually joining the hot helium plenum. Serving as the primary pathway for helium, it flows downward through the pebble bed, whereupon all coolant is collected into the hot helium plenum. Within this plenum, thorough mixing occurs to achieve uniform temperature distribution. Subsequently, the heated helium proceeds from the RPV to the steam generator through the hot gas duct, facilitating heat transfer to the secondary water for steam generation. The cycle repeats as the cold helium, driven by the helium circulator, re-enters the RPV to initiate the subsequent cycle.

3.2. Simulation model

In this section, to simulate the steady-state and transient characteristics of HTR-PM at short time scales, relevant models are established based on the thermal-neutron module in HCP, primarily the MGT-FD and MGT-N modules. The fuel management module and burnup calculations, which are relevant for medium to long-term simulations, will be established in the next section.

A physical thermal-hydraulic model of the HTR-PM is established based on the coupling of the MGT-N and MGT-FD sub-modules in HCP to present the thermal-hydraulic behavior of the reactor core under steady-state and short-term transient conditions. The HTR-PM computational model established based on HCP according to the above data is shown in the Figure 39. This model is capable of analyzing neutron kinetics in the core, fluid flow in the primary loop, solid heat conduction within the reactor, and convection between gases. The model adopts a "r-z" 2D approach to simulate the 3D core modeling scheme.

The model's geometry is defined by 20 meshes in the axial direction and 40 meshes in the radial direction, ensuring comprehensive coverage and accuracy as Figure 39 shows. Key components accounted for in the model include the pebble bed, control rod channel, flow channel in the reflector, carbon brick, and side reflectors, as well as the leakage flow region and air gap. Additionally, the model incorporates the necessary pipes and ducts to simulate the intricate flow dynamics within the system.

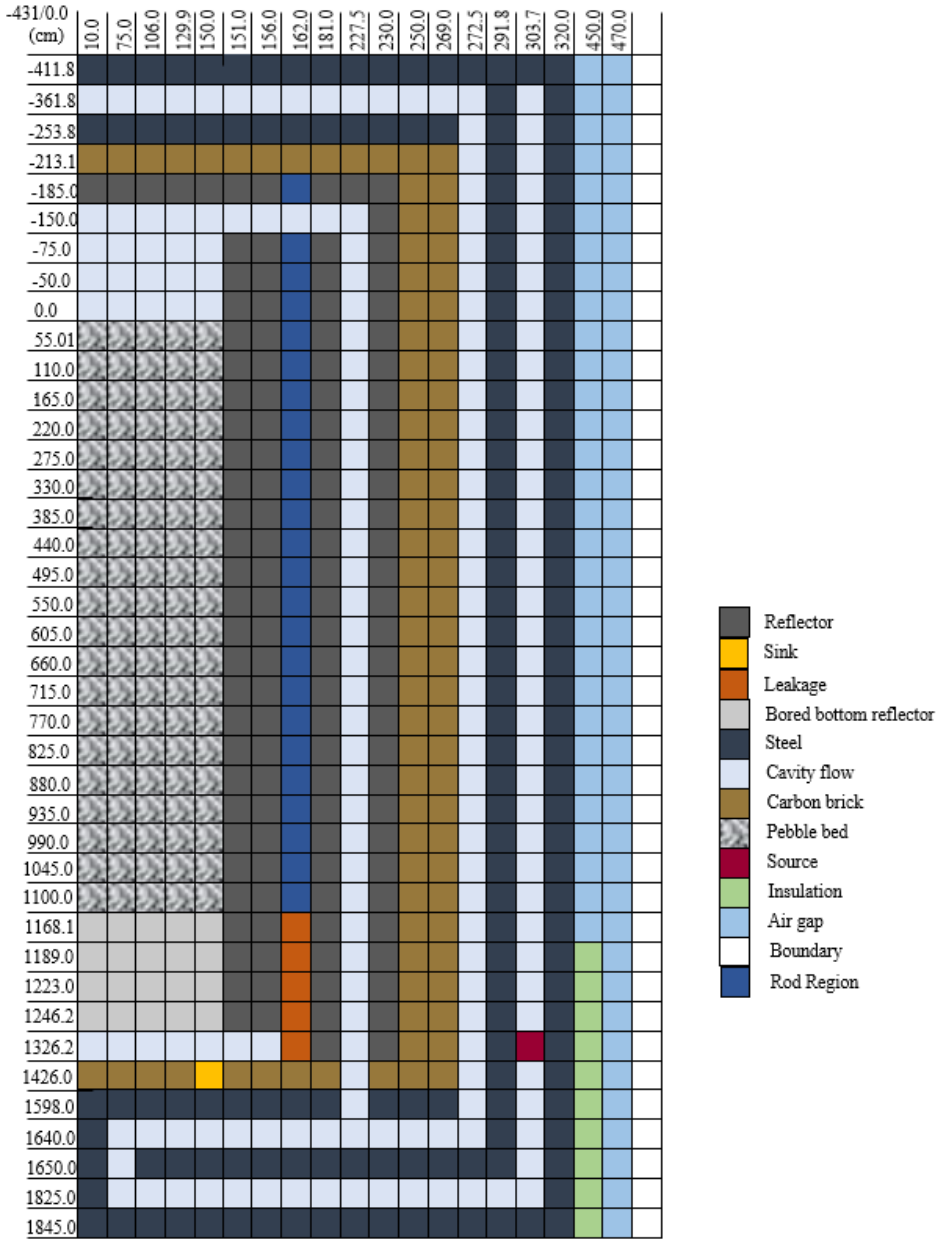

Figure 39 HTR-PM calculation model

3.2.1. Thermal model

The model includes six different calculation domains: fuel, void, nuclear, fluid, solid, and rod, along with the utilization of 38 different components. The pebble bed is represented as a cylinder measuring 150 cm in radial direction and with an average height of 1100.0 cm in the axial direction, encompassing the pebbles within the cone. The pebble bed is characterized as a homogeneous assembly with a filling factor of 0.61, featuring pebbles of 6 cm diameter. Thermal conductivity in the model is governed by a blend of Zehner-Schlünder [46] and Robold laws [47], chosen for their temperature/dose dependency

typical of HTGR pebble beds, with the maximum value of both laws employed. The heat capacity($\frac{J}{cm^3 \cdot K}$) attributed to reactor graphite(NGB-10) is defined in following equation：

$$c_p = 1.75(0.645 + 3.14 \cdot 10^{-3} \cdot T - 2.809 \cdot 10^{-6} \cdot T^2 + 0.959 \cdot 10^{-9} \cdot T^3) \tag{31}$$

The reflector graphite is modeled with a complex approximation that accounts for temperature and dose effects. The conductivity of non-irradiated graphite at 40°C can be expressed as a factor used to characterize the material's thermal properties.

$$\lambda(T, \lambda_0) = \lambda_0 (1 - 1.084(\frac{T}{1000}) + 0.743(\frac{T}{1000})^2 - 0.213(\frac{T}{1000})^3) \tag{32}$$

Where, T denotes the temperature of pebble bed and λ_0 denotes the material factor.

For carbon brick, the heat conductivity is given by:

$$\lambda_b = 0.05 + 0.03 \times 10^{-3} T, \qquad T \le 1000\,°C \tag{33}$$

The specific heat capacity of the carbon brick is:

$$\begin{aligned} &C_v = 1.55 \times (0.645 + 3.14 \times 10^{-3} T - 2.809 \times 10^{-6} T \ + 0.959 \times 10^{-9} T^3) \\ &T \le 1000°C \end{aligned} \tag{34}$$

The pebble bed is encompassed by graphite reflectors, sharing similar material properties. Reflectors' thermal conductivity and heat capacity laws are aligned with those of the reactor graphite. Control rods are depicted as a flexible curtain with fixed nuclide inventories. The inclusion of air gaps, cavities, and gas plenums is essential for understanding heat release from the core during accidents, thus they are duly incorporated into the model. The flow heat transfer parameters elucidate the extent of interaction resulting from temperature disparities between the flowing medium and the solid materials it contacts. These parameters were previously outlined in TINTE [13]. The flow heat transfer equations from solid material to the fluids are shown below:

$$a_f = \frac{A}{V} \frac{\lambda_f Nu}{D} \tag{35}$$

$$q_f = a_f (T_s - T_f) \tag{36}$$

Where,

A = the effect solid surface;

V = volume of the control unit;

λ_f = the thermal conductivity of the fluid;

Nu = the Nusselt number;

d = the equivalent hydraulic diameter;

a_f = the temperature difference proportional parameters of fluids and solid material;

T_s , T_f =the solid temperature and fluids temperature respectively.

For vertical pipe/block or cavity mesh configurations, the Nusselt number calculation distinguishes itself by considering the maximum value among Nu_t, Nu_{l1}, and Nu_{l2}:

$$Nu_t = \frac{\xi^* / 8(\mathrm{Re}-1000)\,\mathrm{Pr}}{1+12.7\sqrt{\xi^* */8}(\mathrm{Pr}^{2/3}-1)}(1+(d/l)^{2/3}) \tag{37}$$

$$Nu_{l1} = \sqrt[3]{3.66^3 + 1.61^3\,\mathrm{Re}\,\mathrm{Pr}\,d/l} \tag{38}$$

$$Nu_{l2} = 0.664\sqrt[3]{\mathrm{Pr}}\sqrt{\mathrm{Re}\,d/l} \tag{39}$$

The Nusselt number is computed in relation to laminar flow, with the maximum value being selected from Nu_{l1} and Nu_{l2}.

Where,

Nu_t = the Nusselt number is evaluated relative to its turbulent flow value;

Re = the Reynolds number;

Pr = the Prandtl number;

l = the length of the mesh;

Here, the Prandtl number and flow resistance coefficient ξ^* are calculated as follows:

$$\mathrm{Pr} = \frac{\mu c_p}{\lambda_f} \tag{40}$$

$$\xi^* = (1.82\log_{10}\mathrm{Re}-1.64)^{-2} \tag{41}$$

Where, c_p denotes the specific heat capacity, μ is the dynamic viscosity.

3.2.2. Kernel Temperature model

The fuel elements of HTGR incorporate a notable quantity of Tri-structural-Isotropic (TRISO) coated particles. Situated at the center of each coated particle is a UO_2 kernel, enveloped successively by a porous carbon buffer, inner pyrolytic carbon, silicon carbide, and outer pyrolytic carbon, extending from the core outward. Notably, in both homogeneous temperature computations and pebble temperature assessments, the fuel temperature—the central temperature of the coated particles—is not factored in. To address this, MGT-3D employs an overheating model to gauge the temperature differential between the fuel kernel and the graphite matrix, by homogenizing the coated materials and assuming a temperature differential between the UO_2 kernel and the graphite matrix.

Illustrated in Figure 40, the particle overheating model establishes a correlation between moderator temperature and fuel temperature.

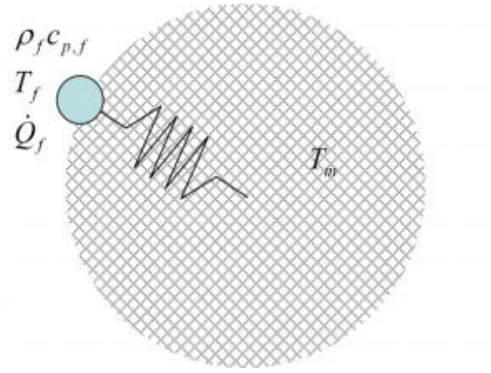

Figure 40 Overheating model [13]

This correlation method adopts an equivalent of a lumped mass heat transfer model, treating the fuel particle as a singular point and the fuel moderator as another point, representative of the pebble's fuel zone's moderator temperature. It's essential to acknowledge that this model's validity hinges on certain assumptions. Firstly, the heat emanating from a fuel particle is assumed to be independent of space, implying uniform distribution throughout the fuel zone, with each particle contributing equally to power generation. Secondly, the UO_2 fuel kernel is presumed to possess substantially higher heat conductivity, capacity, and density compared to the relatively lower values of the coating layers in terms of heat capacity, density, and thickness. Thirdly, owing to the limited understanding of the thermodynamic properties of the UO_2 layers and particle coatings over time, simpler models are preferred for correlation over complex ones. The model equation describing this system is as follows:

$$c_f \rho_f \frac{dT_f}{dt} = \dot{Q}_f''' - \frac{1}{\alpha_f}(T_f - T_m) \tag{42}$$

Where, the ρ_f denotes the density of fuel, $\dot{Q}_f'''$, c_f denotes power density and heat capacity of the fuel respectively, T_f and T_m are the temperature of fuel and moderator . α_f denotes the heat flux resistance.

The primary contribution to heat flux resistance comes from the coating layers, although all heat is assumed to be retained within the fuel kernel. The power density within the fuel kernel is derived from the localized nuclear power density. Subsequently, the power production is integrated into the equation:

$$\dot{T}_f = \frac{1}{\rho_f c_f} \frac{\dot{Q}_f'''}{\dot{Q}_l'''} \dot{Q}_l''' - \frac{1}{\alpha_f \rho_f c_f}(T_f - T_m) \tag{43}$$

Where the $\dot{Q}_l'''$ denotes homogeneous nuclear power density.

At the heart of this correlation method lies the parameter "αf", depicted as a resistor in Figure 40. It serves as the crucial factor in determining the temperature difference between the fuel kernel and the moderator. The effective flux resistance is derived from the equation.

$$\alpha_f' = \frac{\dot{Q}_f''}{\dot{Q}_l'''} \alpha_f \tag{44}$$

Where the $\alpha_f^{'}$ denotes the effective specific resistance of a coated particle. The determination of the effective specific resistance of a coated particle is not conducted within HCP, thus necessitating user input. This task presents difficulty as it relies on the temperature disparity within a reactor. Typical values for this parameter typically fall within the range of 0.5 to 3.

3.3. Simulation results

3.3.1. Fresh core

For this calculation，The HTR-PM models are built based on HCP and SERPENT according to the principles above. In the core and cone area, fresh fuel pebbles are utilized, arranged in a hexagonal regular lattice distribution, achieving a filling factor of 0.6046. This design choice stems from the limitations of Serpent in simulating random pebble distributions within reactors containing a cone area. In this case, control rod zone is considered according to the relevant nuclide composition. The fuel temperature and moderator temperature are fixed at 1000K. The results are shown in Table 6.

Table 6 Results of HCP and Serpent models（He）

Keff_HCP	Keff_SERPENT	Error %
1.26811	1.27270	0.36

The calculation results show that the error between the HTR-PM model established based on HCP and the SERPENT model is only 0.95%, indicating the consistency between them. The error is calculated as follows:

$$Error(\%) = \frac{k_{hcp} - k_{serpent}}{k_{serpent}} \cdot 100\% \tag{45}$$

This not only confirms the high accuracy of HCP but also lays the foundation for simulating other dynamic behaviors of reactor cores.

3.3.2. Control rod movement scenario

In the second section, this thesis presents a method for a "Flexible Curtain" control rod system in HCP based on dynamic changes in nuclide concentrations, which has been implemented in the latest version of HCP. This case study combines the flexible curtain with the HTR-PM model to simulate control rod extension scenarios and compares and analyzes them with the SERPENT model. To simplify the model while ensuring its effectiveness, this case study incorporates the effect of control rods by adding a strong neutron absorber, B-10, in the control rod region, thereby altering the cross-sections within the nodes. In this scenario, the control rods are initially positioned at the top of the control rod channels and are not inserted. At 50s, 100s, and 150s, the control rods are inserted to depths of 110cm, 165cm, and 275cm, respectively. The computed results are shown in Figure 41 and Table 7.

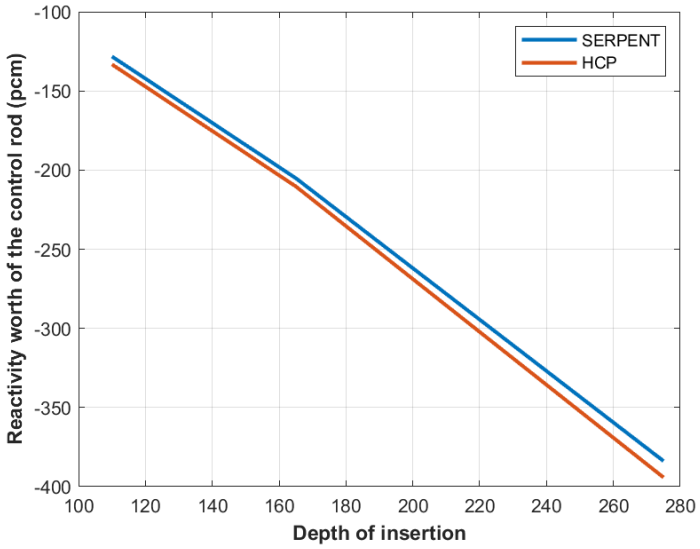

Figure 41 Reactivity of the HTR-PM durig control rod inserting process

Similarly, as shown in Table 7, it can be observed that compared to the SERPENT results, the average reactivity error of HTR-PM after control rod insertions is below 4.0%. In the HCP model, the negative reactivity decreased -128.3pcm, -205.1pcm, and -383.8pcm respectively, after the insertion of multiple control rods, while in the SERPENT model, decreased -133.27pcm, -210.3pcm, and -394.2pcm respectively. The trends of the results from both codes are consistent. The computation in HCP took approximately 278 seconds. This indicates, on the one hand, the high precision of the neutron model for HTR-PM based on HCP, and on the other hand, it demonstrates that the proposed modeling method for the flexible curtain control rods can be well adapted to HCP with a high level of coupling and efficiency.

Table 7 Results of the HTR-PM control rod inserting process

Insertion depth	R_HCP (pcm)	R_SERPENT (pcm)	Error
110	-128.25	-133.27	3.9%
165	-205.14	-210.34	2.5%
275	-383.84	-394.20	2.6%

3.3.3. Steady-state thermal fluids analysis

In reactor design, thermal-hydraulic design is crucial for ensuring the healthy operation of the reactor under various conditions. The task involves predicting thermal-fluid parameters across different operational conditions, analyzing temperature distributions within the reactor and fuel elements, and assessing coolant flow and heat transfer characteristics. Additionally, it ensures that the heat transport capability matches heat generation in the core, guarantees reactor safety during normal operation, and provides a basis for transient analysis of various accident scenarios. In this case, based on HCP, a steady-state thermal-fluid analysis of the HTR-PM equilibrium core was conducted, evaluating parameters

such as maximum fuel temperature, moderator temperature, and primary loop pressure at different power levels.

For an HTGR, the maximum fuel temperature is a critical safety parameter, as exceeding the safety limit could lead to accidents. The safety limit for fuel temperature in the HTR-PM is 1620 ℃, while the normal operating temperature is 1200℃ [43][45]. The rated mass flow rate during normal operation is 96 kg/s. When the reactor operates at rated power, the temperature distribution of solid and fluid inside the reactor is depicted in Figure 42.

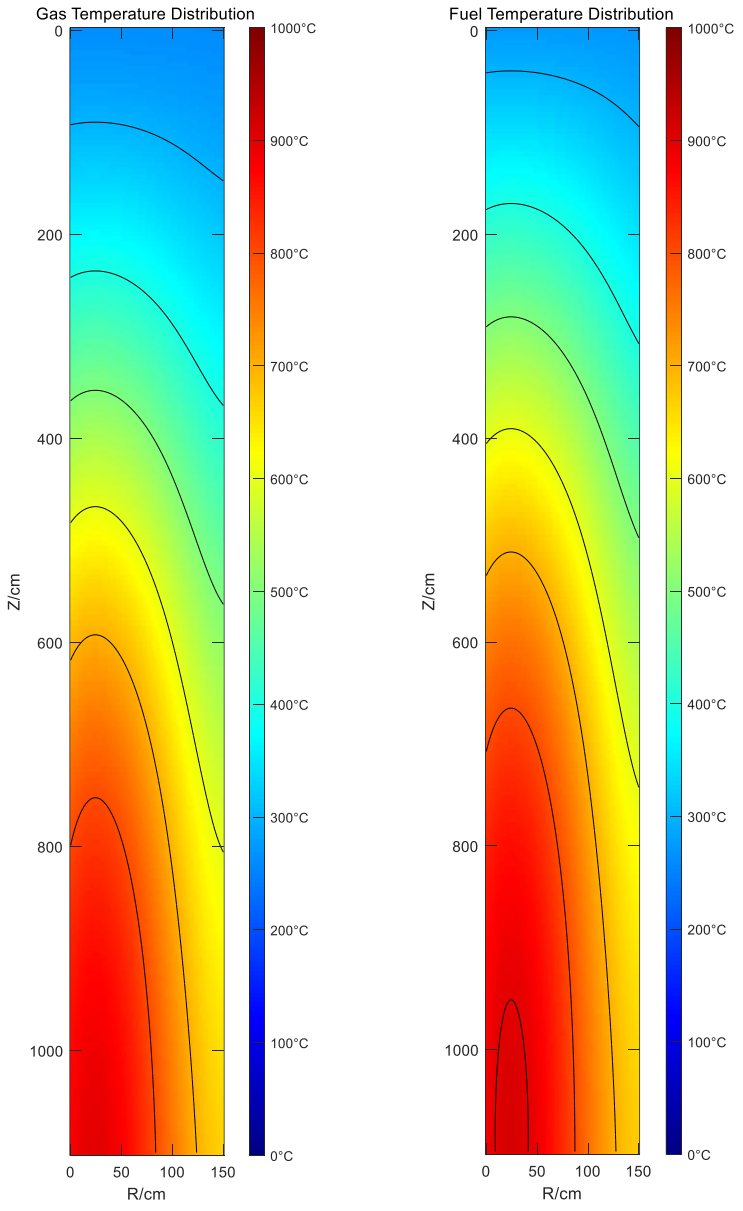

Figure 42 Steady-state temperature distribution of HTR-PM

Helium enters the reactor core at 250°C from the inlet, and the fission heat is transferred to the helium through forced convection. From the isotherm diagram, it can be seen that the coolant mainly heats up along the axial direction, with the helium outlet temperature around 750°C at the reactor outlet. The highest fuel temperature in the core is 901°C, which is far below the design limit of 1620°C. Due to the

combined effects of the helium's cooling capability and the power distribution, the temperature distribution of the helium and the fuel show similar characteristics. The region with temperatures above 900°C is mainly located between 950 and 1100 cm along the vertical axis.

As shown in Figure 43, the radial temperature distribution of helium and fuel at different heights in the core is presented. It can be seen that the temperatures of both helium and fuel vary more significantly near the core outlet. This is partly due to the different power distribution in the core and the varying amount of energy carried away by helium at different locations, with more energy being carried away closer to the core outlet. Compared to the literature results [45], there is a small deviation within the range of r = 0-1.4m, while there is a larger deviation at the edge of the pebble bed from r = 1.4-1.5m. Within the comparable range, the HTR-PM model based on HCP shows a high degree of consistency with the steady-state calculation results and the published reference results.

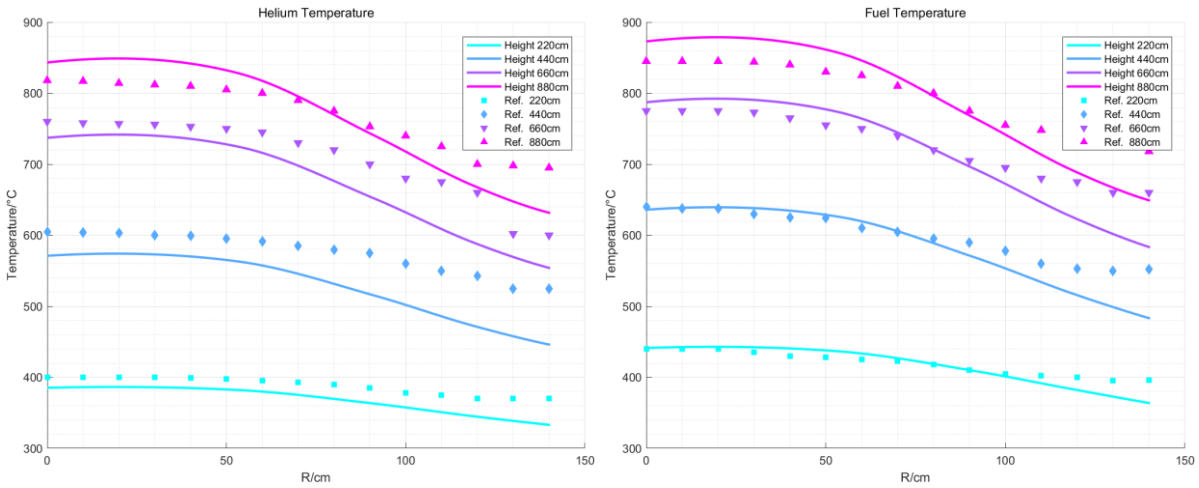

Figure 43 Temperature distribution along the radial direction.

To ensure that the HTR-PM remains within the specified maximum fuel temperature bounds, steady-state results are provided based on conservative estimates of mass flow rate. The standard operational mass flow rate for the HTR-PM is 96 kg/s. Design specifications dictate that 1% of this flow is discharged through the fuel discharge pipe, while 3% is channeled through the control rods; additionally, there exists a leakage flow between the graphite/carbon bricks. In the design of thermal hydraulics, it is conservatively assumed that 6% of the rated mass flow rate is bypassed. Consequently, the effective mass flow rate responsible for cooling the core is estimated at 90%. Furthermore, steady-state conditions serve as the starting point for transient analysis of various accident scenarios. In the current accident analysis of the HTR-PM, 102% of rated power is chosen as the initial condition [43], and the relevant steady-state thermal-hydraulic parameters are calculated accordingly. The results are shown in Table 8.

Table 8 Results under conservative calculation

Property	HCP			Ref	
Reactor thermal power (%)	100	100	102	100	102
Primary helium mass flowrate (kg/s)	96	86.4	86.4	86.4	86.4
Maximum fuel temperature (℃)	901	971	985	967	980
Maximum coolant temperature (℃)	888	955	973	925	937

The calculated results indicate that even under the conservative assumption that 90% of the rated mass flow of helium passes through the core and cools the pebble bed, and under 102% of rated power, the highest fuel temperature is 985°C, significantly lower than the specified limit temperature. Compared to reference 43, the maximum fuel temperature at 102% power is 5°C higher, which is an acceptable range. This may be caused by some deviations in the modelled structure. This demonstrates the rationality and safety of the HTR-PM design.

3.3.4. Thermal-hydraulic dynamic calculation

In this case, simulations and analyses were conducted on some neutron behaviors and thermal-fluids under steady-state conditions based on HCP for HTR-PM. For reactor computations, initial conditions typically start from equilibrium steady state, and a series of operations may lead the reactor to transient changes and enter into new steady states, such as control rod insertion/withdrawal, changes in feedwater valve openings, etc. As the flagship simulation software for HTGR, HCP enables the simulation of complex dynamic operational scenarios for HTGRs to become a reality.

In this case, as shown in Figure 44, the HTR-PM starts operating from equilibrium after steady-state calculations, with a rated power of 250MW and helium inlet temperature of 250°C. After normal operation for 2 minutes, the helium inlet temperature increase to 300°C at a rate of 25°C/min. At this point, the reactor enters transient calculations until the reactor total power stabilizes, followed by another steady-state calculation where the initial conditions are provided by the last iteration of the transient calculation. Xenon neutron absorption effects are ignored here.

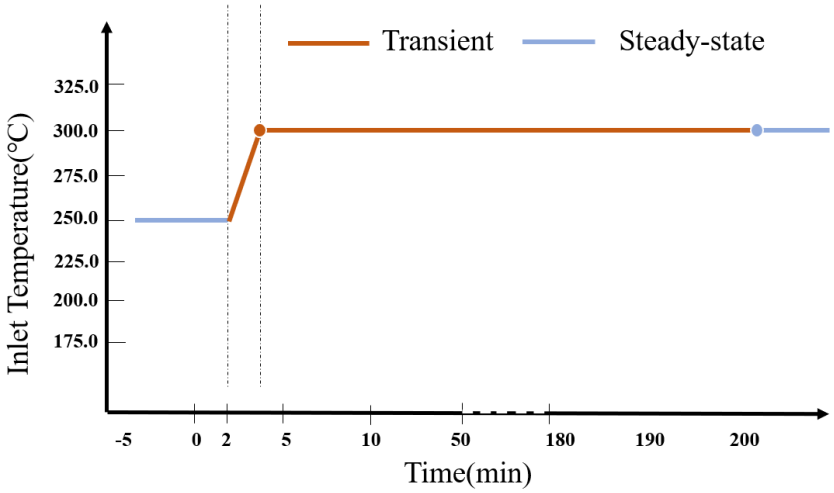

Figure 44 Inlet Helium temperature over time

As shown in Figure 45, the trends of helium outlet temperature and maximum fuel temperature during the transient period are illustrated. HCP starts transient calculations at the 2-minute and continues for 200 minutes before transitioning back to steady-state calculations. Initially, the reactor operates normally for two minutes based on the initial steady-state calculation results. At the 2-minute, the inlet helium temperature increases from 250°C at a rate of 25°C per minute, reaching 300°C by the 4-minute mark and then stabilizing, initiating the transient calculation. As shown in the Figure 45, after the inlet helium temperature changes, the increased coolant temperature causes a decrease in reactivity due to the negative temperature coefficient of reactivity. Consequently, both the power and the maximum fuel temperature exhibit a rapid declining trend until around 6000 seconds, after which the temperature and power changes stabilize. After 200 minutes, the reactor power and maximum fuel temperature reach 221 MW and 874°C, respectively, showing a decrease of 27°C compared to the initial steady-state. Subsequently, the parameters obtained from the transient are used as boundary conditions for steady-state calculations. The calculations indicate that the reactor stabilizes at 220 MW, with a maximum fuel temperature of 873°C, which is only 1°C different from the temperature at the end of the transient period. The initial steady-state calculation yields a k-effective of 1.0034, while the subsequent one results in a slightly lower value of 1.0032. Consequently, based on the transient's calculated data, the reactor enters a stability zone remarkably similar to that observed in the equilibrium state of the first steady-state calculation, occurring at 200 min.

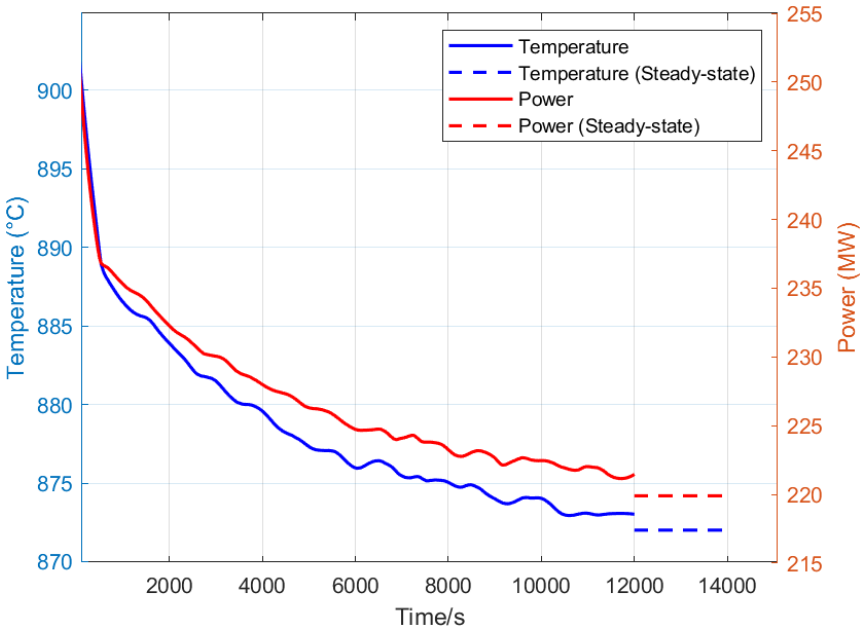

Figure 45 Transient result after inlet tempreture changing

3.3.5. Transient after control rod insertion

This case study investigates the transient response of the HTR-PM reactor following control rod insertion. For HTGRs, control rods are typically made of materials with a high neutron absorption cross-section. When inserted, these materials absorb neutrons within the reactor, thereby slowing down or halting the fission reaction. Operators can control the reactor's power output and ensure safety and stability under various operating conditions by adjusting the position of the control rods. In emergency situations, such as unexpected events or mechanical failures, control rods can be used for emergency shutdowns. By rapidly inserting the control rods into the reactor core, the fission reaction can be quickly stopped, ensuring the reactor's safety.

In this section, the control rods are modeled using a method that maps the addition of strong neutron absorbers. The focus is on exploring the functionality of these control rods and the subsequent dynamic behavior of the HTR-PM.

This case study simulates the insertion of control rods to 165 cm and 275 cm in the HTR-PM using the HCP model based on the flexible curtain method. The results are compared and analyzed against the simulation outcomes from the HTR-PM model based on ATHLET. The HTR-PM model implemented in ATHLET utilizes the prompt neutron group point kinetics equations, incorporating six precursor groups of delayed neutrons. The point kinetics equations are shown as follows:

$$\frac{dn}{dt} = \frac{\rho - \beta}{\Lambda} n + \sum_{i=1}^{6} \lambda_i C_i \tag{46}$$

$$\frac{dC_i}{dt} = \frac{\beta_i}{\Lambda} n - \lambda_i C_i \tag{47}$$

Where, n denotes the normalized neutron flux, β is the total fraction of delayed neutrons, and Λ is the generation time. Here, β is set to 0.00549 and Λ is set to 0.0011 as the reference [48]. Among them,

the reactivity and temperature feedback introduced by the control rod are included. For the calculation method of reactive feedback, we refer to the literature [45] here:

$$\rho = \rho_{rod} + (\alpha_f + \alpha_m)(T_m - T_{c0}) + \alpha_r (T_r - T_{r0}) \tag{48}$$

Where,

$$a_f = -4.36 \times 10^{-5} \quad 1/K$$
$$\alpha_m = -0.94 \times 10^{-5} \quad 1/K$$
$$\alpha_r = 1.49 \times 10^{-5} \quad 1/K$$

Here, a_f α_m and α_r are the fuel temperature reactivity coefficient, moderator temperature reactivity coefficient and reflector temperature reactivity coefficient respectively. T_{c0} is the steady-state core temperature and T_{r0} is the reflector temperature.

As shown in Figure 46, the trends of the maximum fuel temperature are depicted for control rod insertions of 110 cm and 275 cm, respectively. Initially, the HTR-PM operates normally at full power, then the control rod insertion operation begins, and HCP performs transient calculations. From the figure, it can be observed that after the control rods are inserted, the fuel temperature starts to decrease rapidly. This is due to the negative reactivity introduced by the control rods, which causes a reduction in reactor power. For the case of inserting the control rods to 110 cm, a new steady state is approached around 180 seconds, with the maximum fuel temperature in the core being 865°C, which is 36°C lower than the maximum temperature before the insertion.For the case of inserting the control rods to 275 cm, the reactor reaches a new steady state after about 230 seconds, with the maximum fuel temperature being 838°C, a decrease of 63°C from the initial state.It is important to note that the concentration of the strong neutron absorber B10 used here does not match the dosage used in Section 3.3.2 but is instead a more moderate concentration.

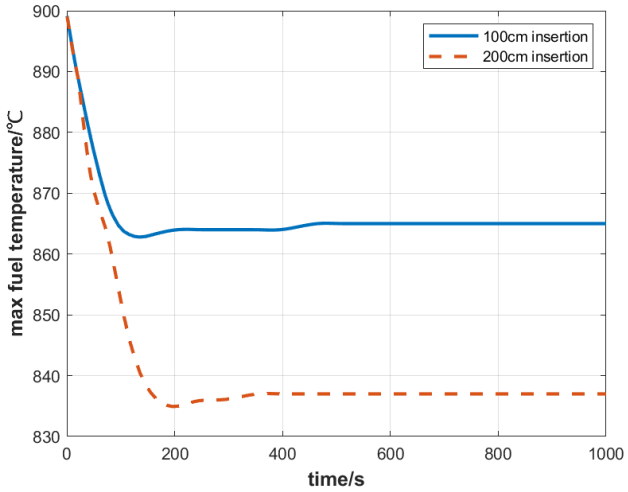

Figure 46 Max fuel temperature after rod insertion

As mentioned in Section 2.3.6, due to ATHLET not being the primary tool for HTGR modeling, there are some assumptions in the thermal-hydraulic modeling that may lead to errors. Here, only ATHLET

and HCP are compared for the power variation after control rod insertion. As shown in the Figure 47 (a), after inserting the control rod 110 cm, both the HCP and ATHLET models rapidly decrease to around 69% and 82% of rated power, respectively. Then, both models start to oscillate rapidly, and after 300 seconds, they both converge to 94% of rated power.

For the case of inserting the control rod 270 cm (Figure 47 (b)), both the HCP and ATHLET models similarly decrease to around 58% and 70%, respectively, and then return to 89% relative power after 400 seconds. This result demonstrates good consistency between the two codes in HTR-PM modeling. The control rod modeling based on the flexible curtain method provides support for transient and steady-state results of control rod movement in HTR-PM, enhancing the capability of HCP in HTGR safety analysis.

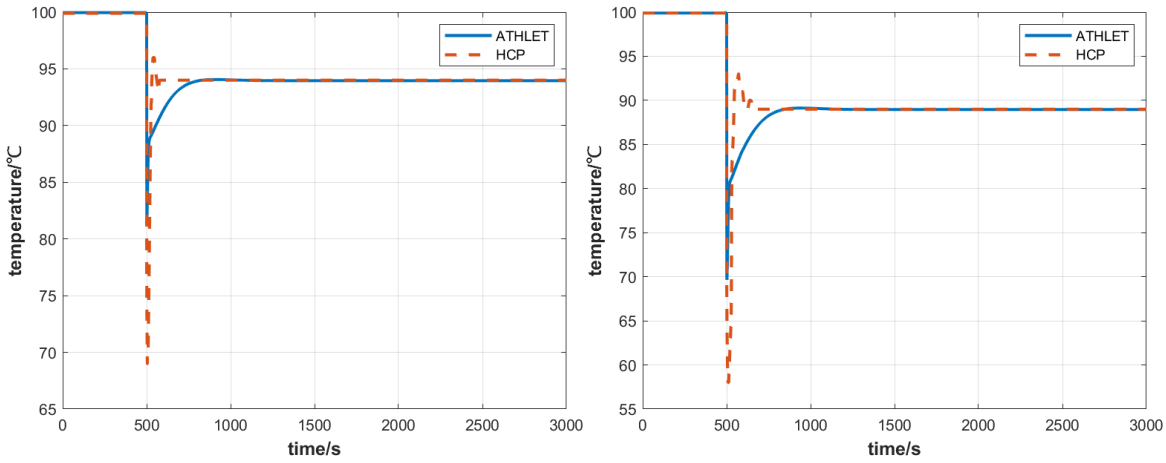

Figure 47 Power changing after rod insertion

3.3.6. PLOFC accidents results

Pressurized Loss of Forced Cooling (PLOFC) is a typical accident condition in HTGRs, such as the failure of helium blower or power loss, resulting in the cessation of forced coolant circulation. During PLOFC, assuming that the pressure control system of the primary circuit can operate normally and maintain the pressure of the primary circuit at the working pressure, natural convection can easily be established due to temperature differences within the core. At this time, the decay heat of the fuel can be carried away through the equivalent conduction of the reflector and natural convection of pressurized helium.

In this case, the reactor initially operates at 100% power. Subsequently, the helium coolant flow rate decreases to 0 kg/s within 1 second. Figure 48 illustrates the power changes during the first 360 seconds following the incident. It can be observed that the reactor power drops sharply due to an emergency shutdown, with decay heat becoming the primary heat source in the core region. The primary circuit pressure is maintained at 60 bar.

When compared to the reference [62], the power decline curve is quite similar, with the relative power dropping to around 5% approximately 100 seconds after the incident. By 300 seconds, all three curves indicate that decay heat has become the dominant heat source.

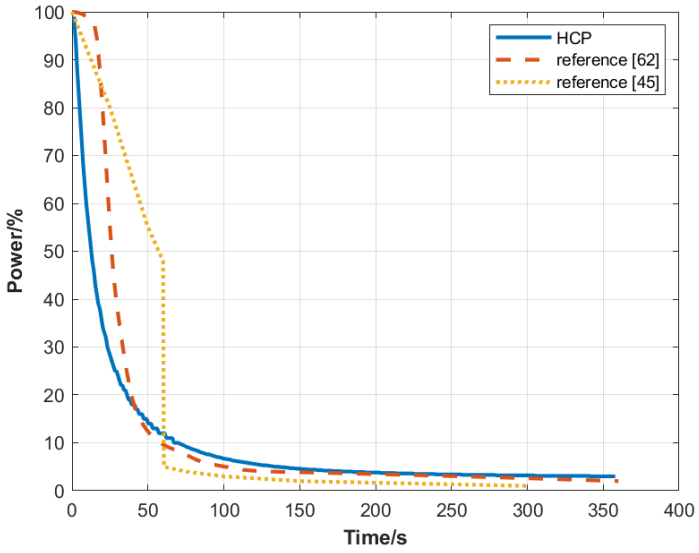

Figure 48 Total power during the first 360s

Figure 49 illustrates the progression of the maximum temperature throughout the simulation period. Over the course of the simulation, the peak fuel temperature can manifest in various regions of the pebble bed. The analysis spans 4,160 calculation time steps, during which no discernible variation is observed in any significant digit of the physically meaningful variables.

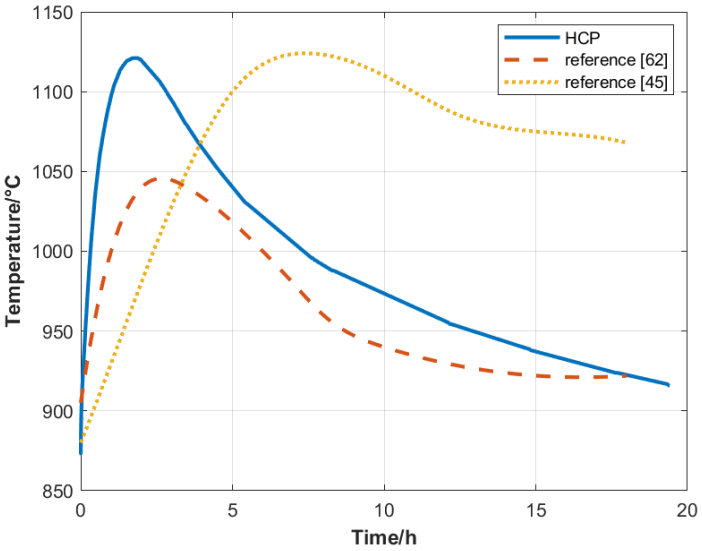

Figure 49 Maximum fuel temperature after PLOFC

At steady-state operation, the highest fuel temperature is 874°C. Compared to Section 3.3.3, the reactor has undergone some refueling operations, resulting in a decrease in the maximum fuel temperature. After the incident, the highest fuel temperature starts to rise, reaching 1125°C at 6300 seconds. In reference [62], the maximum temperature is approximately 1050°C, occurring around 8000 seconds. In reference [45], due to a linear decrease in reactor power 60 seconds before the incident followed by a manual shutdown, more heat remains in the core, resulting in the maximum fuel temperature occurring around 7.5 hours, later than in this study and reference [62].

However, all three results show a consistent trend. Additionally, the maximum temperature remains well below the design limit for the fuel, demonstrating the safety of the HTR-PM high-temperature gas-cooled reactor design.

4. Multi-time scale complex scenario

On a long-term scale, dynamic simulations can be used to study the long-term operational behavior of the HTGR, such as fuel burnup, fuel depletion, and the accumulation of radioactive products over several months or years. These simulations help predict the fuel life under different operating conditions, optimize fuel management strategies, and assess potential issues that may arise during extended operation.

On a short-term scale, dynamic simulations can be used to study the reactor's rapid response and accident scenarios. This includes situations such as startup, shutdown, load changes, and emergency responses. By simulating these scenarios, it is possible to evaluate the stability and safety of the reactor under various operational conditions, providing guidance for operators to take appropriate actions to address potential challenges.

Furthermore, coupling long-term and short-term scale simulations can provide a more comprehensive and realistic understanding of the reactor's dynamic characteristics, enabling the optimization of reactor performance, safety, and stability. For safety, the coupled simulations on both time scales allow for a better understanding of their mutual influences. Coupled long-term and short-term scale simulations can more accurately model the actual operating conditions of the reactor. In real-world operations, a reactor experiences various changes over different time scale. By considering these changes comprehensively, the simulation results can be more reflective of real conditions, thereby improving the accuracy and credibility of the simulations. Such coupled simulations help evaluate the reactor's safety under diverse operating conditions. By simulating long-term behavior, potential safety issues during extended operation can be assessed. Simulating short-term transient behavior, on the other hand, allows for evaluating the reactor's response to sudden events or operational changes. This comprehensive approach provides a more thorough assessment of the reactor's overall safety, enabling the implementation of necessary measures to ensure its safe operation.

Therefore, in this section, to overcome the limitations of past HTGR software that could only simulate specific parts of the reactor, we will utilize the HTR-PM neutron and thermal models established in Chapter 3 and further extend HCP to include fuel management and burnup models. This approach allows HCP to comprehensively simulate and evaluate the dynamic behavior of HTR-PM across both long-term and short-term time scales using a unified model.

This section is organized as follows: First, we will provide a brief introduction to the SHUFFLE fuel management module and the TNT burnup module within HCP. Then, we will establish the HTR-PM fuel management and burnup models based on SHUFFLE and TNT, and couple them with the neutron and thermal models to form an integrated multi-time scale simulation model for HTR-PM. Next, we will simulate the initial core loading pattern of the HTR-PM, analyze its key physical parameters, and evaluate the relevant schemes. Finally, we will simulate and analyze the combined long-term and short-term operational conditions of HTR-PM, discussing some of the interdependencies, assessing the overall safety of the reactor, and addressing new issues arising from the coupling of various codes.

4.1. HTR-PM fuel management and depletion

4.1.1. Seepage and flow tube model

The continuous movement of fuel pebbles is a key feature in Pebble Bed High-Temperature Gas-Cooled Reactors (PB-HTGR). Therefore, accurate fuel modeling is crucial for design, operation, and safety. Here are several important reasons:

1. Temperature and Heat Distribution Variations: The movement of fuel pebbles leads to changes in the temperature and heat distribution within the reactor core. This directly impacts the reactor's thermal characteristics, such as fuel cooling efficiency and the formation and distribution of hot spots. Accurate simulation of fuel pebble movement helps engineers better understand and predict the thermal behavior of the reactor, guiding reactor design and operation.
2. Improved Fuel Redistribution: The movement of fuel pebbles promotes fuel redistribution, thereby improving fuel utilization and the thermal performance of the core. Correctly modeling fuel movement can help optimize fuel management strategies, extend fuel life, and maximize energy output efficiency.
3. Safety Assessment: Fuel pebble movement is critical for reactor safety assessment. In dealing with emergencies or abnormal situations, fuel redistribution and cooling are key factors to ensure safe reactor operation. Proper modeling of fuel movement enables engineers to more accurately assess reactor safety performance under various conditions and develop corresponding countermeasures.
4. Performance Impact: Fuel pebble movement can affect reactor performance, including fuel utilization and thermal efficiency. By accurately modeling fuel movement, engineers can optimize reactor design and operational strategies to maximize reactor performance and economic benefits.

For the purpose, HCP has developed a fuel management module named Software for Handling Universal Fuel Elements (SHUFLE), which includes two management models: seepage and Flowtube.

The seepage model, has been developed to simulate fuel management utilizing the same mesh grid employed for fluid dynamics and neutronics. In this approach, fuel shuffling is represented by a series of seepage processes, illustrated in Figure 50. During the discharge of clusters of pebbles from the lower end of the pebble-bed, one or more voids are created in the lower part of the core. As the discharge progresses, the volume of the pebble-bed situated above these voids may remain stable for a brief period. However, at a certain juncture, the configuration becomes unstable, prompting pebbles to flow and refill the newly formed voids. Consequently, the voids gradually migrate upwards, as depicted in Figure 50. The seepage process continues iteratively until the voids reach the surface of the pebble-bed, at which point the process concludes.

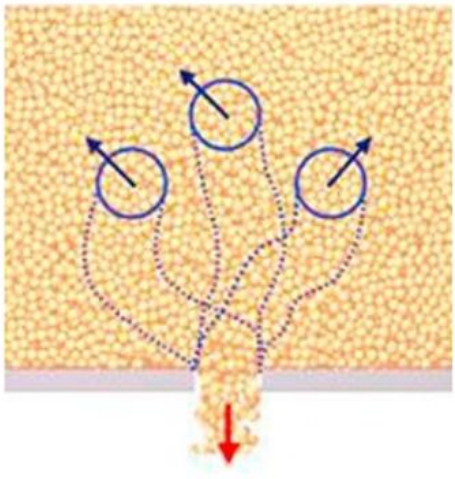

Figure 50 Seepage model[38]

In addition, HCP, referencing traditional codes such as VSOP, has further developed the Flowtube model and coupled it with other HCP modules, making it the primary fuel management model used in HCP.

In the flow tube model, the continuous movement of pebbles is approximated by transferring the contents of larger volumes at discrete time intervals. To facilitate straightforward box-wise movement, the core is divided into flow channels, each further divided into nodes of uniform geometric volume. In VSOP, these nodes are referred to as regions. Pebbles are treated akin to an incompressible fluid, traversing a flow tube with clearly defined boundaries. During a fuel management step, the contents of each node are shifted downward to the node below. The number of nodes within a channel dictates the flow velocity of pebbles within it. However, despite this typically irregular node grid, Cartesian or cylindrical mesh grids are utilized for fluid dynamics and neutronics calculations. Due to the disparity in grids, data must be mapped from one grid to another. To facilitate this mapping, the code requires knowledge of which mesh(es) correspond to which node and to what extent, and vice versa. A shared volume refers to a volume that is shared by or coincides with a single mesh and a single node. Therefore, a shared volume lies entirely within a single mesh and a single node. The shared volume is explained in section 2.1.5.

SHUFLE employs graph theory to facilitate fuel shuffling. Utilizing the Boost Graph Library (BGL), a peer-reviewed C++ library, the code harnesses its versatile functionalities tailored for graph operations. Before commencing calculations, the graph encapsulating all fuel management data is initialized. The node's actual geometry is inconsequential; solely its geometric volume, maximum filling factor, occupied volume by contained batches, and connections to other nodes are vital for fuel shuffling computations. This principle applies to both the flow tube and seepage model.

In the flow tube model, nodes within the pebble-bed form sequential chains, each node having a single precursor and successor node. This differs from junctions in the seepage model. Only nodes eligible for content shuffling are included in this graph, with connections established between nodes where pebbles (batches) can be transferred. Additionally, each inlet and discharge tube correspond to an inlet or outlet port, respectively, modeled as nodes. When discharging a specific volume from the outlet, the code initiates a recursive process, transferring batches to the node below. If the discharged solid volume matches the sum of solid volumes of a single node in each channel, it mirrors the legacy code's behavior. However, discharging any volume from the core may result in batch splitting, increasing the batch count. The ports introduce a vertex between the inlet port and each upper-end pebble-bed node, storing distribution fractions between the inlet port and surface nodes. Figure 51 depicts a reactor core example with four flow channels, each with varying numbers of nodes. Consequently, the pebble-flow isn't parallel. These channels connect to one inlet port at the upper end and one outlet at the lower end. For differing node volumes at the core's upper end, the values are specific to each flow channel.

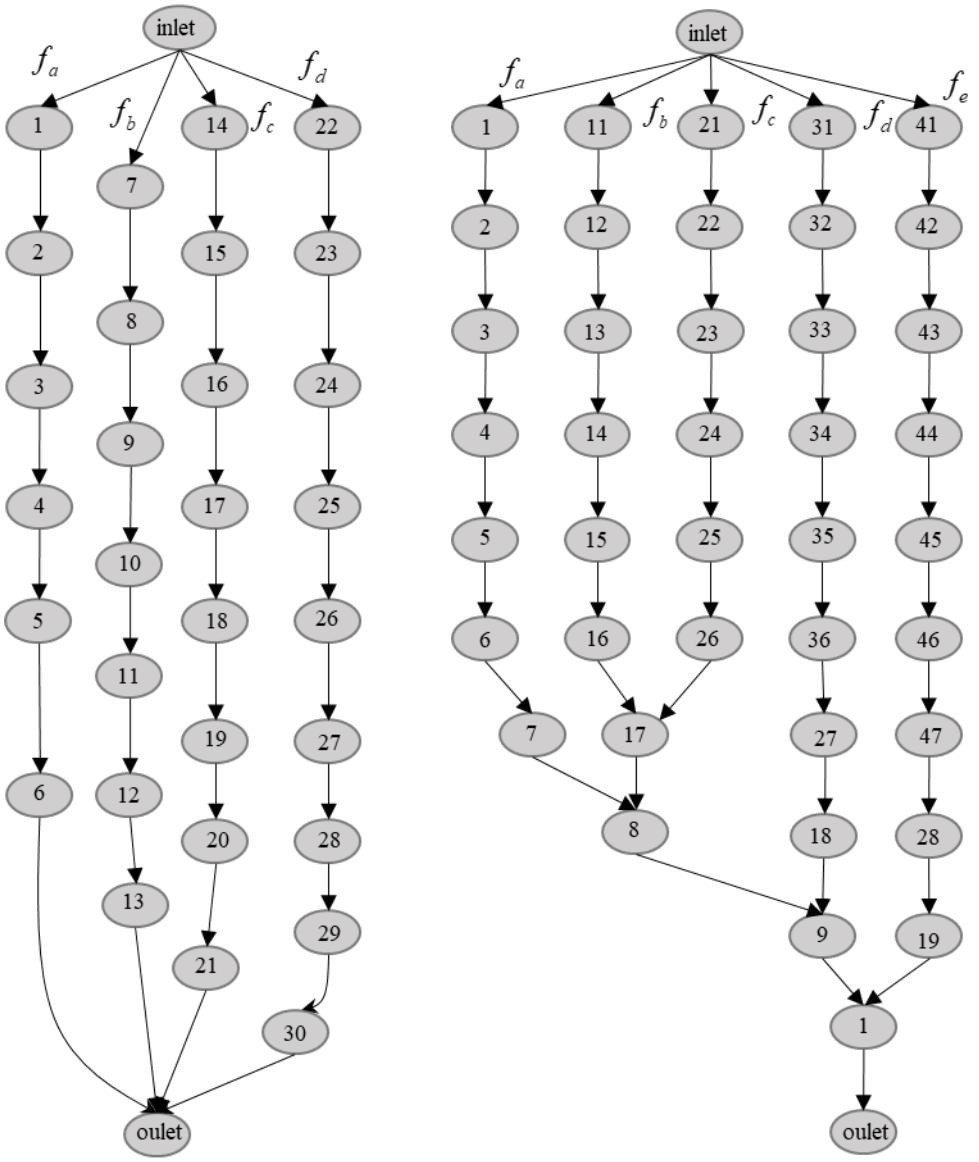

a) Flow tube model b) Seepage model

Figure 51 Exemplary node graphs of core [38]

Following the discharging phase, the topmost point of each flow path remains vacant. Restoring the core to its original level requires introducing pebbles with a combined volume matching the sum of solid volumes fitting into these points through the inlet. In OTTO fuel rearrangement, this volume comprises solely fresh fuel elements, while in fuel rearrangement, it involves a blend of fresh and recycled discharged elements. The inlet initiates a distribution of batch across various channels by partitioning the batches based on predetermined fractions at the nodes.se fractions are predetermined during the pre-processing stage by the code module to ensure that the initial configuration of the pebble-bed surface is reestablished at the conclusion of a fuel rearrangement step. The fractions are calculated as follows:

$$f_i = \frac{V_{Solid,i}}{\sum_i^n V_{Solid,i}} \tag{49}$$

4.1.2. Depletion code TNT

In Section 2.1.7, this study briefly describes TNT. Here, we will introduce the new physical and programming features of TNT compared to ORIGEN.

From a physics perspective, a new feature involves the use of energy-dependent fission yields, when available in the data library. The ENDF/B-VII.0 data files provide fission yields for 30 heavy metal nuclides. Among these, five nuclides have yields for two incident neutron energies, while seven nuclides have yields for three different energies. Another example is the flexibility to add reactions supported by the code. To date, the following processes have been implemented:

- Decay processes: α, β+, β−, EC, IT, SF, n-emission, p-emission, and any combinations (e.g., β−/n).
- Neutron-induced reactions: (n, f), (n, γ), (n, 2n), (n, 3n), (n, p), (n, α).

Another significant enhancement is the capability to provide problem-specific neutron energy spectra and cell data, enabling the dynamic generation of broad-group cross-sections for all nuclides at each burn-up time step. This allows users to move beyond precompiled cross-section sets tailored for typical reactors, giving them the flexibility to input internal data derived from a spectrum code. Additionally, the separate calculation of nuclear power for decay, fission, and capture processes, including both local and non-local heat generation, is an important feature. Unlike traditional methods that use average capture Q values for a given fuel and reactor, TNT utilizes the most up-to-date nuclide vector and distinct Q values for all capture processes available in the data library

In terms of programming, TNT has also made a lot of changes compared to the past. It is developed from scratch with a focus on modern software engineering principles. Written in C++, it utilizes an object-oriented approach, enhancing readability and facilitating future extensions by encapsulating problem-specific data types like Nuclide and Reaction. The code separates data handling routines from algorithms, improving clarity and simplifying implementation. The key features include:

1). Automated Data Generation: TNT automatically generates and stores essential nuclear data such as decay data, cross sections, and scattering matrices for each nuclide. This data is extracted from sources like ENDF/B-VII and serialized into a binary format for efficient storage and retrieval.

2). Library Utilization: The code incorporates well-established libraries like boost and Eigen. Boost provides utilities and data structures, while Eigen facilitates efficient linear algebra operations. Template metaprogramming is extensively used, enabling high-level abstraction and ease of implementation.

3). Efficient Data Processing: By separating data generation and storage concerns, TNT ensures quick setup times and optimized runtime performance. This approach minimizes errors and streamlines computational tasks.

4.2. HTR-PM fuel management model based on HCP

4.2.1. Seepage model

Although HCP currently relies heavily on the FLOWTUBE model for analyzing fuel management in HTGR, here we still build on the SEEPAGE model as a proven model in the past to be used for comparative validation. To simulate the seepage refueling strategy of a HTR-PM in HCP, the reactor core is divided into 5 channels radially and 20 layers axially, as shown in Figure 52. This division creates 100 material regions of equal volume, which serve as the basic units for neutron spectrum calculations.

Each material region is further divided into 15 fuel batches of equal volume, resulting in a total of 1500 batches. Here, each region contains 15 batches to facilitate the modelling of multiple pass strategies.

These batches are the fundamental units for fuel burnup calculation and fuel shuffling. During reactor operation, fuel batches with the highest burnup are discharged from the bottom of the core, while other fuel batches are returned to the top, and fresh fuel batches are loaded at the top to maintain a stable total quantity of fuel spheres. In the core's middle region, fuel batches are shuffled down to neighboring material regions along the channels. This method effectively simulates the multi-pass refueling strategy of the pebble-bed reactor.

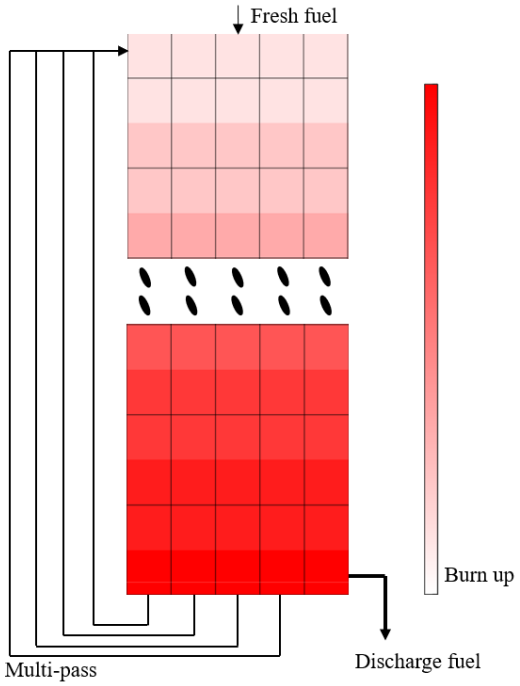

Figure 52 HTR-PM seepage model

4.2.2. Flowtube model

Due to the conical structure at the bottom of the High-Temperature Gas-Cooled Reactor core and the design of the central fuel pebble discharge outlet, the flow behavior of the fuel pebbles varies across different parts of the core. The conical bottom guides the fuel pebbles toward the central discharge outlet, resulting in higher flow velocities in the central region and lower flow velocities in the peripheral regions. The geometry of the conical structure may cause different accumulation patterns of fuel pebbles at various heights and radial positions, thereby affecting their flow behavior. The design of the central discharge outlet leads to higher flow velocities for fuel pebbles near the center and lower velocities for those farther from the center.

To analyze this, the HCP's Flowtube model is used to divide the HTR-PM into five flow paths, as shown in Figure 53. Unlike SEEPAGE, the flow paths in this model follow an S-curve, with fuel pebbles moving downwards along the flow paths. According to the sphere flow experiments and history data from AVR, each flow path consists of a different number of nodes: 12:12:14:24:48, respectively [42]. Each node has only one predecessor node and one successor node. When refueling begins, a certain volume is discharged from the outlet, causing the batch of fuel pebbles in the upstream nodes to move

to the subsequent nodes. Due to the varying number of nodes in each flow path, the radial flow velocities of the fuel pebbles differ as well.

Under the single-pass strategy, fresh fuel pebbles replenish the upper regions vacated by the discharged pebbles. In contrast, under the multi-pass strategy, both fresh fuel and screened old fuel are used to fill the regions vacated by the discharged pebbles.

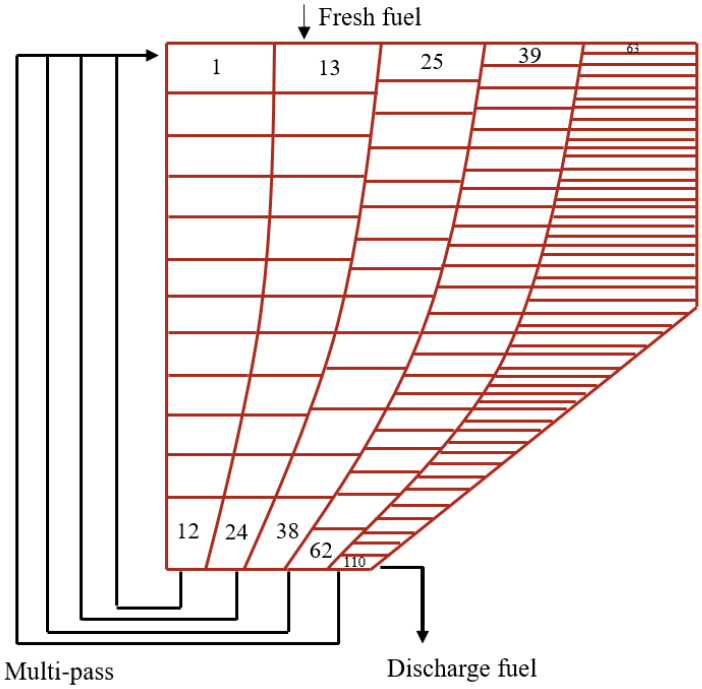

Figure 53 HTR-PM Flowtube model

4.2.3. Benchmark of two models

Here, this study compares the above two models (Seepage and Flowtube) with SERPENT in various benchmark scenarios to establish them as reliable models for subsequent fuel management analysis.

The initial loading process of a pebble-bed reactor (PBR) necessarily starts from a cold state with an air atmosphere. This involves achieving the first physical criticality by gradually loading fuel, then continuing to load fuel to compensate for reactivity changes due to core temperature increase, burnup, and fission product accumulation. The process ultimately leads to a fully loaded core operating at full power in a hot state, known as the initial core state. As a typical representative of PBRs, the HTR-PM must go through fuel loading, atmosphere switching, temperature and pressure ramp-up, and power increase phases to reach the initial core state from the first physical criticality. This process is called the initial core establishment process. Benchmark test scenarios will be designed based on the different stages of this startup process. First, the two models will be tested in an air atmosphere.

In this case， the helium coolant featured in the previous HTR-PM fresh core benchmark is substituted with dry air at 27°C, while all other parameters remain unchanged. Dry air consists of 78% nitrogen-14 (N-14) and 21% oxygen-16 (O-16). The effective multiplication factor (keff) results calculated by HCP model and SERPENT are shown in the Table 9, with an error between them of 0.2%. Compared to the scenario with helium coolant, in both HCP and SERPENT calculations, the Δk decreased by 0.65 and 0.60 niles respectively, demonstrating consistency between the two models. Δk is calculated as follows:

$$\Delta k = keff\_He - keff\_Air \tag{50}$$

Table 9 Results of HCP and Serpent models（Air）

Keff_Seepage	Keff_Flowtube	Keff_SERPENT	Error %
1.2632	1.2632	1.2659	0.2

Scenario Two involves the HTR-PM during the break-in phase. Due to the accumulation of fission products and deep burnup of fuel spheres, in the equilibrium core, although the fresh fuel spheres loaded into the core have an enrichment of 8.5%, the average fuel enrichment in the HTR-PM core is only 4.58%. For an initial core with almost no burnup, loading only fresh fuel spheres with an enrichment of 8.5% would result in excessive reactivity, making it difficult to control. To avoid this, it is necessary to add some boron-containing absorber spheres or reduce the number of fissionable fuel spheres in the core, which can be achieved by adding some graphite spheres or lowering the enrichment of the fuel spheres.

Therefore, Scenario Two simulates two cases of the initial HTR-PM core filled with fuel and graphite spheres, with a ratio of fuel spheres to pure graphite pebbles being 7:8 and a fuel enrichment of 4.1%. As shown in Figure 54, the left core has graphite pebbles and fuel pebbles uniformly distributed throughout the core. In contrast, for the right core, the upper half (7/15) is filled with fuel pebbles, and the lower half (8/15) is filled with graphite pebbles. In the figure, red spheres represent fuel spheres, and blue spheres represent graphite spheres.

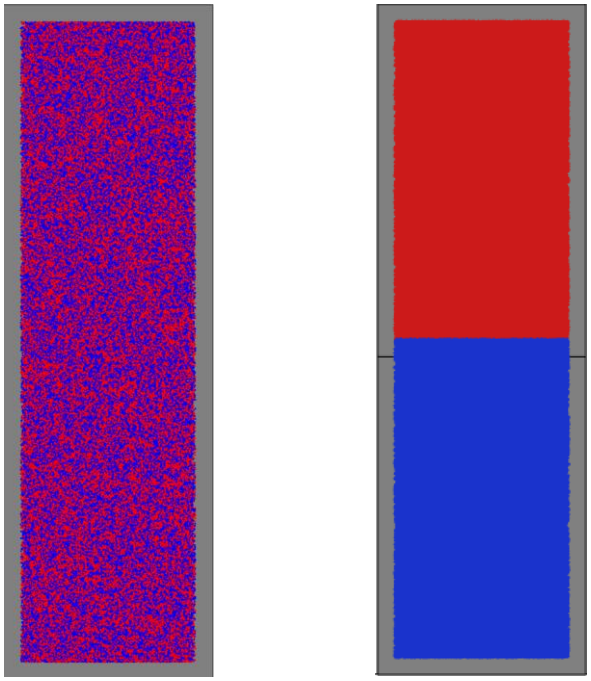

Figure 54 Physical Considerations of the Initial Core

In both scenarios, the packing factor remains 0.6046. The simulation results from HCP and SERPENT are shown in Table 10.

Table 10 Results of HCP and Serpent models(Mix and Separated)

	Keff_Mix	Error %	Keff_Separated	Error %
Serpent	1.0819		1.0685	
Seepage	1.0784	0.3%	1.0661	0.2%
Flowtube	1.0784	0.3%	1.0662	0.2%

As can be seen, for the case of a core with mixed fuel spheres and graphite spheres, the calculation result from SERPENT is 1.0819, while the results from the Seepage and Flowtube modules are both 1.0784, showing a deviation of 0.3%. This demonstrates a high level of consistency. For the second scenario, where the upper half of the core is filled with fuel spheres and the lower half with graphite spheres, the calculation result from SERPENT is 1.0685, while the results from Seepage and Flowtube are 1.0662, showing a deviation of 0.2%. Both refueling models demonstrate very high consistency. Whether using the Seepage model or the Flowtube model, both can serve effectively as benchmark models for simulating core behavior in fuel management.

4.3. Fuel loading patterns of HTR-PM

This part aims to comprehensively explore the fuel loading patterns of the initial core in HTR-PM, and provide theoretical support for the design of nuclear reactors by delving into their physical properties. As a representative of new nuclear reactor technologies, the design of the initial core in HTR-PM is crucial for the performance and safety of the reactor. To achieve this goal, the study employs the HCP code for simulation and encompasses various representative loading schemes. Through an analysis of key physical parameters, including fuel enrichment, flux distribution, and temperature coefficients, as well as the power and charging rates of fuel pebbles, the research explores the relationship between these parameters and the volume fraction of fuel pebbles in the initial core. This study aims to provide theoretical support and data basis for determining the optimal fuel loading scheme for the initial core, ensuring the efficient operation and safety of the reactor.

The HTR-PM's initial core is initially composed solely of fresh fuel pebbles, potentially with graphite pebbles for full power operation. Over time, this core stabilizes through gradual burn-up and replacement, known as the bedding-in phase. Despite the fresh fuel pebbles having an enrichment of 8.5%, the equilibrium core exhibits an average fuel enrichment of 4.58% due to fission product accumulation and deep fuel pebble burn-up. Loading only fresh fuel pebbles into the nearly unburned initial core poses challenges in excess reactivity control, requiring the addition of boron-containing absorber pebbles or a reduction in fissile fuels by adding graphite pebbles or decreasing fuel pebble enrichment. Fuel loading modes for the initial HTR-PM core include various combinations involving fuel pebbles with <8.5% enrichment, graphite pebbles, and absorber pebbles, or exclusively using fuel pebbles with extremely low enrichment.

Choosing the appropriate fuel loading mode involves considering several factors such as fuel pebble enrichment, absorber pebble utilization, and graphite pebble addition. Consistency in enrichment simplifies procurement, manufacturing, and management while moderating individual fuel pebble power. Incorporating a few absorber pebbles can enhance fuel pebble count and reduce individual fuel pebble power, albeit with considerations regarding pebble movement randomness. Adding graphite pebbles can boost fuel pebble enrichment, narrow the enrichment gap between initial and equilibrium

cores, smooth the bedding-in phase, and enhance fuel utilization, making it a planned strategy for HTR-PM implementation [55].

4.3.1. Initial fuel loading strategy

Determining the ratio of fuel pebbles to graphite pebbles is critical in the initial core loading design of the HTR-PM. This ratio has a significant impact on the core's physical properties, including the distribution of thermal neutron flux, temperature feedback, the power output of each fuel pebble, and the loading rate. These factors are closely linked to the volume fraction of fuel pebbles in the initial core.

According to reference [56], the HTR-PM employs a multi-pass fuel management strategy. Fuel spheres enter the reactor core through the central fuel loading tube and exit via a discharge pipe at the bottom of the core. After being discharged, the fuel spheres pass individually through the burnup measurement facility. Based on their burnup levels, they are either directed to the spent fuel storage tank upon reaching their intended burnup or reintroduced into the reactor for another pass through the core.

The fuel passes through the core fifteen times. Therefore, in this study, the unit for the volume fraction of fuel pebbles is set as 1/15 to facilitate simulating the refueling process. As mentioned earlier, using fuel and graphite pebbles with different volume units has a significant impact on the initial core. Hence, we simulated the relationship between the enrichment of fuel and graphite pebbles with different volume units at the full-power initial critical state.

The results are shown in Figure 55. When the volume fraction of graphite pebbles in the initial core is 14/15, the enrichment of fuel needs to reach 21.8% to ensure the core operates normally at maximum power. Conversely, when the volume fraction of graphite pebbles is 10/15, a fuel enrichment of 5.2% is sufficient to meet the requirements. In summary, only when the fuel enrichment is less than 8.4% can the requirements be met. Therefore, the volume fraction of graphite pebbles should be at most 12/15. In other words, the volume fraction of fuel pebbles should be at least 3/15.

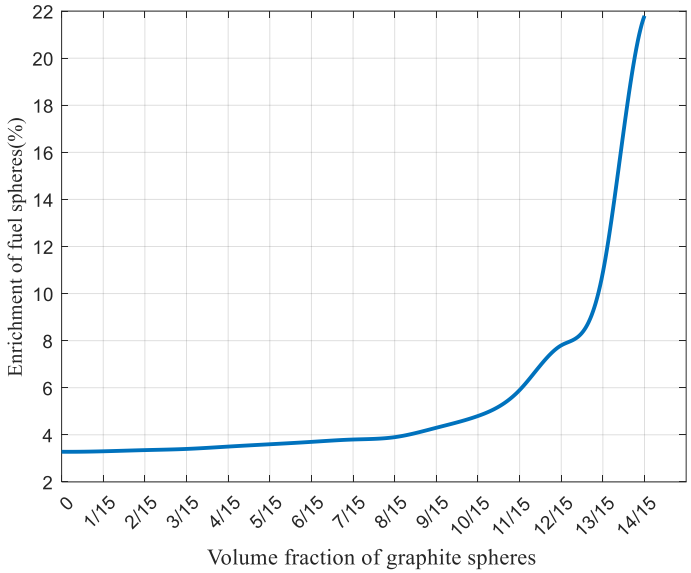

Figure 55 Relationship between fuel enrichment and volume fraction of Graphite spheres

To ensure that the maximum power of a single fuel sphere does not exceed the safety limit of 3.5 kW, it is necessary to minimize the number of graphite spheres in the initial core. At the same time, to

improve fuel utilization and ensure a smooth break-in phase, the enrichment level of the fuel spheres in the initial core needs to be increased, which means increasing the number of fuel spheres. Additionally, the maximum fuel temperature in the fuel region should not exceed 1620°C, which requires adding as many fuel spheres as possible to the initial core. These objectives need to be balanced by adjusting the volume ratio of fuel spheres to graphite spheres in the core.

According to HCP calculations, Figure 56 shows the relationship between the volume fraction of individual fuel spheres power and the initial core fuel spheres, while Figure 57 demonstrates the relationship between the maximum fuel temperature and the volume fraction of the initial core fuel spheres.

From Figure 56, it is evident that when the volume fraction of fuel spheres in the initial core exceeds 5/15, the maximum power of a single fuel sphere is about 3.3 kW, which is below the safety limit of 3.5 kW. In other words, when the volume fraction of fuel spheres is below 5/15, the power of a single fuel sphere is too high, failing to meet the design requirements of the HTR-PM. Moreover, to allow for a safety margin, it is recommended that the volume fraction of fuel spheres should be at least 6/15, at which point the maximum power of a single fuel sphere is approximately 3.1 kW, ensuring a safety margin of over 10%.

Similarly, from Figure 57, it can be seen that when the volume fraction of fuel spheres in the initial core is less than 3/15, the maximum fuel temperature in the core will exceed the upper limit of 1650°C. Therefore, the volume fraction of fuel spheres should be greater than 3/15.

In summary, the initial volume fraction of fuel spheres should be at least 6/15 to meet the above design requirements of the HTR-PM.

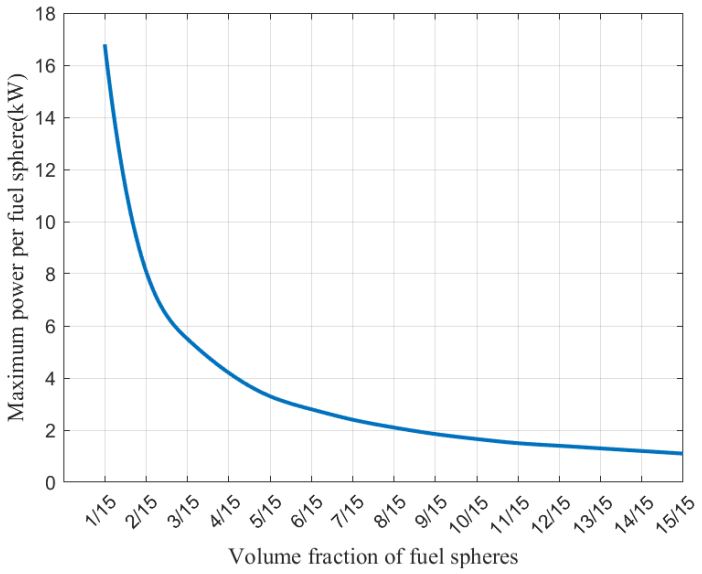

Figure 56 Relationship between volume fraction maximum power per fuel sphere and maximum power per fuel sphere

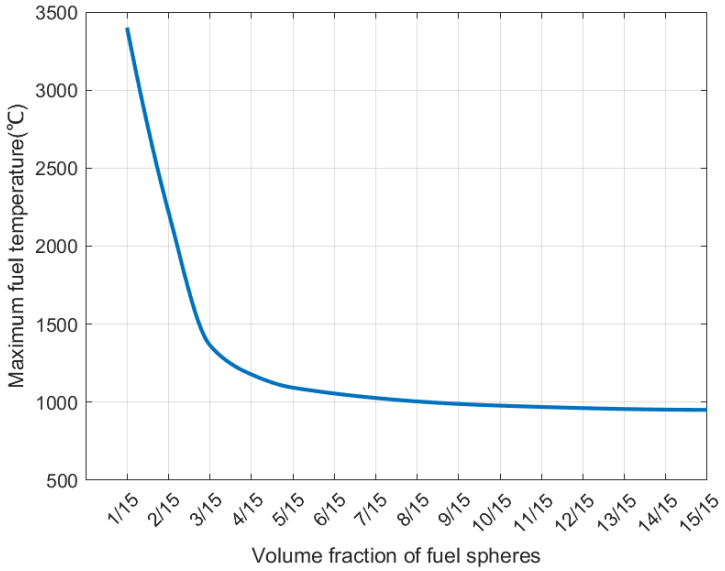

Figure 57 Relationship between volume fraction of fuel and maximum fuel temperature

4.3.2. OTTO and multi-pass strategy

For PB-HTGRs, the dynamic nature of their core allows for continuous flow of spherical fuel elements, enabling the possibility of online refueling. HTGRs typically employ three fuel loading strategies: OTTO, PAP, and Multi-pass [57].

In the OTTO scheme, fuel is loaded into the reactor core once and is not replaced or reprocessed during operation; it is simply discharged after use. The PAP scheme involves online fuel loading and offline fuel discharge. The Multi-pass scheme entails multiple cycles of fuel circulation through the reactor. In a multi-pass strategy, fuel cycles involve multiple loading and unloading processes to maximize fuel utilization. By reusing fuel multiple times, its lifespan in the reactor is prolonged, and fuel waste is minimized.

As a result, pebbles of fuel will pass through the core multiple times. The contribution of high-burnup fuel pebbles, rather than fresh fuel, to the power output at the top of the reactor core is relatively minor. This not only ensures a more uniform power density distribution but also increases power density overall.

To ensure optimal fuel utilization and safety, this section analyzes and compares the OTTO and Multi-pass strategies for HTR-PM using HCP. The simulations and analyses are conducted using the HCP Flowtube model.

The physical design of the core and the corresponding fuel management are based on the flow patterns of the pebbles. The velocity of pebble flow varies at different locations within the core. Near the center of the core, the pebbles flow faster and have shorter residence times, whereas near the edges, the pebbles flow slower and have longer residence times. This results in significant differences in fuel burn-up in different regions.

In Section 4.2.2, to simulate the flow of pebbles, the core is divided into five radial regions. Therefore, in this direction, the average residence times of the fuel pebbles are 12:12:14:24:48. Consequently, the pebble bed is divided into equal-volume regions with residence times of 12:12:14:24:48 across the five

radial regions. During each refueling cycle, pebbles move down one layer from top to bottom. The core is divided into 110 nodes, with a sparser distribution on the left side compared to the right side.

When refueling occurs, newly loaded fuel pebbles are introduced from the top of the core and flow from top to bottom. In the OTTO strategy, fuel pebbles are not reused after being discharged from the bottom. In contrast, the Multi-pass strategy involves selecting discharged fuel pebbles for reuse. Fuel pebbles are reused if they meet both the criteria of having fewer than the specified number of passes and having a burn-up depth below the rated limit. If the fuel pebbles do not meet these conditions, they are stored in a spent fuel tank and are no longer used.

The discarded fuel pebbles are partially replaced by fresh fuel pebbles. Fresh fuel pebbles are introduced into nodes 1, 13, 25, 39, and 63, and subsequently discharged from the core at the bottom nodes 12, 24, 38, 62, and 110.

Starting from the initial loading, the HTR-PM is operated until it reaches equilibrium according to the specifications. At this point, based on the design parameters, the average burn-up is 90 GWd/tU, and the core power is 250 MW. The core contains approximately 420,000 fuel pebbles, with each pebble containing 7 grams of uranium. The average residence time of each fuel pebble in the core can be calculated using the following formula:

$$Average\ Residence\ Time = \frac{Total\ Energy\ Output}{Core\ Power} \tag{51}$$

Fuel spheres remain in the reactor core for an average of approximately 1058 days. For the OTTO strategy, the refueling interval P can be calculated using Equation (52).

$$P = \frac{t_a}{(12+12+14+24+48)/5} \tag{52}$$

The calculated time interval is approximately 48 days. In other words, around 400 new fuel spheres need to be loaded and 400 old fuel spheres removed each day. For the HTR-PM, a 15-pass strategy is typically used. This also requires the daily addition of the same number of fuel spheres as in a single pass. Therefore, the refueling time P2 is P/15, which is approximately 3.2 days. Each day, 6000 fuel spheres need to be added, with fresh fuel spheres accounting for 1/15 of the total.

Calculations were performed on different fuel management models of HTR-PM in the HCP. The simulation utilized SHUFLE, MGT-N, MGT-FD, TRISHA, and TNT. This section focuses on the performance of HTR-PM under steady-state normal operation and the fuel management calculation capabilities of the HCP. Therefore, the calculations began with a fresh core.

As illustrated, since the fresh core initially lacks strong neutron absorbers such as Xe-135, a one-day steady-state burnup calculation was first performed to generate the relevant nuclides. Further steady-state calculations were then performed to obtain cross sections for many nuclides over long burnup time steps.

During the refueling cycle, to avoid repetitive input, the HCP used a series of ACTION repeat commands. First, steady-state calculations were performed based on MGT-N, MGT-FD, and TRISHA. Then, TNT was used for burnup calculations over a fixed time period. After the burnup calculations, steady-state calculations were performed again, and finally, the core was refueled using the ACTION command. These operations were repeated to simulate the refueling scenario under normal operation of the HTGR.

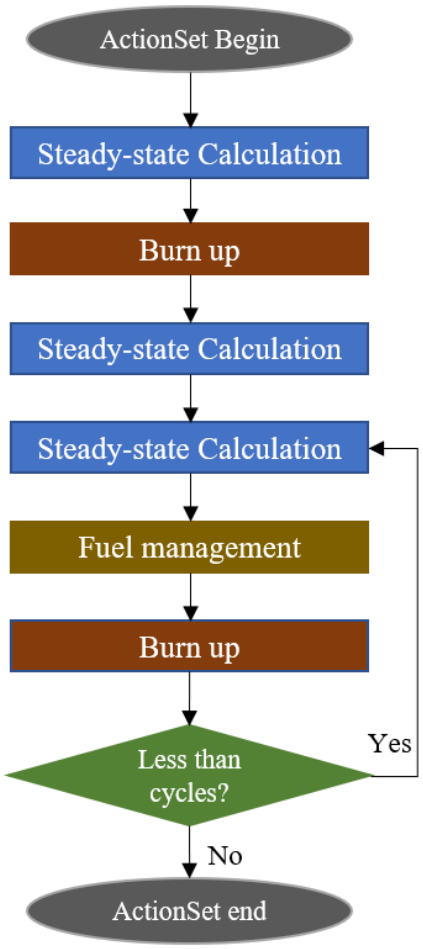

Figure 58 Flowchat of ActionSet

As shown in Figure 58, the OTTO and Multi-pass strategies depict the process from a fresh core to a gradually burnt and equilibrium core. For safety reasons, the entire burnup period was extended to 2000 days. To ensure that the final core's keff is slightly greater than 1.0, maintaining the core's steady state, multiple tests were conducted. The average residence time of the fuel spheres in the core was found to be slightly less than 1058 days, approximately 900 days. Here, to improve computational efficiency, the number of nodes has been appropriately reduced in proportion.

This adjustment is due to two main reasons. Firstly, to prevent some fuel spheres from exceeding the specified burnup depth (100 Gwd/tU), some fuel spheres are discarded when they approach the average burnup depth, resulting in a final average burnup slightly less than 90 Gwd/tU. Secondly, the parameters such as the number of fuel spheres (420,000) and fuel enrichment levels used in the calculations are approximate values. The final results and actual operation will inevitably have some discrepancies, which is reasonable. The specific operational strategy should be determined based on actual experimental data.

Although the once-through and multi-pass strategies involve the same number of fresh fuel pebbles being introduced daily, the power distribution differs significantly. During normal reactor operation with the once-through strategy, the power is concentrated at the top of the core, resulting in higher heat generation by the fuel pebbles at the top. As helium flows in from the top, it aids in cooling these fuel pebbles. In contrast, with the multi-pass strategy, the power distribution is more uniform, leading to

higher power density at the bottom compared to the once-through strategy. Consequently, more heat is generated at the bottom. Since helium has already increased in temperature by the time it reaches the bottom, its cooling effect is less effective there. This results in slightly higher temperatures for the fuel pebbles at the bottom. However, this temperature increase remains within acceptable limits.

Figure 59 shows the relative power density curves for the first flow channel and the radially averaged core after approximately 500 days under the once-through and multi-pass strategies. It can be observed that in the once-through strategy, the power density increases from the top to the bottom and then decreases, with significant variation. The peak power point appears around z=1 meter. This is because, in the once-through strategy, the closer to the top of the core, the fresher the fuel, and since this strategy results in each region burning fuel for a much longer time than the multi-pass strategy, most of the heat is generated at the top of the core. By the time the fuel gradually descends to the lower part of the core, it is near the target burnup, and the heat generated is much less than at the top of the core. In contrast, the multi-pass strategy includes fuel with different burnup depths in each region, resulting in a more uniform power distribution. The peak power point in this strategy is lower, closer to the middle of the core. The figure also shows that, whether considering the average power across multiple flow channels or the axial power distribution at R=0 cm, the power distribution in the multi-pass strategy is more uniform.

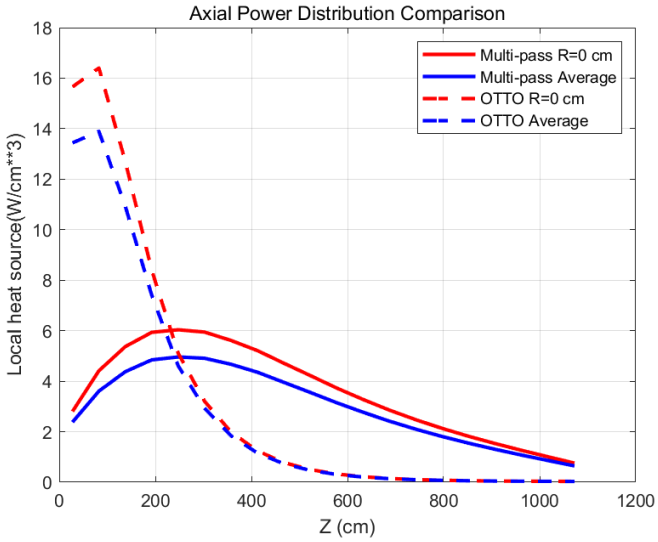

Figure 59 Axial power distribution comparison between OTTO and Multi-pass strategies

Due to the ability of the Multi-pass fuel management strategy to achieve a more uniform power distribution within the core, calculations indicate that the Multi-pass strategy can effectively prevent localized high temperatures, making the core safer. Therefore, this thesis concludes that the Multi-pass refueling strategy is more suitable for the HTR-PM fuel management scheme, offering enhanced safety for the HTR-PM.

4.3.3. LOCA analysis under different fuel loading strategy

As indicated in the previous section, the power peak points and distribution of the HTR-PM core vary under different refueling strategies. Therefore, based on steady-state calculations, this thesis analyzes the PLOFC accident for both the OTTO strategy and the multi-pass refueling strategy using the MGT-FD and MGT-N models for the equilibrium core.

After 500 days of fuel management calculations, the reactor operates normally at 100% power. At this point, the helium coolant flow suddenly decreases to 0 kg/s within 60 seconds. The reactor power sharply declines due to an emergency shutdown, and after about 200 seconds, decay heat becomes the primary heat source in the core. The primary circuit pressure is maintained at 60 bar.

Figure 60 shows the time-dependent maximum fuel temperature curves following a loss of flow accident for the equilibrium core under both refueling strategies. During this period, fuel management operations are halted, and no further refueling is performed. The figure indicates that the maximum fuel temperature in the core under the multi-pass strategy is consistently lower than under the OTTO strategy, with a peak of 1121°C, which is 31°C lower than that of the OTTO strategy.

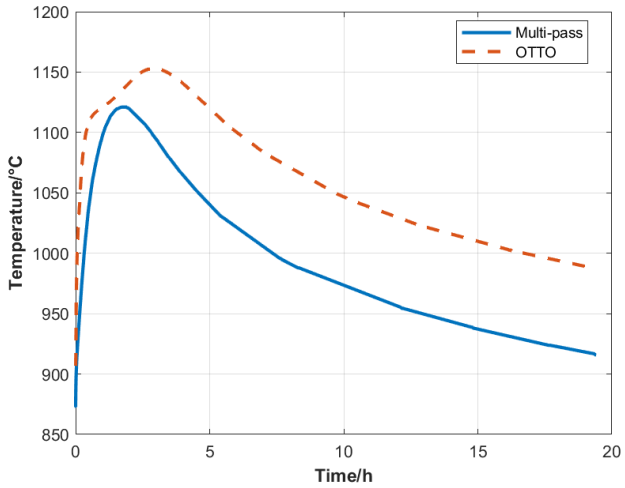

Figure 60 Comparision of maximum fuel temperature tendency after PLOFC accident

The maximum fuel temperatures in both scenarios are below the safety limit, demonstrating the safety of both strategies. However, the Multi-pass strategy results in a lower peak fuel temperature during the accident, providing better protection for the reactor. Thus, the reactor operates in a safer condition under similar average burnup with the Multi-pass strategy.

5. Conclusion

This doctoral research provides a comprehensive exploration of the multi-timescale complex dynamic characteristics of Modular HTGRs, with a particular focus on the development and application of HCP. The study's contributions span several critical domains of HTGRs design, safety, and operational efficiency, advancing the state-of-the-art in nuclear reactor technology. The primary contributions of this research are detailed as follows:

1) Innovative Development of Control Rod Systems: The research introduced the "Flexible Curtain" control rod method within the HCP framework, representing a significant advancement in the simulation of HTGR dynamics. This method was rigorously validated against established international codes such as SERPENT, confirming its precision in modeling control rod behavior. The successful implementation of this method enhances HCP's capability to perform detailed dynamic analyses over both long-term and short-term timeframes, thus improving the safety and operational control of HTGRs.
2) Comprehensive Neutron and Fluid Dynamics Models for HTR-PM: Detailed neutron and fluid dynamics models for the HTR-PM were developed and integrated into the HCP framework. These models facilitated accurate simulations of various short-term operational scenarios, including control rod movements, power fluctuations, and temperature variations. The simulations validated the design safety and reliability of the HTR-PM, demonstrating its robustness under different operational conditions and enhancing confidence in its performance.
3) Evaluation of Fuel Management Strategies: The study investigated multiple fuel management strategies using the SHUFFLE and TNT modules within HCP, specifically analyzing OTTO and multi-pass refueling scenarios. The comparative analysis provided critical insights into the benefits and challenges of each strategy, contributing to the optimization of reactor performance and fuel utilization. The ability of HCP to integrate long-term and short-term simulations demonstrated its effectiveness in handling complex reactor dynamics over extended operational periods.
4) Multi-Timescale Analysis Capability: The HCP's ability to conduct multi-timescale analyses—from instantaneous reactions on the order of microseconds to long-term operational dynamics spanning years—provides a holistic understanding of HTGR behavior. This capability is crucial for optimizing reactor performance, ensuring safety, and managing the lifecycle of reactor components. By addressing both short-term transients and long-term operational strategies, the research offers a comprehensive framework for analyzing and improving HTGR systems.

Future research should build upon the advancements made in this study, focusing on several critical areas to further enhance the capabilities and applications of the High-Temperature Reactor Code Package (HCP). Continued development and optimization of HCP, particularly in refining control rod system modeling and improving spectrum codes, are essential for increasing its accuracy and reliability. Expanding the application of HCP to other reactor types, such as PWRs and BWRs, will provide broader insights into reactor dynamics and facilitate advancements in nuclear reactor technology. Integrating advanced safety systems and passive safety features within the HCP framework will contribute to more comprehensive safety analyses, incorporating innovative materials and cooling technologies. Additionally, research should focus on the sustainability and environmental impact of HTGRs, including lifecycle emissions, waste management strategies, and the potential for integrating HTGRs with renewable energy systems to create a more sustainable and low-carbon energy infrastructure. These future research directions will collectively enhance the safety, performance, and environmental benefits of nuclear reactors.

In conclusion, this doctoral research has made substantial contributions to the field of HTGR technology. The development and validation of the HCP have addressed critical gaps in reactor simulation capabilities, providing a robust tool for the dynamic analysis of HTGRs. These advancements not only improve the safety and efficiency of current reactor designs but also pave the way for future innovations in nuclear reactor technology. The research provides a solid foundation for future work aimed at enhancing the safety, performance, and sustainability of nuclear reactors, contributing to the ongoing development of advanced nuclear energy systems.

REFERENCES

[1] IEA World energy outlook. 2023.

[2] World Nuclear Performance Report 2022, world-nuclear.org/getmedia/9dafaf70-20c2-4c3f-ab80-f5024883d9da/World-Nuclear-Performance-Report-2022.pdf.aspx.

[3] Handbook of generation IV nuclear reactors[M]. Woodhead Publishing, 2016.

[4] Tang C, Li Z, Zou Y, et al. Irradiation testing of matrix material for spherical HTR-10 fuel elements[J]. Nuclear engineering and design, 2008, 238(11): 2886-2892.

[5] High Temperature Gas Cooled Reactor Fuels and Materials. IAEA-TECDOC-1645. 2010.

[6] Kugeler, K., Zhang, Z. (2019). General Aspects of High-Temperature Reactors. In: Modular High-temperature Gas-cooled Reactor Power Plant. Springer, Berlin, Heidelberg.

[7] Qu X, Zhao G, Wang J. Thermodynamic evaluation of hydrogen and electricity cogeneration coupled with very high temperature gas-cooled reactors[J]. International Journal of Hydrogen Energy, 2021, 46(57): 29065-29075.

[8] Wang Q, Liu C, Li D, et al. Optimization and comparison of two improved very high temperature gas-cooled reactor-based hydrogen and electricity cogeneration systems using iodine-sulfur cycle[J]. International Journal of Hydrogen Energy, 2022, 47(33): 14777-14798.

[9] Retrieved from https://www-pub.iaea.org/

[10] Allelein H J, Verfondern K. Major milestones of HTGR development in Germany and still open research issues[J]. Annals of nuclear energy, 2018, 116: 114-127.

[11] Dazhong W, Daxin Z, Yuankui X. Present status of research and development for HTGR in China[J]. Energy, 1991, 16(1-2): 159-167.

[12] Rütten H J, Haas K A, Brockmann H, et al. VSOP (99/05) computer code system[J]. 2005.

[13] Gerwin H. Das Zweidimensionale. Reaktordynamikprogramm TINTE. Teil 1: Grundlagen und. Lösungsverfahren. Jül-2167. November. 1987.

[14] Gerwin H. Das zweidimensionale Reaktordynamikprogramm TINTE Teil 2: Anwendungsbeispiele[R]. Publikationen vor 2000, 1989.

[15] Scherer W, Gerwin H, Kindt T, et al. Analysis of reactivity and temperature transient experiments at the AVR high-temperature reactor[J]. Nuclear Science and Engineering, 1987, 97(1): 58-63.

[16] Lee B, Gerwin H, Niessen H F, et al. On the validation of the reactor-dynamics code-sytem TINTE post-calculation of the SANA I experiments with radial insulator[J]. Interner Bericht KFA-ISR-IB-2, 1995, 95.

[17] Gerwin H, Scherer W. Zur Validierung des Reaktordynamik-programmsystems TINTE: Graphit-Korrosion mit Luft, Vergleichsrechnungen zum Experiment VELUNA[J]. Institut für Sicherheitsforschung und Reaktortechnik (ISR), KFA-ISR-IB-8/92, 1992.

[18] Krohn H, Finken R. FRESCO-II: ein Rechenprogramm zur Berechnung der Spaltproduktfreisetzung aus kugelförmigen HTGR-Brennelementen in Bestrahlungs-und Ausheizexperimenten[R]. Publikationen vor 2000, 1983.

[19] Verfondern K. PANAMA-Ein Rechenprogramm zur Vorhersage des Partikelbruchanteils von TRISO-Partikeln unter Storfallbedingungen[J]. Jul-Spez-298, 1985.

[20] Moormann R. Source term estimation for small sized HTGRs[M]. Forschungszentrum, Zentralbibliothek, 1992.

[21] Stöcker B, Hurtado A, Struth S. Component exposure in hypothetical accidents with very fast depressurization in a HTGR module reactor[J]. Nuclear engineering and design, 1999, 190(3): 297-302.

[22] Allelein H J, Xhonneux A, Herber S C. Progress on the development of a fully integrated HTR code package[J]. Nuclear engineering and design, 2012, 251: 400-406.

[23] Rütten H J, Haas K A. NAKURE-99, Computer code for the calculation of the decay power of the fuel of Pebble-Bed HTGRs[J]. FZ-Jülich, Internal Report ISR-IB-1, 2003.
[24] Muir D W, Boicourt R M, Kahler A C. The NJOY nuclear data processing system, version 2012[J]. Los Alamos, USA: Los Alamos National Laboratory, 2012.
[25] Nyffenegger U, Schlösser J. The New Cross Section Library of the Dragon Project. Dragon Project Report[R]. Organization for Economic Co-Operation and Development, 1964.
[26] Nordheim L W. A Program of Research and Calculations of Resonance Absorption. Final Report[R]. General Atomics, San Diego, CA (United States), 1961.
[27] Schlösser J. MUPO: an IBM—7090 Programme to Calculate Neutron Spectra and Multi-Group Constants. Dragon Project Report[R]. Organization for Economic Co-Operation and Development, 1963.
[28] P. Lourens. Verification of the mathematical models for the neutron flux of the code TINTE. Internal documents of PBMR project, 2004.
[29] Y. Naito, M. Maekawa, K. Shibuya. A leakage iterative method for solving thethree-dimensional neutron diffusion equation. Nuclear Science and Engineering, 58: 182-192, 1975.
[30] Deutsches Institut f¨ur Normung. Berechnung der Nachzerfallsleistung der Kern brennstoffe von Hochtemperaturreaktoren mit kugelf¨ormigen Brennelementen. DIN 25485, 1990.
[31] J.Schlösser. MUPO An IBM-7090 programme to calculate neutron spectra and multi-group constants. O.E.C.D. High temperature reactor project dragon. 1963.
[32] U. Nyffenegger, J.Schlösser. The new cross section library of the dragon project. O.E.C.D. High temperature reactor project dragon. 1964.
[33] G. Golub, C. Van Loan. Matrix Computations (3rd ed.). 1996.
[34] Brockmann, H. TOTMOS: an integral transport code for calculating spectra and multi-group cross section, Jül-4325.
[35] Bende E E, Hogenbirk A H, Kloosterman J L, et al. Analytical calculation of the average Dancoff factor for a fuel kernel in a pebble bed high-temperature reactor[J]. Nuclear Science and Engineering, 1999, 133(2): 147-162.
[36] Ji W, Martin W R. Application of the chord method to obtain analytical expressions for Dancoff factors in stochastic media[J]. Nuclear science and engineering, 2011, 169(1): 19-39.
[37] Tantillo F, Allelein H J, Bardow A, et al. Design, implementation and validation of a new neutron spectral code for high temperature gas reactors[R]. Lehrstuhl für Reaktorsicherheit und-technik, 2019.
[38] Xhonneux A, Lambertz D, Allelein H J. The enhanced fuel management models of the HTR code package (HCP) module SHUFLE[J]. Nuclear Engineering and Design, 2018, 329: 177-191.
[39] Xhonneux A, Allelein H J. Development of an integrated fission product release and transport code for spatially resolved full-core calculations of V/HTGRs[J]. Nuclear engineering and design, 2014, 271: 361-369.
[40] Gerwin H. Das zweidimensionale Reaktordynamikprogramm TINTE.: Grundlagen und Lösungsverfahren[M]. Kernforschungsanlage Jülich, 1987.
[41] Druska C, Nünighoff K, Kasselmann S, et al. Code-to-code comparison between TINTE and MGT for steady state scenario[J]. Nuclear engineering and design, 2012, 251: 111-116.
[42] Kugeler, K., Zhang, Z. (2019). Reactor Components. In: Modular High-temperature Gas-cooled Reactor Power Plant. Springer, Berlin, Heidelberg.
[43] Chen F, Han Z. Steady-state thermal fluids analysis for the HTR-PM equilibrium core[J]. International Journal of Advanced Nuclear Reactor Design and Technology, 2021, 3: 11-17.
[44] J. Zhang, J. Guo, F. Li, and Y. Sun, “Research on the fuel loading patterns of the initial core in Chinese pebble-bed reactor HTR-PM,” Annals of Nuclear Energy, vol. 118, pp. 235–240, 2018.

[45] Guan C, Chai X, Zhang T, et al. Transient coupling analysis of loss-of-coolant accidents in HTR-PM based on CFD approaches[J]. Annals of Nuclear Energy, 2022, 173: 109097.
[46] Zehner P., Schlünder E.U.: Einfluss der Wärmestrahlung und des Druckes auf den Wärmetransport in nichtdurchströmten Schüttungen. Chem.-Ing. Techn.,1972
[47] Robold K.: Wärmetransport im Innern und in der Randzone von Kugelschüttungen, Forschungszentrum Jülich, Jülich, 1982
[48] Zheng Y, Shi L, Dong Y. Thermohydraulic transient studies of the Chinese 200 MWe HTR-PM for loss of forced cooling accidents[J]. Annals of Nuclear Energy, 2009, 36(6): 742-751.
[49] Ortensi J, Ougouag A M. Improved prediction of the temperature feedback in TRISO-Fueled reactors[R]. Idaho National Lab.(INL), Idaho Falls, ID (United States), 2009.
[50] Shi D. Extension of the Reactor Dynamics Code MGT-3D for Pebblebed and Blocktype High-Temperature-Reactors[M]. Nukleare Entsorgung und Reaktorsicherheit, 2015.
[51] J. Ortensi, A. M. Ougouag. Improved prediction of the temperature feedback in TRISO-fueled reactors. Report INL/EXT-09-16494, 2009.
[52] O. Ubbink, P. S. Toit, P. Lourens, W. R. Joubert. PBMR fuel kernel model forthe prediction of accurate temperature profiles. ICONE16, Orlando, Florida, USA, May 11-15, 2008.
[53] Kamrin K, Rycroft C H, Bazant M Z. The stochastic flow rule: A multi-scale model for granular plasticity[J]. Modelling and Simulation in Materials Science and Engineering, 2007, 15(4): S449.
[54] Kasselmann S, Schitthelm O, Tantillo F, et al. Development of a new nuclide generation and depletion code using a topological solver based on graph theory[J]. Nuclear engineering and design, 2016, 306: 154-159.
[55] Zhang J, Li F, Sun Y. Physical analysis of the initial core and running-in phase for pebble-bed reactor HTR-PM[J]. Science and Technology of Nuclear Installations, 2017, 2017.
[56] Zhang J, Guo J, Li F, et al. Research on the fuel loading patterns of the initial core in Chinese pebble-bed reactor HTR-PM[J]. Annals of Nuclear Energy, 2018, 118: 235-240.
[57] Wu S R, Wu S C, Chao D S, et al. Burnup computations of online refueling process for HTR-10 using shell-by-shell fuel movement[C]//Proceedings of International Symposium on Symbiotic Nuclear Power Systems for 21st Century (ISSNP2016), September 26-28, Chengdu, China. 2016.
[58] Trabadela R. High-temperature reactor code package thermo-fluid dynamics development[J]. 2020.
[59] Shi D. Extension of the Reactor Dynamics Code MGT-3D for Pebblebed and Blocktype High-Temperature-Reactors[M]. Nukleare Entsorgung und Reaktorsicherheit, 2015.
[60] Kasselmann S, Xhonneux A, Tantillo F, et al. Verification of the HTR code package (HCP) as a comprehensive HTGR steady state and transient safety analysis framework[J]. Nuclear engineering and design, 2018, 329: 167-176.
[61] Guan C, Chai X, Zhang T, et al. Transient coupling analysis of loss-of-coolant accidents in HTR-PM based on CFD approaches[J]. Annals of Nuclear Energy, 2022, 173: 109097.
[62] Zheng Y, Stempniewicz M M, Chen Z, et al. Study on the DLOFC and PLOFC accidents of the 200 MWe pebble-bed modular high temperature gas-cooled reactor with TINTE and SPECTRA codes[J]. Annals of Nuclear Energy, 2018, 120: 763-777.

ACKNOWLEDGMENTS

As I come to the end of my PhD journey, I would like to take this opportunity to express my sincere gratitude to all those who have supported and helped me along the way.

First and foremost, I would like to thank my supervisor, Prof. Rafael Macián-Juan, for his guidance, patience, and support throughout my doctoral studies. His dedication to research and careful mentorship have been truly invaluable to my academic growth.

I am also grateful to all the colleagues and friends in the Nuclear Technology Research Group at TUM. Thank you for your collaboration, encouragement, and the many meaningful discussions that have helped shape this work.

My sincere thanks also go to the members and partners of the KONHCP project. Working on this project has been a rewarding experience that taught me both technical skills and the value of teamwork.

I would like to thank the TUM Graduate Center and the funding bodies for their support, which made my research and exchange opportunities possible.

I owe my deepest gratitude to my family, especially my parents, for their unwavering support and understanding throughout these years. Your encouragement has been my greatest source of strength.

Lastly, I would like to thank myself—for not giving up, for staying the course through challenges, and for continuing to believe that every step forward counts.